Carnegie Mellon University
Mellon College of Science

Thesis

Submitted in partial fulfillment of the requirements for the degree of Ph.D. in Biological Sciences

Title Different Phases of Refinement in a Developing Inhibitory Circuit.

Presented by Jineta Banerjee

Accepted by the Department of Biological Sciences

Major Professor Karl Kandler **Date** March 17, 2014

Department Head Nathan Urban **Date** March 17, 2014

Approved by the MCS College Council

Dean Frederick Gilman **Date** March 24, 2014

A Study of the Different Phases of Refinement of an Inhibitory Circuit in the Mouse Auditory Brainstem.

by

Jineta Banerjee
B.Sc in Zoology (Honors), University of Calcutta
M. Sc in Biotechnology, University of Calcutta

Submitted in partial fulfillment of the requirements for the degree of
Doctor of Philosophy

at

Carnegie Mellon University
Department of Biological Sciences
Pittsburgh, Pennsylvania

Advisor: *Dr. Karl Kandler, PhD*

March 3, 2014

Abstract

Crudely assembled neuronal circuits with exuberant innervations are refined into precise adult-like circuits by functional silencing and structural pruning of the surplus connections during early development. Such reorganizations are evident in several excitatory circuits as well as in the inhibitory circuit between the medial nucleus of trapezoid body (MNTB) and the lateral superior olive (LSO).

LSO neurons integrate excitation from the glutamatergic inputs from ipsilateral anteroventral cochlear nucleus (AVCN) and inhibition from the contralateral AVCN via GABA/glycinergic inputs from the ipsilateral MNTB (Cant and Casseday, 1986; Spangler et al., 1985). The tonotopic arrangement of the circuit ensures that the excitatory and inhibitory inputs corresponding to the same sound frequency converge on to the same population of LSO neurons. Due to this tonotopic arrangement, the medial part of the circuit responds to high frequency sound stimulus and the lateral part of the circuit responds to low frequency sound stimulus (Kandler and Friauf, 1993; Friauf, 1992; Tsuchitani, 1977). In the first two postnatal weeks of pre-hearing development, the medial part of the circuit undergoes extensive functional refinement during which single LSO neurons lose 75 % of their initial MNTB connections and the remaining inputs are strengthened by 8 fold (Kim and Kandler, 2003; Noh et al., 2010). The neurotransmitter phenotype of this circuit also transforms from

a GABA/Glycine/Glutamate co-release to primarily glycinergic release during this period (Kotak et al., 1998; Gillespie et al., 2005). However, it is still unclear whether functional elimination and strengthening of inputs occurs simultaneously or in succession and which factors influence these processes.

In this study I investigated the course of refinement of the medial and lateral MNTB inputs to the LSO in acute brainstem slices of E 18 to P 13 mice using whole-cell patch clamp technique. I determined the strength of single MNTB inputs using minimal stimulation technique. I estimated the number of inputs on to each LSO cell by calculating the convergence ratio derived from the postsynaptic response amplitudes to minimal and maximal stimulation of MNTB fibers. I also investigated the role of transient glutamatergic and GABAergic co-release from the MNTB inputs in the process of refinement and strengthening of the inputs.

I observed three distinct phases in the pre-hearing refinement of the MNTB-LSO circuit. The first phase or the proliferation phase (between embryonic day 18 and postnatal day (P) 2-3) is followed by a functional elimination phase (between P 3 and P 5). This is then followed by a strengthening phase (between P 6 and P 9) of the retained MNTB inputs. I observed extensive proliferation and functional elimination of inputs in the medial part of the circuit while no significant elimination occurred in the lateral part. Both medial and lateral inputs strengthened about 3-4 fold in the first two weeks of development. I also observed that the transient glutamate co-release, which is essential for the refinement and strengthening of the medial MNTB-

LSO projections, does not seem to play an important role in the strengthening of the lateral MNTB inputs. I further investigated the role of GABA co-release in the process of refinement of the MNTB-LSO circuit using a conditional Gad1 knockout mouse. However, the study of the role of GABA co-release in the MNTB-LSO circuit was inconclusive due to the lack of phenotypic alteration of the GABAergic input in the MNTB-LSO circuit of the Gad1 knockout mice.

Thus from the present study it is clear that, during the pre-hearing development, functional elimination of specific inputs occurs before strengthening of the inputs in the medial MNTB-LSO circuit. So the strength of single inputs does not seem to be a key factor in determining which inputs are functionally eliminated. Significant strengthening occurs in the lateral MNTB-LSO circuit even in the absence of any functional elimination. Further, while glutamate co-release in the circuit seems to be crucial for the elimination and strengthening of medial MNTB-LSO projections, it does not seem to be important for the lateral part of the circuit. These observations collectively suggest that the functional elimination phase and the strengthening phase in the pre-hearing refinement of the MNTB-LSO circuit seem to be independent of each other with different underlying mechanisms.

Acknowledgments

I would like to begin by thanking my advisor Karl Kandler for his guidance and support throughout my dissertation work. I really appreciate how patient he has been with me as I worked through the various ups and downs of research. I would also like to thank my research advisory committee members Nathan Urban and Alison Barth for taking time out from their very busy schedules to hear about my research and provide valuable feedback. Contrary to most students, I have really enjoyed my yearly thesis committee meetings through my years of Ph.D. The feedback that I got during these meetings have helped me immensely in keeping my eye on the target and prevented me from getting lost in the vastness of the ocean of science. Apart from the scientific discussions, the informal chats I have had with Alison, Nathan and Karl have helped me grow as a person.

I would like to thank Dr. Rebecca Seal (University of Pittsburgh) and Dr. Richard Palmiter (University of Washington) for graciously gifting transgenic mice.

I would also like to thank Thanos and Lania for their feedback on my research during our weekly lab meetings. I would also like to acknowledge all past and present members of the auditory research group for their helpful discussions and friendly banter. I have enjoyed our casual chats as well as scientific discussions as part of the close knit auditory research group in the Department of Otolaryngology in University of Pittsburgh. I would like to specially mention Amanda Clause for teaching me how to patch a cell, Tuan Nyugen for helping me with setting up my rig, Catherine Weisz

for various helpful discussions, and Santosh Chandrasekaran for being a great friend and classmate. I would like to thank Hannah Roos for helping me out with mice work and Xinyan Gu for helping me out with immunofluorescence stainings. I would also like to acknowledge Dorothy O'Hara for friendly chats over the regular morning coffee. All of these together have helped me enjoy the roller-coaster ride of research.

I would like to acknowledge the administrative staff of the Department of Biological Sciences and the Center for Neural Basis of Cognition (CNBC) Ena Miceli, Emily Stark, Kristen McConnell, Nate Frezzell, Melissa Stupka, Barb Dorney and Lisa Bopp for their help with various administrative formalities and paperwork.

My acknowledgements would be incomplete without mentioning Jayanta Mondal, Anindita Dutta, Rachana Nevrekar and Sourish Chaudhuri who made the last five years of my life extremely special. Their presence made the easier days more fun and the tough days easier to bear. Carnegie Mellon and Pittsburgh will always occupy a special place in my heart. The close, personal and collaborative scientific community that CMU provides was perfect for my growth as a student and I could not have wished for a better place to live than Pittsburgh.

Finally, I would like to dedicate this thesis to my parents Jayanta Banerjee and Kalyani Banerjee. Their hard work, support, and guidance is the foundation of all my achievements. Their love and wisdom has always urged me to look beyond the ordinary and seek excellence in every sphere of life. To them, I owe it all !

Abbreviations

ABBV	**Name**
MNTB	Medial Nucleus of Trapezoid Body
LSO	Lateral Superior Olive
SPON	Superior ParaOlivary Nucleus
AVCN	AnteroVentral Cochlear Nucleus
DCN	Dorsal Cochlear Nucleus
IC	Inferior Colliculus
NMJ	Neuromuscular Junction
CF	Climbing Fiber
PC	Purkinje Cell
RGC	Retinal Ganglion Cell
LGN	Lateral Ganglion Cell
MSO	Medial Superior Olive
IPSC	Inhibitory Postsynaptic Current
P	Postnatal day
ILD	Interaural Level Difference
ITD	Interaural Time Difference
VGlut-3	Vesicular Glutamate Transporter 3
GABA	Gamma Amino Butyric Acid

Contents

List of Tables

List of Figures

Chapter 1

Introduction

1.1 Developmental refinement in neural circuits

Properly functioning mature neural circuits show precise and stereotypic connectivity among different nuclei. The initial projections of the immature neurons are targeted to the appropriate locations guided by genetics and neurotrophic factors (Goodman and Shatz, 1993). But the microstructure of the circuit is imprecise because of exuberant connections, commonly seen during the early stages of assembly and development (Colman et al., 1997; Lichtman and Colman, 2000). In course of development, a select few connections are strengthened, followed by the elimination of surplus weaker connections (Colman et al., 1997; Lichtman and Colman, 2000; Cohen-Cory, 2002). Such reorganization or refinement of the developing connections is generally guided by activity dependent mechanisms (Changeux and Danchin, 1976; Lohof et al., 1996; Nguyen and Lichtman, 1996; Katz and Shatz, 1996) leading to the formation of precisely connected adult-like circuits.

1.2 Refinement in the excitatory neural circuits

Evidences of such reorganizations have been observed in several well studied model excitatory neural circuits like the neuromuscular junctions (Purves and Lichtman, 1983; Colman et al., 1997), climbing fiber - Purkinje cell (CF-PC) circuit (Hashimoto and Kano, 2003; Hashimoto et al., 2009), and retinal ganglion cell - lateral geniculate nucleus (RGC-LGN) circuits (Shatz, 1990; Katz and Shatz, 1996).

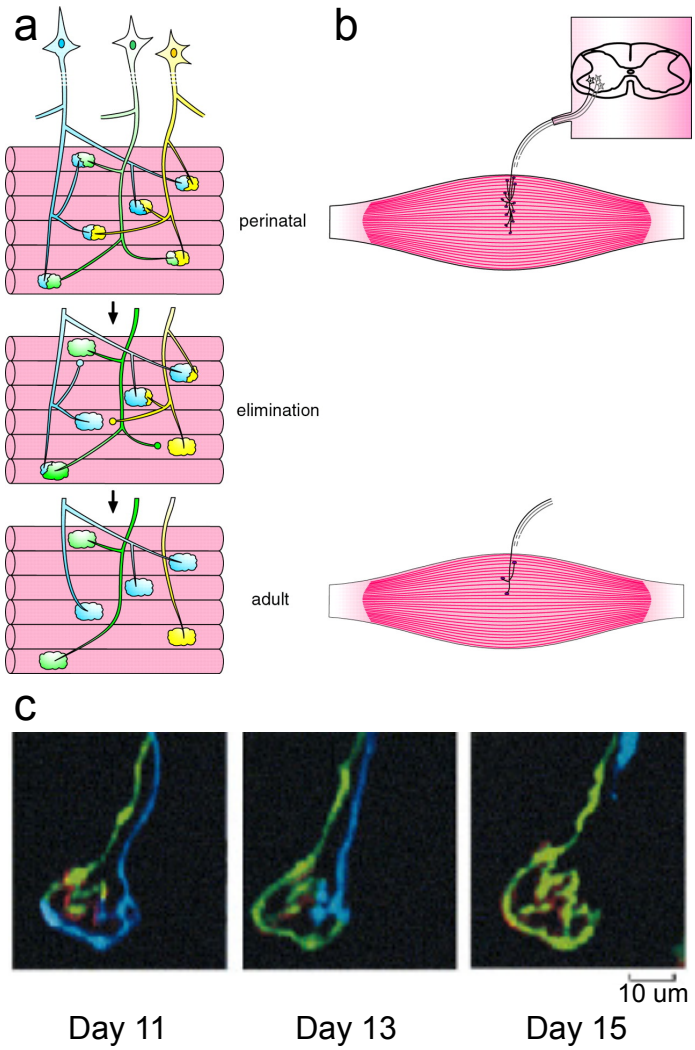

Figure 1.1: **Synaptic competition at the developing neuromuscular junction.**
(a, b) Schematic representation of elimination of inputs at the neuromuscular junction during development.
(c) Confocal image of the competing synaptic inputs at a neuromuscular junction showing active competition (flip-flop) between two synaptic inputs during development. Left panel shows "winning" blue input at day 11, Middle and right panel shows green axon taking over in subsequent days. Modified from (Walsh and Lichtman, 2003)

1.2.1 Neuro-Muscular Junction

Synaptic reorganization or refinement is very well studied in the developing neuromuscular junction. At birth, each muscle fiber receives inputs from a number of spinal motor neurons, showing a multi innervation state. At each junction, the postsynaptic membrane possesses an oval plaque with a high density of acetylcholine receptors (AchRs), where numerous motor axons of similar strength converge and intermingle (Sanes and Lichtman, 1999; Gan and Lichtman, 1998). Over the next few postnatal weeks, the relative strength of one of the competing axonal inputs become progressively higher than the rest due to an increase in the amount of neurotransmitter released (quantal content) by the input (Colman et al., 1997). This disparity in the input strengths along with asynchrony in the activity patterns of the different synaptic inputs, help to initiate active competition between the inputs (Balice-Gordon and Lichtman, 1994; Walsh and Lichtman, 2003). As a result of this competition, the stronger or the more synchronously active inputs are preferentially maintained (Colman et al., 1997; Busetto et al., 2000) (Fig 1.1). The other relatively weak inputs become progressively weaker and finally lose territory on the postsynaptic surface and are ultimately eliminated (Balice-Gordon and Lichtman, 1993; Balice-Gordon et al., 1993). The selectively maintained inputs form a monoinnervated junction which is both functionally and anatomically mature.

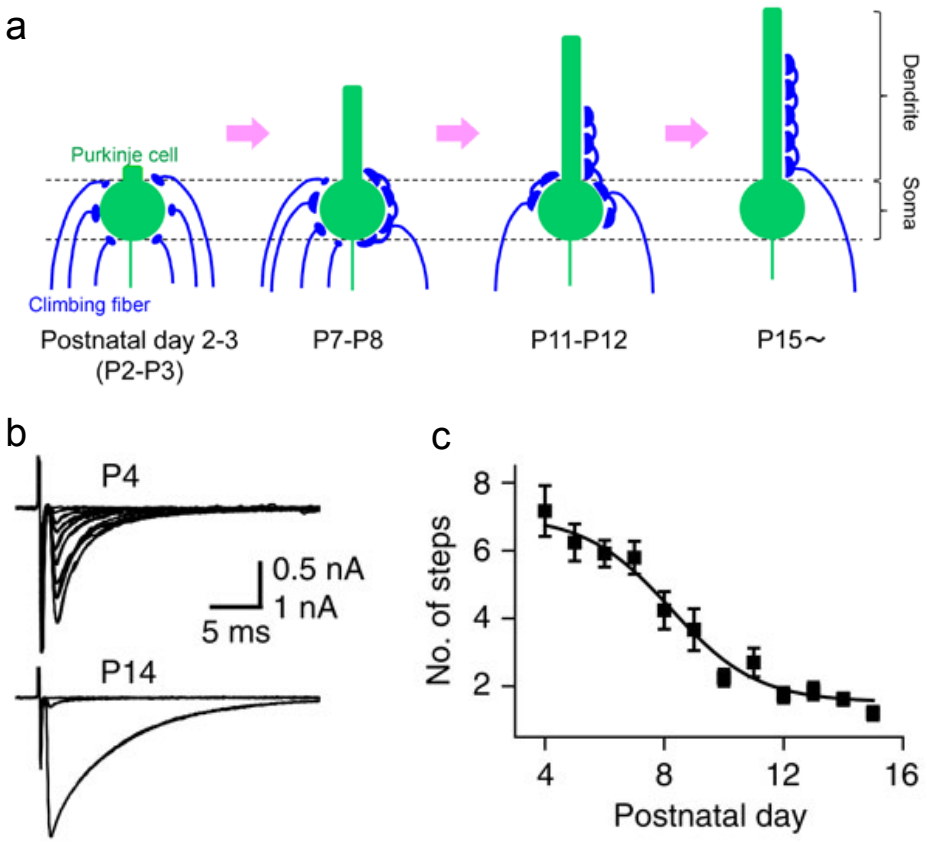

Figure 1.2: **Synaptic competition at the developing climbing fiber - Purkinje cell circuit in the cerebellum**.
(a) Schematic representation of elimination of weak climbing fiber inputs at the climbing fiber - Purkinje cell synapse during development.
(b, c) Whole cell recording showing reduction in number of climbing fiber inputs from P4 to P14 reported by reduction in number of steps in the synaptic response of Purkinje cell. Modified from (Hashimoto et al., 2009; Kawamura et al., 2013)

1.2.2 Climbing Fiber - Purkinje Cell circuit

Another well studied circuit showing extensive reorganization of synaptic inputs is the climbing fiber - Purkinje cell circuit in the cerebellum. In the mature cerebellum, the Purkinje cell (PC) receives a single strong glutamatergic climbing fiber (CF) input, originating from the inferior olive, on the proximal dendrites, as well as numerous parallel fiber inputs on mostly the distal dendrites (Eccles et al., 1966). During the first three weeks of postnatal development, this CF-PC circuit transforms from a multiple-innervation state to a mono-innervation state (Hashimoto and Kano, 2005). At postnatal day (P) 3-4, each Purkinje cell is innervated by many weak perisomatic climbing fiber inputs (Mason et al., 1990; Crepel et al., 1976; Lohof et al., 1996). Out of these weak fibers, the fiber with a higher probability of multivesicular release at the synapses, strengthens significantly over the next week of postnatal development (Wadiche and Jahr, 2001; Hashimoto and Kano, 2003). The strengthening of a single climbing fiber is not only facilitated by the higher probability of multivesicular release, but also governed by the Hebbian rule of plasticity. The repeated pairing of the stimulation of a CF and the postsynaptic depolarization of the PC causes homosynaptic strengthening of the stimulated CF and heterosynaptic depression of other CFs to form the mono-innervation pattern (Bosman et al., 2008; Bosman and Konnerth, 2009). The fiber, strengthened by the above mentioned methods, then extensively innervates the proximal dendrite of the Purkinje cell and is retained while the other weaker fibers are subsequently eliminated (Hashimoto and

Kano, 2003). This elimination of weaker fibers is also facilitated by the activation of mGluR1 (Ichise et al., 2000) mediated heterosynaptic depression resulting from parallel fiber activity (Nusser et al., 1994). At around P 12 each Purkinje cell is innervated with only one strong climbing fiber (CF-mono) or one strong and a few weak fibers (CF-multi) (Hashimoto and Kano, 2005) (Fig 1.2 a).

1.2.3 Retinal Ganglion Cell - Lateral Geniculate Nucleus circuit

A similar trend of elimination of surplus innervations has also been observed in the retinal ganglion cell - lateral geniculate nucleus (RGC-LGN) circuit. In this circuit, coordinated spontaneous bursts of spiking activity in the retinal ganglion cells helps the segregation of eye-specific inputs in the LGN (Shatz, 1990; Katz and Shatz, 1996; Wong and Oakley, 1996; Mooney et al., 1996). Coordinated spontaneous activity of ipsilateral ganglion cells causes long term potentiation or LTP in the inputs from the ipsilateral eye (homosynaptic potentiation) to the LGN and causes long term depression or LTD in the inputs from the contralateral eye (heterosynaptic depression) to the same LGN neurons (Wong et al., 1993; Wong and Oakley, 1996). The synapses weakened by LTD are most likely removed during development and the inputs strengthened by LTP are most likely retained, so that at the end of the period of refinement, the LGN neurons receive input from only one specific eye (Wong et al., 1993; Wong and Oakley, 1996).

From the extensive study of different model excitatory circuits, a common theme of

refinement seems to emerge. Refinement typically consists of two phases: firstly a few of the numerous initial weak inputs strengthen considerably by different physiological processes including increase in quantal content, multi-vesicular release, and LTP in the strengthening phase (Purves and Lichtman, 1983; Colman et al., 1997; Hashimoto and Kano, 2003). Then a phase of elimination occurs either simultaneously or in succession to ensure that the relatively weaker or asynchronous inputs lose out in the competition with the stronger or more synchronous inputs (Ichise et al., 2000; Maejima et al., 2001; Miyata et al., 2000; Wong and Oakley, 1996; Mooney et al., 1996) and are successively structurally pruned. The selectively maintained strong inputs form circuits that are anatomically and functionally mature (Colman et al., 1997; Hashimoto and Kano, 2005; Shatz, 1990; Katz and Shatz, 1996).

1.3 Refinement in the inhibitory neural circuits

While the excitatory circuits have been extensively studied, the developmental changes in the inhibitory circuits have been studied to a lesser degree. Most of the inhibition in the brain comes from intricate local networks of inhibitory interneurons. Recurrent connectivity and complex interactions of the inhibitory circuits with the excitatory circuits make these circuits difficult to manipulate and study. However, the inhibitory circuits in the auditory brainstem like that of the medial superior olive (MSO) and the lateral superior olive (LSO) have relatively linear circuitry free from the above mentioned complexities. Refinement of inhibitory circuits has been studied

in these model circuits.

1.3.1 Medial Nucleus of Trapezoid Body - Medial Superior Olive circuit

The MSO receives binaural excitatory inputs from the cochlear nuclei (Joris et al., 1998) and binaural inhibitory inputs from the lateral nucleus of trapezoid body (LNTB) and the medial nucleus of trapezoid body (MNTB) (Cant and Hyson, 1992; Grothe and Sanes, 1994) (Fig 1.3 a). The ipsilateral and contralateral excitatory inputs converge on to the same MSO cells but are spatially segregated in a frequency specific manner between lateral and medial dendrites respectively (Smith et al., 1993; Russell and Moore, 1995). The inhibitory inputs however undergo reorganization during development. The inhibitory inputs are present uniformly along the soma and dendrites in the juvenile animals before hearing onset (Kapfer et al., 2002). Under the influence of sound-evoked activity, the inhibitory inputs then reorganize by elimination of synapses such that the retained synapses are mostly perisomatic after hearing onset (Kapfer et al., 2002) (Fig 1.3 b). The MNTB-MSO projections have also been shown to undergo significant axonal refinement during this time of synaptic reorganization (Werthat et al., 2008) (Fig 1.3 c). The axonal spread and branch points of the MNTB axons decrease significantly after hearing onset to make the circuit anatomically more precise (Werthat et al., 2008).

Another inhibitory circuit where refinement of an immature inhibitory neural circuit has been studied extensively is the MNTB-LSO circuit. In this circuit, the orga-

nization of the mature circuit is extremely well known. Furthermore, reorganization of synaptic inputs in this circuit occurs both before and after hearing onset i.e in the absence as well as presence of external stimulus. The presence of a pre-hearing phase of refinement in this circuit provides an excellent opportunity to study the different phases of refinement in an inhibitory circuit occurring in absence of external stimulus and the intrinsic factors that may influence such refinement.

1.4 The Medial Nucleus of Trapezoid Body - Lateral Superior Olive circuit

The MNTB-LSO circuit is a part of the sound localization pathway in the mouse auditory brainstem. It helps in localization of sound using the interaural level difference or ILD of sound stimuli (Boudreau and Tsuchitani, 1968). The difference in the intensity of sound (ILD) in the two ears provides a primary cue for the horizontal direction of the sound source. As the first binaural nucleus in the sound localization pathway in vertebrates (Boudreau and Tsuchitani, 1968; Guinan et al., 1972a), the LSO integrates excitation from the ipsilateral ear and inhibition from the contralateral ear to compute the ILD in a frequency dependent manner (Boudreau and Tsuchitani, 1968; Guinan et al., 1972a; Sanes and Rubel, 1988) (Fig 1.3 a). The LSO neurons receive glutamatergic inputs from the ipsilateral anteroventral cochlear nucleus (AVCN) and inhibition from the contralateral AVCN via the GABA/glycinergic inputs from the ipsilateral MNTB (Cant and Casseday, 1986; Spangler et al., 1985; Boudreau and Tsuchitani, 1968; Caird and Klinke, 1983; Sanes and Rubel, 1988; Fri-

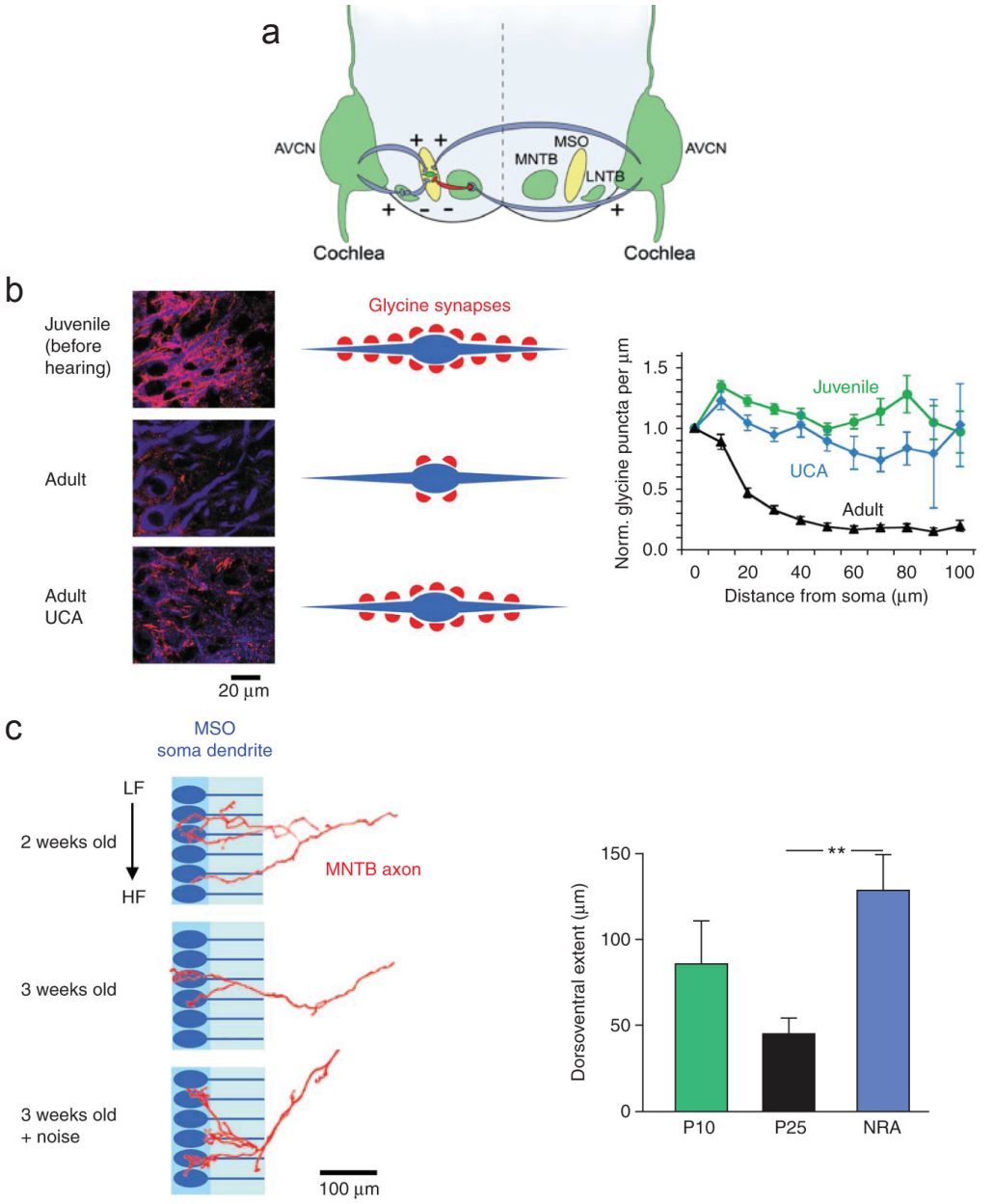

Figure 1.3: **Refinement in the MSO circuit**
(a) Schematic representation of the auditory brainstem showing excitatory and inhibitory inputs into the MSO
(b) (left) Immunofluorescence staining of MSO cells showing the redistribution of glycine positive puncta in the MSO from juvenile to adult, and lack of redistribution in unilateral cochlear ablation(UCA) animals; (middle, right) schematic showing reorganization of glycinergic boutons along the MSO dendrites
(c) (left) Schematic representation showing post-hearing refinement MNTB axons in the MSO, and lack of refinement in noise reared animal (bottom panel); (right) barplot showing the spread of the MNTB axons in the MSO at different ages. (Kandler et al., 2009)

auf and Ostwald, 1988) (Fig. 1.3 b). As a result, the LSO cells show higher spiking activity when the sound intensity at the ipsilateral ear is greater than that of the contralateral ear (Tollin et al., 2008) (Fig 1.3c). To help in computation of the ILDs in a frequency specific manner, the bilateral inputs are tonotopically arranged such that the excitatory and inhibitory inputs corresponding to the same sound frequency converge on to the same population of LSO neurons. The tonotopic map of the MNTB-LSO circuit is aligned such that the medial part of the circuit responds to high frequency sound stimulus and the lateral part of the circuit responds to low frequency sound stimulus (Friauf, 1992; Kandler and Friauf, 1993; Kil et al., 1995; Tsuchitani, 1977; Sanes et al., 1989; Sanes and Siverls, 1991).

1.4.1 Refinement in the developing MNTB - LSO circuit

The tonotopic map of the MNTB-LSO circuit undergoes extensive reorganizations to form narrow and precise frequency bands (Kim and Kandler, 2003; Sanes and Siverls, 1991; Sanes et al., 1992b), possibly for optimum frequency discrimination. These reorganizations occur both before as well as after hearing onset (Kim and Kandler, 2003; Sanes and Siverls, 1991; Sanes et al., 1992b). The GABA/glycinergic inputs in the MNTB-LSO circuit are functional prenatally and are arranged in an imprecise tonotopy at birth (Kandler and Friauf, 1995a, 1993). Then, in the first two postnatal weeks of development (before hearing onset), the medial MNTB-LSO connections undergo extensive silencing or functional elimination of almost 75% of the initial MNTB connections (Kim and Kandler, 2003). This functional elimination

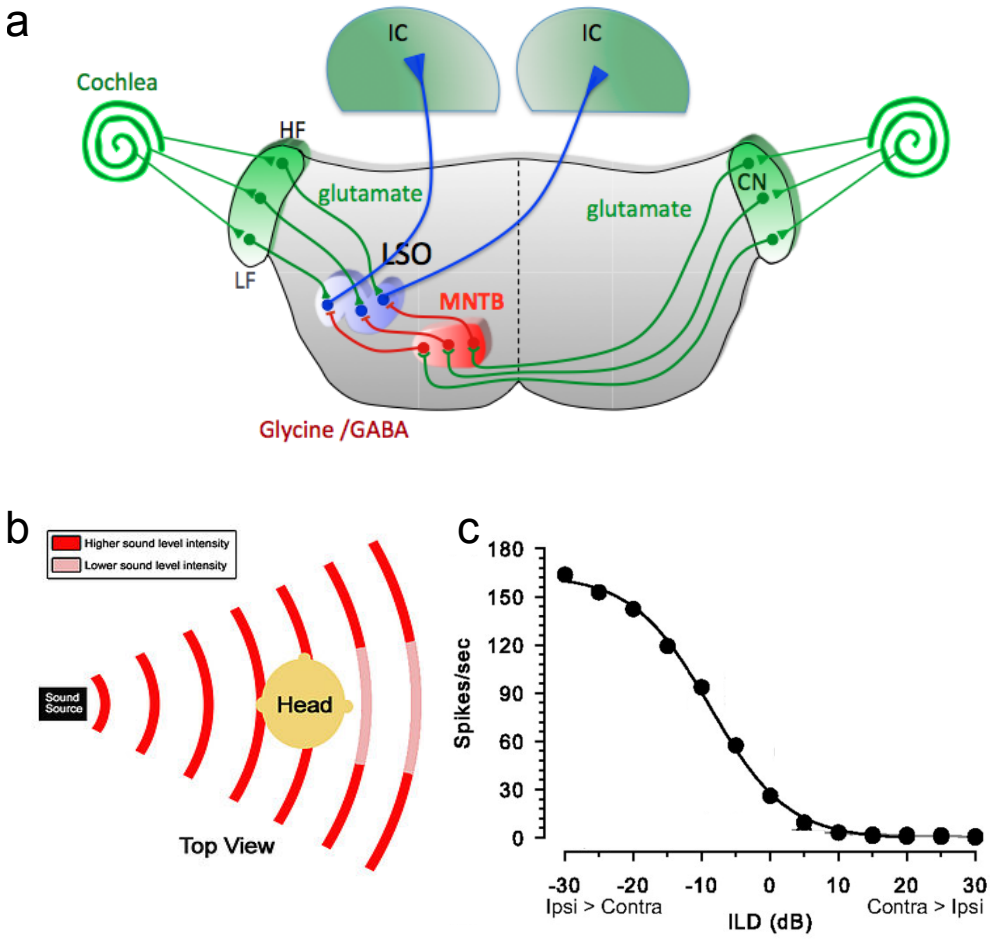

Figure 1.4: **The MNTB-LSO circuit**

(a) Schematic showing the afferent and efferent connections of LSO. HF: high frequency, LF: low frequency, CN: cochlear nucleus, MNTB: medial nucleus of trapezoid body, LSO: lateral superior olive, IC: inferior colliculus.
(b) Interaural level difference (ILD) as a primary cue for sound localization. Dark red: high intensity sound, light red: low intensity sound.
(c) Plot showing spiking activity of LSO neurons in response to different ILDs. Modified from (Tollin et al., 2008)

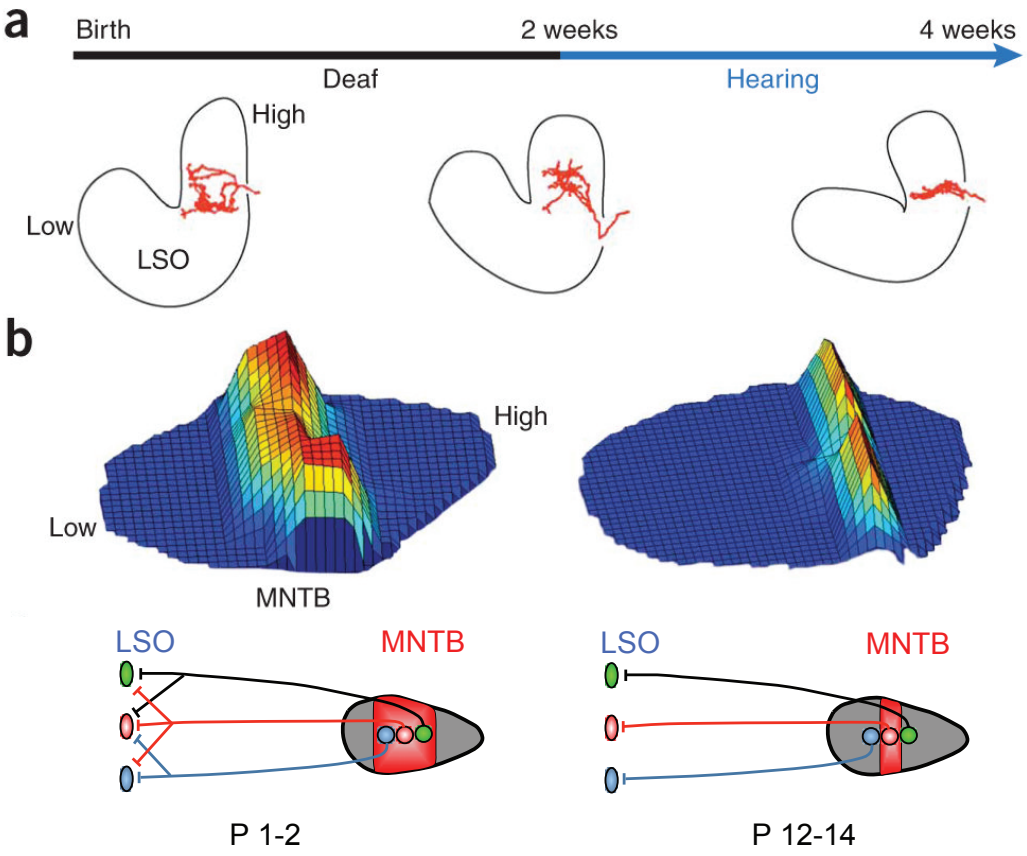

Figure 1.5: **Refinement in the MNTB-LSO circuit**
(a) Schematic representation showing structural pruning of MNTB axonal boutons after hearing onset
(b) Schematic representation showing sharpening of MNTB input maps before hearing onset. Modified from (Kandler et al., 2009)

causes sharpening of the initial crude tonotopy such that the frequency specific MNTB input map is reduced by 50% (Kim and Kandler, 2003; Noh et al., 2010) (Fig. 1.4 b). Along with the functional silencing, the remaining inputs are strengthened 12 fold (in rats) (Kim and Kandler, 2003) due to increase in the quantal content and addition of new release sites (Kim and Kandler, 2003, 2010).

After hearing onset, a second phase of tonotopic refinement ensues leading to structural reorganization of the MNTB-LSO connections (Sanes et al., 1989). Axonal pruning of MNTB inputs and structural elimination of synaptic boutons occur in the first week after hearing onset (Sanes and Siverls, 1991; Sanes et al., 1992a,b). This presynaptic axonal pruning is complimented with a narrowing of the dendritic tree of the postsynaptic LSO cells (Sanes et al., 1990). This structural reorganization resulting in sharpening of the frequency map in the LSO (Sanes and Siverls, 1991; Rietzel and Friauf, 1998; Sanes and Chokshi, 1992) requires normal neurotransmission in the circuit and is impaired in animals with cochlear ablation or chronic blockade of glycinergic transmission in the circuit (Sanes and Takács, 1993; Sanes and Chokshi, 1992).

1.4.2 Role of transient neurotransmitters in the developing MNTB - LSO circuit

Very little is known about the different factors that influence the different phases of early postnatal refinement in the MNTB-LSO circuit. The first phase of functional refinement in the circuit occurs in the pre-hearing period, in the absence of any external sound stimuli (Kim and Kandler, 2003). However, spontaneous activity

in the cochlea driving the activity of downstream auditory nuclei is hypothesized to play a key role in the pre-hearing refinement in the MNTB-LSO pathway (Tritsch et al., 2007). Thus the neurotransmitters released by MNTB neurons in response to such spontaneous activity in the cochlea may be key candidates that influence the pre-hearing refinement in the MNTB-LSO circuit. The MNTB-LSO neurons are known to co-release three different neurotransmitters during this pre-hearing period (Kotak et al., 1998; Gillespie et al., 2005). While the MNTB-LSO projections in the adult circuit are primarily glycinergic in their function, during the first two postnatal weeks they release GABA (Kotak et al., 1998) and glutamate (Gillespie et al., 2005) in addition to glycine. Glutamate and GABA are released only during the first two postnatal weeks and their levels decline significantly at hearing onset (Kotak et al., 1998; Case and Gillespie, 2011). The transient nature of the release of glutamate and GABA release and their presence specifically during the period of functional refinement in the circuit make them excellent candidates for a role in influencing the pre-hearing refinement in the MNTB-LSO circuit.

Glutamate is a fast excitatory neurotransmitter in the central nervous system and GABA is a primary inhibitory neurotransmitter in the adult brain. However, during the early stages of development, both glutamate and GABA are known to elicit excitatory postsynaptic potentials (Kandler and Friauf, 1995a; Ben-Ari et al., 2007) and cause calcium influx into the postsynaptic cell (Leinekugel et al., 1995). During the first two postnatal weeks, glutamate released from the MNTB terminals activate

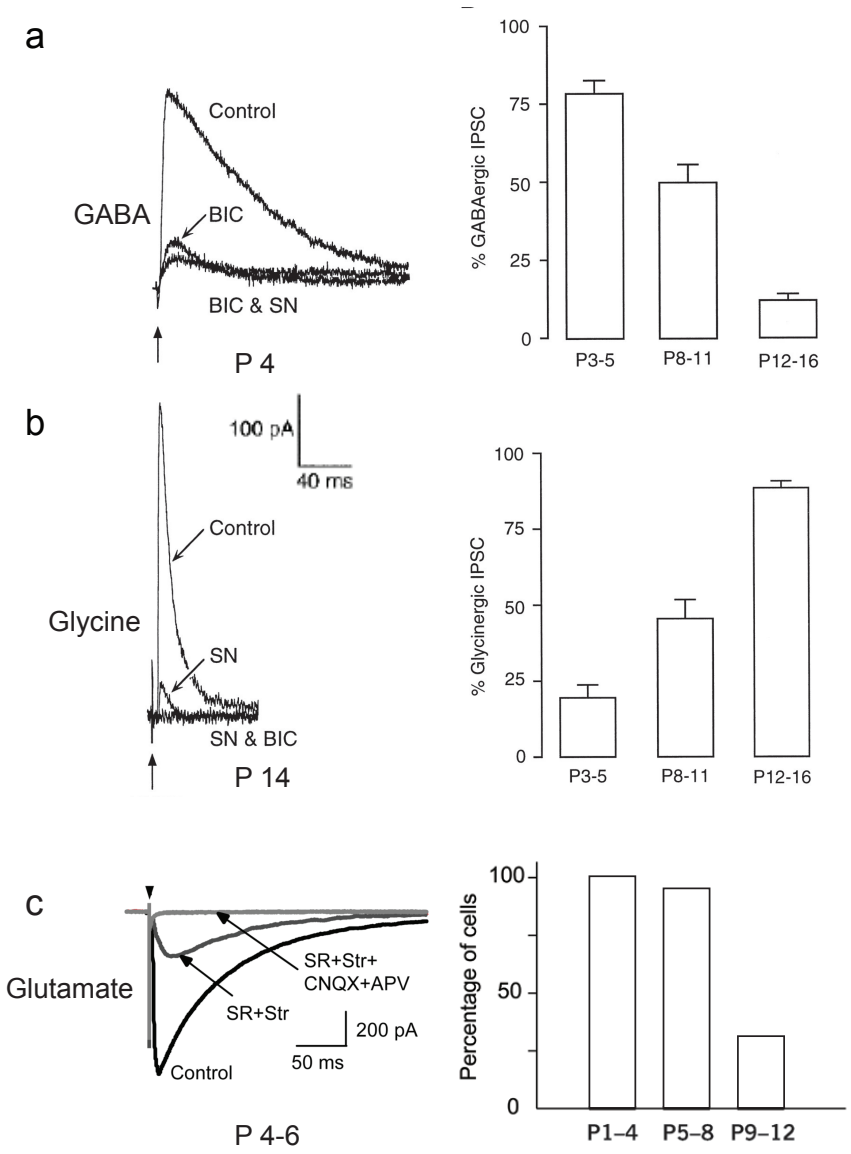

Figure 1.6: **GABA, Glycine and Glutamate co-release in the MNTB-LSO circuit**
(a) MNTB evoked GABAergic response in P 4 LSO cells blocked mostly by addition of bicucculine (BIC). (right) Percentage of GABAergic IPSCs decrease over the first two weeks.
(b) MNTB evoked Glycinergic response in P 14 LSO cells blocked mostly by addition of Strychnine (SN). (right) Percentage of Glycinergic IPSCs increase over the first two weeks.
(c) MNTB evoked Glutamatergic response in P 4-6 LSO cells blocked by addition of CNQX and APV. (right) Percentage of cells showing Glutamatergic response decrease over the first two weeks.
Modified from (Kotak et al., 1998; Noh et al., 2010)

the GluN2B containing NMDA receptors leading to calcium influxes into the post-synaptic LSO cells (Case and Gillespie, 2011). During these developmental stages, GABA can also elicit prolonged depolarizations due to the high intracellular chloride concentrations in the developing LSO cells (Kandler and Friauf, 1995a; Kullmann and Kandler, 2001) . Such depolarization by GABA in the postsynaptic cell is capable of causing calcium influx into the postsynaptic LSO cell (Kullmann et al., 2002). These depolarization induced calcium influxes in the postsynaptic cell may activate different synaptic plasticity mechanisms that may be required for the refinement and strengthening of developing synapses. The presence of transient glutamate release in the MNTB-LSO circuit has been shown to be essential for the refinement and strengthening of the inputs in the medial part of the circuit during the pre-hearing stages (Noh et al., 2010). However, almost nothing is known regarding the role of the transient GABAergic transmission in the refinement of the MNTB-LSO circuit during the early developmental ages.

While the medial or the high frequency sensitive part of the MNTB-LSO circuit has been studied extensively leading to detailed information about postnatal synaptic refinement in this inhibitory circuit, very little is known about the refinement in the low frequency sensitive lateral part of the circuit. In this thesis I have attempted to elucidate the pre-hearing refinement of the medial and the lateral part of the MNTB-LSO circuit in finer detail and also investigated the possible role of Glutamate and

GABA co-release in the refinement process.

First, I investigated the detailed course of refinement in both the medial and the lateral part of the MNTB-LSO circuit. The study revealed three phases in the process of refinement. The medial part of the circuit shows an early phase of proliferation of synaptic inputs followed by an elaborate phase of silencing or functional elimination of synaptic inputs. The elimination is further followed by a phase of strengthening of the remaining inputs. This chronology of phases is very different from the process of refinement seen in other model excitatory circuits where the strengthening phase precedes the elimination phase. This observation suggests that the strength of the MNTB inputs may not play a role in the determination of which inputs are to be selectively maintained or eliminated. I also observed that this elimination phase is absent in the lateral part of the circuit. But even in the absence of the elimination phase, strengthening occurs normally in the lateral projections. This suggests that the two phases may be independent of one another.

Second, I investigated the possible role of glutamate co-release on the refinement of the lateral MNTB inputs. Glutamate co-release that has been shown to be essential for the strengthening of the medial MNTB inputs, seems to be non-essential for the strengthening of the lateral inputs. This suggests that the process of strengthening of lateral MNTB-LSO connections may be influenced by different underlying factors compared to that of the medial connections.

Third, I investigated the role of transient GABAergic co-release in the process

of functional elimination of synaptic inputs in the medial part of the circuit using a conditional Gad1 knockout mouse made by Cre-loxP method of recombination. However, the study using the conditional knockout mouse was inconclusive due to the lack of a deletion phenotype.

Chapter 2

Materials and Methods

2.1 Materials and Methods:

2.1.1 Animals and slice preparation:

All experimental procedures were performed in accordance with NIH guidelines and were approved by IACUC at the University of Pittsburgh. Whole cell patch clamp experiments were performed in acute brainstem slices of postnatal mice of strain C57bl (Jaxson Mice Laboratory) (ages E18 - P13), *vglut3-/-* (ages P2 - P13), and *gad1 -/-* (ages P2 - P13) of both genders.

The animals were deeply anesthetized by isofluorane inhalation. Anesthetized embryos and postnatal animals were decapitated and the brains were quickly removed and submerged in cold artificial cerebrospinal fluid (ACSF; composition in mM: NaCl-124, $MgSO_4$.7H2O 1.3, KCl- 5.0, KH_2PO_4- 1.25, Dextrose-10.0, $NaHCO_3$- 26.0, $CaCl_2.2H_2O$- 2.0, bubbled in 95 % O_2/ 5 % CO_2, pH 7.4, RT, Kynurenic Acid- 1.0 was added during slicing. 350um coronal slices of the brainstem were prepared as described previously (Noh and Kandler, 2010, Kandler and Friauf, 1995).

To obtain E18 animals, young adult mice were paired overnight and the first 24-hour period after pairing was considered E1. The timed pregnant females were deeply anesthetized by isofluorane inhalation. All the embryos were quickly removed by Cesarean section and further anesthetized by hypothermia by submerging in ice cold artificial cerebrospinal fluid (ACSF). The anesthetized female was euthanized after the extraction of embryos. For postnatal animals, the animals were deeply

anesthetized by isofluorane inhalation. Anesthetized embryos and postnatal animals were decapitated and the brains were quickly removed and submerged in cold artificial cerebrospinal fluid as described above.

For *gad1 -/-* experiments, after setting up the breeding scheme and obtaining the offsprings of the appropriate generation, all the experiments were done blind to the genotype to avoid experimenter's bias. The data were analysed and then regrouped according to the genotyping results.

2.1.2 Electrophysiological recordings and electrical stimulation:

Whole cell recordings were obtained from visually identified bipolar LSO neurons in the medial (high frequency) and lateral (low frequency) limb. Intracellular recordings were made using patch pipettes of 2-3 MOhm resistances. Patch pipettes were filled with internal solution of the following composition in mM; D-gluconic acid-54.0, CsOH-49.0, CsCl-56.0, Na-phosphocreatine-3.0, $MgCl_2.6H_2O$-1.0, $CaCl_2$-1.0, HEPES-10.0, EGTA-11.0, Na-GTP-0.3, Mg-ATP-2.0, QX-314-5.0, Alexa-568-0.2%.

Recordings were performed in a submersion chamber mounted on an upright microscope (Zeiss AxioExaminer1). Whole cell currents in voltage clamp were recorded using a Multiclamp700B amplifier (Axon instruments) and a Digidata 1440A digitizer (Axon instruments) using pClamp10 software. All currents were Bessel filtered at 10KHz. Series resistance was compensated up to 65 %. Recordings were made

while holding the cells at -60mV (after liquid junction potential correction).

Afferent fiber bundle from MNTB to the LSO was stimulated with a low resistance patch pipette (¡ 1 MOhm, filled with ACSF). Stimulation pulses (0.1ms duration) were delivered using a stimulation isolation unit (Isoflex, AMPI) at 0.1 Hz.

2.1.3 Minimal and maximal stimulation:

Electrical stimulation was gradually increased from 0 uA until it produced a synaptic success rate of ¡ 50 %. Any further increase would decrease the failure rate without increasing the mean peak amplitude of successful synaptic input. 50-100 responses were recorded at this stimulus intensity to estimate mean peak amplitude of a single input.

For maximal stimulation, the stimulus intensity was increased gradually. An increase in response amplitude was noted commensurate with the increased stimulus. A stimulus response curve was obtained until a plateau in response amplitudes was reached where any further increase in stimulus amplitude caused a decrease in response amplitude presumably due to damage to fibers near the stimulus electrode. The mean of at least 10 consecutive plateau responses was used to estimate the maximal synaptic strength for a given LSO neuron.

2.1.4 Data Analysis:

Preliminary analyses of recorded traces were done using Clampfit10.0 software. Further analyses and statistical tests were done using Graphpad prism and custom

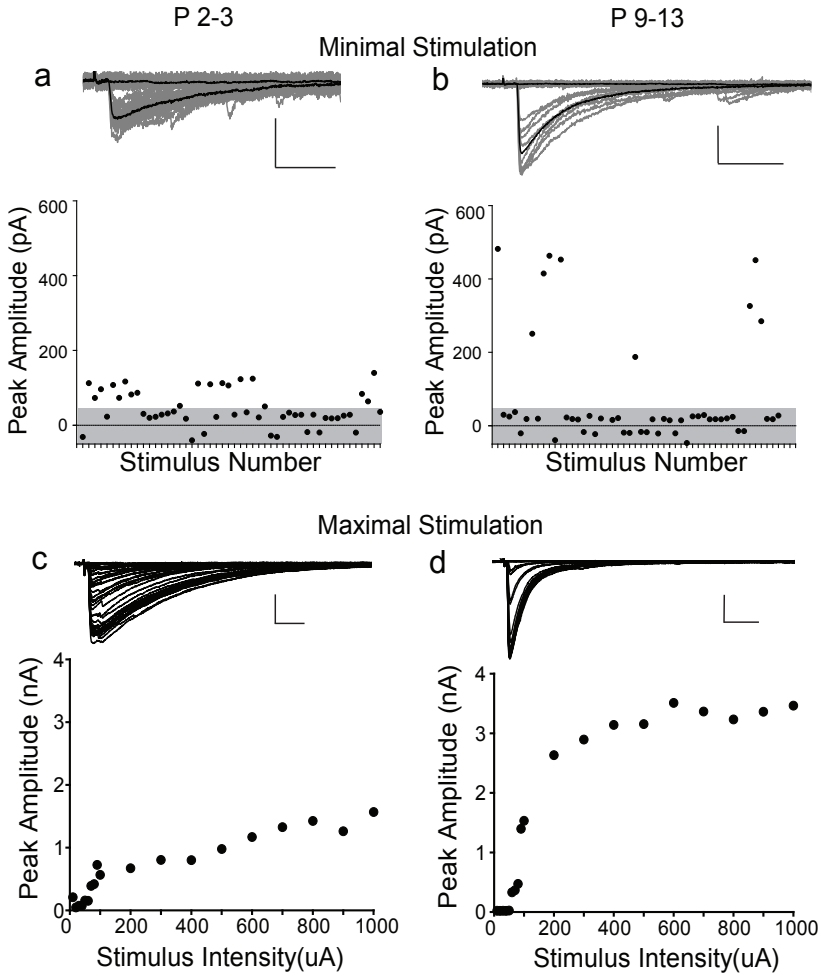

Figure 2.1: **Examples of minimal and maximal stimulation experiments**
(a) Example traces of minimal stimulation responses of postsynaptic medial LSO cells at P 2-3 (Grey: single traces, Black- average traces of 20-40 responses). Scale bars: 200pA, 20ms. Bottom panel shows peak response amplitudes to repeated trials of the minimal stimulation intensity. Grey bar indicates noise level (peak to peak amplitude of baseline trace).
(b) Example traces of minimal stimulation responses of postsynaptic medial LSO cells at P 9-13 (Grey: single traces, Black- average traces of 20-40 responses). Scale bars: 200pA, 20ms. Bottom panel shows peak response amplitudes to repeated trials of the minimal stimulation intensity. Grey bar indicates noise level (peak to peak amplitude of baseline trace).
(c) Example traces of maximal stimulation responses of postsynaptic medial LSO cells at P 2-3. Scale bars: 1nA, 20ms. Bottom panel shows stimulus response plot of the maximal stimulation experiment
(d) Example traces of maximal stimulation responses of postsynaptic medial LSO cells at P 9-13. Scale bars: 1nA, 20ms. Bottom panel shows stimulus response plot of the maximal stimulation experiment

software written in Matlab. Data are presented as mean+/- SEM (except for bootstrap analysis of convergence ratio where mean and standard deviations are plotted). Data were tested for normal distribution and parametric (Students t test, ANOVA with Bonferroni post test) and nonparametric (Mann U Whitney, Kruskal-Wallis with Dunns post test) significance tests to determine statistical differences between groups of data.

For a more accurate estimation of convergence ratio in MNTB-LSO pathway, bootstrap resampling with replacement was performed on the observed dataset of minimal and maximal synaptic input. 10,000 sample data sets were constructed by resampling the minimal and maximal peak amplitudes with replacements from the experimental dataset. 10,000 different maximal and minimal mean peak amplitudes were then calculated from each resampled data set, each of which was then used to calculate 10,000 convergence ratios. The mean of the calculated convergence ratios and the standard deviation were used for statistical analysis.

2.1.5 Immunohistochemistry of brainstem sections:

The immunohistochemistry of brain slices for VGlut-3 expression was done by a former lab member Kristy Cihil. The animals were anesthetized using isofluorane until cessation of reflexes. The animals were then perfused pericardially with chilled 4% PFA for 15 to 20 mins. The fixed brains were then postfixed in 4 % PFA at 4 deg C overnight. The fixed brains were then cryoprotected to 30 % sucrose. After cry-

oprotection, the brains were sectioned using a sliding microtome. The 100um sections were transferred into a 24 well plate and incubated in PBS. The tissue was then permeabilized using 0.2 % TritonX-100. After further washes with PBS, the tissue was incubated in a blocking solution containing 4% bovine serum albumin. Then primary antibodies specific for VGlut3 were added to the tissue and incubated overnight at 4 deg C. The tissue was washed thoroughly and incubated with biotinylated secondary antibodies for 2 hours and then washed thoroughly. Then the tissue was reacted with an avidin-biotin reagent (ABC Elite Kit, Vector Laboratories, Burlingame, CA) in blocker for two hours at room temperature. Sections were then washed in PBS and reacted with 0.05 % diaminobenzidine-tetracholoride (DAB; Sigma, St. Louis, MO) in a solution containing 1 % $CoCl_2$, 1 % $Ni(NH_4)_2SO_4$, and 0.3 % H_2O_2 in PBS. Sections were washed in PBS, mounted on gelatinized glass slides, dehydrated in an ethanol/xylene series, and coverslipped with Permount (Fisher Scientific, Fair Lawn, NJ).

2.1.6 Fluorescence immunostaining of brainstem sections:

The fluorescence immunostaining of the *gad1 -/-* brain slices were done blind to the genotype by Xinyan Gu. The animals were anesthetized using isofluorane until cessation of reflexes. The animals were then perfused pericardially with chilled 4 % PFA for 15 to 20 mins. The fixed brains were then postfixed in 4 % PFA at 4 deg C overnight. The fixed brains were then cryoprotected to 30 % sucrose.

After cryoprotection, the brains were sectioned using a cryostat (Microm HM 550). The 30um sections were transferred on to glass slides and incubated in PBS. The tissue was then permeabilized using 0.2 %TritonX-100. After further washes with PBS, the tissue was incubated in a blocking solution containing 4 % bovine serum albumin. Then primary antibodies specific for VGlut3 were added to the tissue and incubated overnight at 4 deg C. The tissue was washed thoroughly and incubated with fluorescent secondary antibodies for 2 hours and then washed thoroughly. Sections were coverslipped with Fluoro-gel (EMS), an aqueous mounting medium.

2.1.7 Image J analysis of fluorescent images:

Raw grayscale images of fixed duration were taken using the epifluorescence microscope. Region of interests were marked in the medial and lateral parts of the LSO. The absolute grey values (AGV) of the region of interest were calculated using Image J and normalized to the gray values of a region of interest outside LSO. The relative grey values (RGV) of 3 different animals were then used to calculate the mean grey value (MGV) of the region. The mean gray values were compared between wildtype and *gad1-/-* animals.

2.1.8 Adenoviral injections into P1 mice brain:

P1 pups of homozygous floxed $GABA_AR$ mice were anaesthetized using hypothermia and positioned in a stereotax specially designed for small pups. A small incision

was made in the skull between the bregma and lambda to expose the inferior colliculus (IC). 10-50 ul of the GFP tagged Adcre virus (Baylor College of Medicine virus facility) (5 x 1011 pfu/ml) was injected via a glass pipette using a Nanoject (Drummond) at a slow rate. The pipette was kept in place for few minutes after injection to allow for diffusion. The pup was kept cold all throughout the procedure. After the injection, the skin was sutured or glued back. Mercaine was injected into the skin around the suture to serve as an analgesic. The pup was then revived by placing it on a heating platform. After the pup started responding to the toe pinch and started to right itself when turned on its side, it was assumed to be out of anesthesis and returned to the mother for nursing. The cage with the mother and pup was monitored for 30 mins before returning to the housing racks to ensure the mother had started nursing the pup. The cages were again checked in 3 hours time to ensure survival of the pup.

Chapter 3

Independent phases of pre-hearing refinement in the MNTB-LSO circuit

3.1 Introduction:

Evidences of activity dependent reorganizations of immature neural connections have been observed in several model excitatory neural circuits like the neuromuscular junctions (Purves and Lichtman, 1983; Colman et al., 1997), climbing fiber - Purkinje cell circuit (Hashimoto and Kano, 2003; Hashimoto et al., 2009), and the retinal ganglion cell-lateral geniculate nucleus circuit (Shatz, 1990; Katz and Shatz, 1996). From extensive study of these different model excitatory circuits it is clear that developmental refinement typically consists of two phases: firstly, a few of the numerous initial weak inputs strengthen by different physiological processes (like LTP or multivesicular release) in the strengthening phase creating a disparity among the inputs (Purves and Lichtman, 1983; Colman et al., 1997; Hashimoto and Kano, 2003). Then a phase of elimination occurs, either simultaneously or in succession, to ensure that the relatively weaker or asynchronous inputs are outcompeted by the stronger or more synchronous ones (Ichise et al., 2000; Maejima et al., 2001; Miyata et al., 2000; Wong and Oakley, 1996; Mooney et al., 1996). These weaker inputs are then structurally pruned to form circuits that are anatomically and functionally mature (Colman et al., 1997; Hashimoto and Kano, 2005; Shatz, 1990; Katz and Shatz, 1996).

Such organized refinement is also evident in the circuit between the medial nucleus of trapezoid body (MNTB) and the lateral superior olive (LSO). The MNTB forms topographically organized inhibitory connections with the LSO (Spangler et al., 1985;

Guinan et al., 1972b; Kim and Kandler, 2003; Kandler et al., 2009). The LSO neurons integrate excitation from the ipsilateral ear via the glutamatergic inputs from ipsilateral anteroventral cochlear nucleus (AVCN) and inhibition from the contralateral ear (contralateral AVCN) via GABA/glycinergic inputs from the ipsilateral MNTB in a frequency dependent manner (Cant and Casseday, 1986; Boudreau and Tsuchitani, 1968; Caird and Klinke, 1983; Sanes and Rubel, 1988; Friauf and Ostwald, 1988; Guinan et al., 1972a). The medio-lateral tonotopic map of the MNTB-LSO circuit is highly organized, so that the medial part of the circuit responds to high frequency sound stimulus and the lateral part of the circuit responds to low frequency sound stimulus (Friauf, 1992; Kandler and Friauf, 1993; Kil et al., 1995; Tsuchitani, 1977; Sanes et al., 1989; Sanes and Siverls, 1991).

The inputs in the rat MNTB-LSO circuit are functional prenatally and are arranged in a crude tonotopy even at birth (Kandler and Friauf, 1995a, 1993). Then, in the first two postnatal weeks of development (before hearing onset), the medial part of the circuit undergoes a phase of extensive functional silencing during which single LSO neurons lose almost 75 % of their initial MNTB connections and the remaining inputs are strengthened significantly (by almost 12 fold in rats, 8 fold in mice). This functional silencing causes sharpening of the initial crude tonotopy. As a result, the frequency specific input map of the MNTB is reduced by almost 50 % (Kim and Kandler, 2003, 2010; Noh et al., 2010).

This model of postnatal refinement of this inhibitory circuit is based on the de-

tailed information gathered from the extensive study of the medial (high frequency sensitive) part of the MNTB-LSO circuit. However, little is known about the lateral (low frequency sensitive) part of the circuit. Classical reports suggested that the cells in the lateral part of the circuit were mostly monoaural and thus did not receive inhibitory inputs from the ipsilateral MNTB (Boudreau and Tsuchitani, 1968; Batra et al., 1997). But it was established through later anatomical studies that the lateral LSO cells, similar to medial cells, also receive inputs from both ipsilateral cochlear nucleus as well as the ipsilateral MNTB (Glendenning et al., 1985; Smith et al., 1998).

Even though the medial and the lateral parts of this circuit receive inputs from similar nuclei, there are some differences between them. Some post hearing onset anatomical studies of the refinement of this circuit suggest that synaptic pruning of the MNTB inputs in the lateral part of the circuit does not occur as extensively as in the medial part. The narrowing of the dendritic tree of the LSO cells, which compliments the synaptic pruning of the MNTB inputs, is also less in the lateral part compared to the medial part (Sanes and Siverls, 1991; Sanes et al., 1990). Some electrophysiology studies have noted that the GABA to glycine switch in the LSO may follow a gradient along the tonotopic axis (Kotak et al., 1998; Löhrke et al., 2005). Other studies have also shown that the expression levels of many proteins such as calbindin (Henkel and Brunso-Bechtold, 1998), endocannabinoid (CB1) receptors (Chi and Kandler, 2012), glycine receptors (Sanes and Wooten, 1987), gephyrin

(Kotak et al., 1998), K_v1 channels (Barnes-Davies et al., 2004) also show a gradient along the tonotopic axis.

Functional studies of the LSO have reported that while the medial LSO cells rely only on interaural level difference (ILD), the lateral LSO cells are capable of responding to ILD as well as interaural time difference (ITD) for low frequency stimulus (Spitzer and Semple, 1995; Joris and Yin, 1995; Tollin and Yin, 2005), since the low frequency afferents from both the cochlear nucleus and the MNTB preserve the temporal fine structure of the incoming sound (Joris et al., 1994; Smith et al., 1998). Furthermore, lateral LSO cells can also phase lock to low frequency ipsilateral stimulation (Tollin and Yin, 2005). In view of these anatomical, physiological and functional differences between the medial and lateral LSO cells, it is important to investigate whether the process of pre-hearing refinement also differs along the tonotopic axis in the MNTB-LSO circuit.

In this chapter, I investigated the course of refinement of the MNTB inputs to both the medial and lateral parts of the LSO, between the ages of E 18 to P 13 (Fig. 3.1). I observed two distinct phases in the refinement of proliferated inputs in the MNTB-LSO circuit: an elimination phase (between P 2-3 and P 5-6), followed by a strengthening phase (between P 5-6 and P 9-13) of the retained MNTB inputs. I also observed that the extensive elimination of inputs that occurs for the medial circuit between P 2-3 and P 5-6 is absent in the lateral part of the circuit. After the phase of elimination, all inputs (both medial and lateral) strengthen about 3-4 fold

between P 5-6 and P 9-13. Since the medial MNTB-LSO connections show elimination preceding strengthening of inputs and the lateral connections show strengthening even in the absence of elimination, I believe that the two processes of elimination and strengthening are independent of one another.

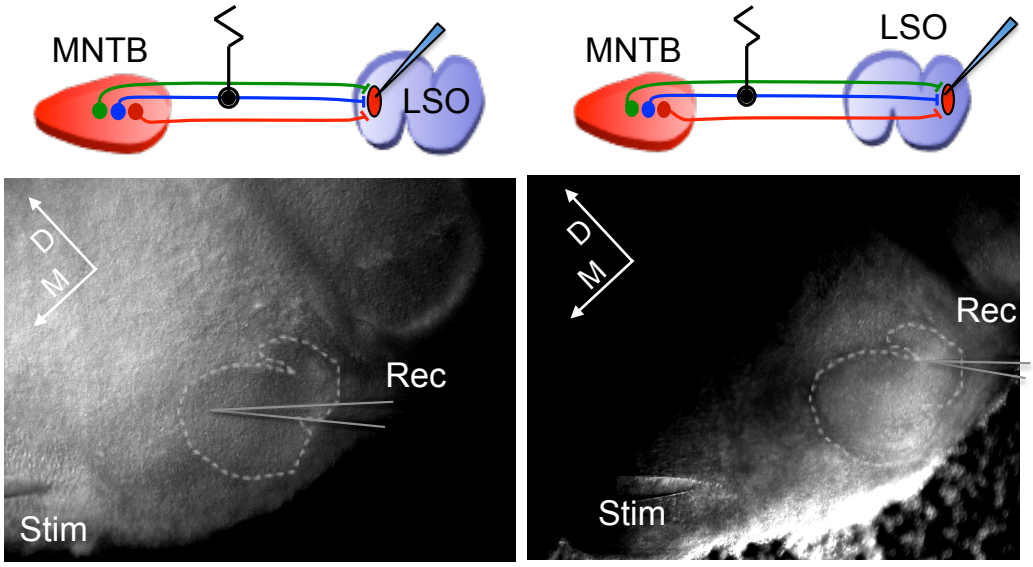

Figure 3.1: **Electrophysiological recording setup for medial and lateral LSO cells**
(Left) DIC image of recording setup of medial LSO cells in a P9 slice containing the MNTB and LSO. The position of the stimulation and recording electrodes are marked.
(Right) DIC image of recording setup of lateral LSO cells in a P9 slice containing the MNTB and LSO. The position of the stimulation and recording electrodes are marked.

3.2 Results:

3.2.1 In the embryonic stages, medial LSO cells receive only one or two active immature MNTB inputs:

Extensive reorganization of synaptic inputs occurs in the medial part of the MNTB - LSO circuit in postnatal rodents even before hearing onset. The convergence of MNTB inputs on to LSO cells at P 2-3 is very high (20 active inputs) but it becomes low (7-8 active inputs) at P 9-13 due to extensive functional elimination causing refinement of the circuit and increase in the precision of connectivity (Kim and Kandler, 2003; Noh et al., 2010). However, very little is known about whether refinement also happens in the embryonic stages. Previous studies have shown that the MNTB-LSO synapses are functional at E18 (rats) (Kandler and Friauf, 1995b). To investigate whether refinement of the MNTB inputs occurs in the embryonic stages, I recorded the synaptic currents elicited by minimal and maximal stimulation of the MNTB fiber bundle which corresponded to the amplitudes of responses due to a single input and the total number of inputs converging on to a single LSO cell respectively. The ratio of the maximal response to the minimal response was the convergence ratio, which estimated the number of active inputs on a given LSO cell at this age (Kim and Kandler, 2003; Noh et al., 2010).

At E 18, I found responsive cells in both medial and lateral part of the LSO in an acute brainstem slice (Fig. 3.2 a). While 57 % of medial cells responded to the electrical stimulation of the MNTB fiber bundle (Fig. 3.2 d), this response rate was

much lower compared to the response rate at the early postnatal age P 2-3 (>90 %). The absence of response from 43 % of the medial LSO cells indicated a possibility that all MNTB axons might not have reached the LSO yet. I injected the tracer fluorescein dextran into the MNTB in the E 18 slices and observed tracer filled axons traveling into the medial as well as the lateral part of the LSO (Fig 3.2 b, c). These observations indicate that, at E 18, even though MNTB fibers are present in the entire LSO, a large number of the inputs were still inactive. However the presence of LSO cells that responded to MNTB stimulation testifies that the MNTB-LSO synapses in mice are functional at E 18.

I estimated the strength of single MNTB inputs to the LSO from the response of postsynaptic LSO cells to minimal stimulation of the MNTB fibers. The mean peak amplitude for a single synaptic input for the responsive medial cells at E 18 was similar to that at P 1 (Fig. 3.2 e, f and h, Fig 3.3 a, c, Table1; row: Medial; p value >0.05, Students t-test). Thus the synaptic inputs at E18 are examples of immature inputs that later strengthen over the pre-hearing period of development.

However, the corresponding maximal synaptic response at E 18 was significantly smaller compared to the responses found at P 1 (Fig 3.2 e, g and i, Table 2, row: medial; p value = 0.001, Mann-Whitney test). The estimation of the number of inputs by convergence ratio calculations showed that only 2 (CR = 1.96 ± 0.47; Bootstrap analysis) medial MNTB-LSO connections were active at E 18.

These data together indicate that in agreement with previous studies in rats (Kan-

dler and Friauf, 1995b), MNTB-LSO connections were also functional for medial LSO cells in mice at E 18. These connections were weak, suggesting that the inputs were immature. These data also indicate that at E 18, the number of active inputs in the medial part of the circuit was lower than that at P 1. Thus synaptic elimination did not occur between E 18 and P 1.

3.2.2 Strengthening of single inputs, in the medial MNTB-LSO circuit, occurs after P 5-6.

To ascertain the precise pattern of strengthening of the medial MNTB-LSO circuit, I investigated the minimal synaptic amplitudes at various time points (E 18, P 1, P 2-3, P 5-6, and P 9-13) during the pre-hearing development.

Table 3.1: **Summary of minimal stimulation response amplitude at different ages.** The p values represent comparisons between medial and lateral LSO cells.

Position	E 18	P 1	P 2-3	P 5-6	P 9-13
Medial	49.64 ± 7.36 pA (n=8 of 14)	68.15 ± 6.38 pA (n=17)	135.5 ± 54.63 pA (n=12)	85.63 ± 8.52 pA (n=12)	423.2 ± 114.8 pA (n=17)
Lateral	42.05 ± 0.27 pA (n=4 of 17)	73.66 ± 13.89 pA (n=10)	90.80 ± 13.72 pA (n=23)	108.3 ± 20.07 pA (n=10)	301.1 ± 88.65 pA (n=17)
P Values	1.0 (Mann-Whitney test)	0.7 (Mann-Whitney test)	0.68 (Mann-Whitney test)	0.57 (Mann-Whitney test)	0.31 (Mann-Whitney test)

For the medial LSO cells, the single input strength increased significantly from E 18 to P 2-3 as indicated in Table 3.1 (row: Medial) and Fig. 3.3 c (p value = 0.02; Mann-Whitney test). The increments in strength of inputs between E 18 and P 5-6

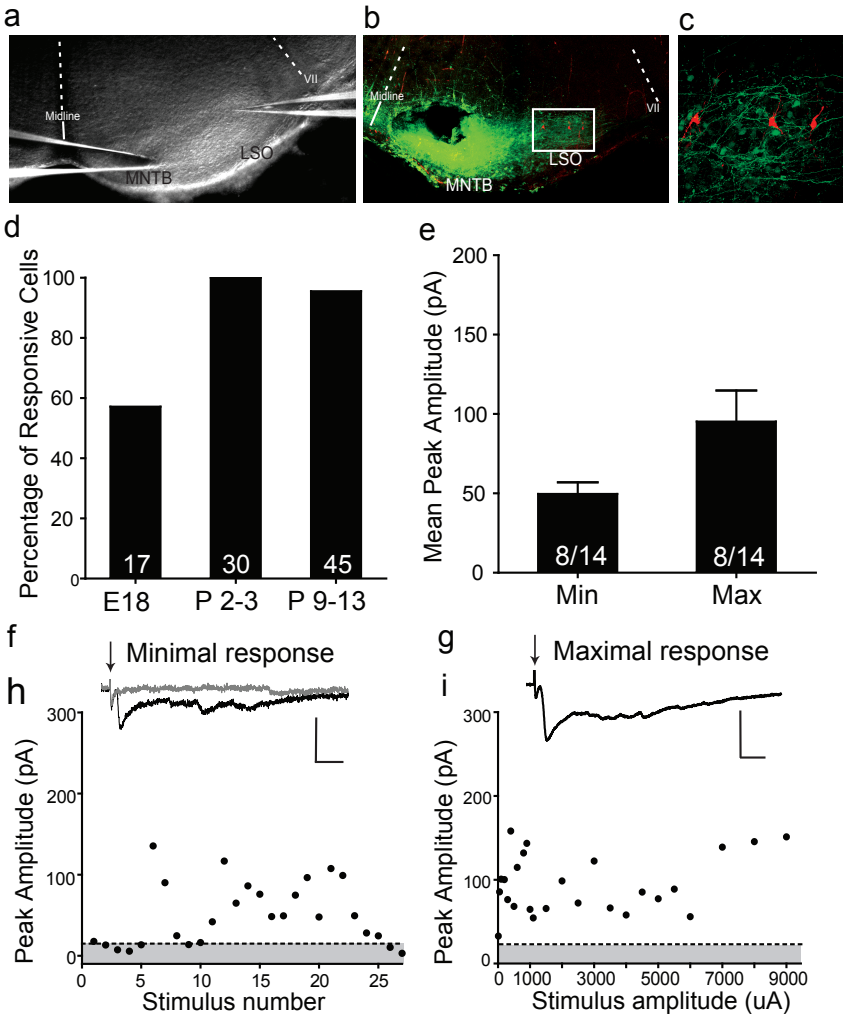

Figure 3.2: **Weak MNTB inputs to LSO neurons are present at embryonic day 18**
(a) DIC image of recording setup of E18 slice containing the MNTB and LSO. The position of the midline and VIIth nerve are marked.
(b) Confocal image of the same E18 slice after Fluorescein-dextran injection in the MNTB and fixation of slice.
(c) Magnified image (60X) of highlighted area in (b) showing three recorded neurons filled with Alexa-568.
(d) Population data showing percentage of recorded neurons in medial LSO showing synaptic responses to minimal or maximal MNTB stimulation at different ages.
(e) Mean response amplitudes of medial LSO neurons at E18 to minimal (49.64 $\pm$ 7.356 pA (n=8 of 14)) and maximal stimulation (97.74 $\pm$ 27.18 pA (n=8 of 14)).
(f-g) Average traces of E18 medial LSO cells; minimal stimulation (d); maximal stimulation (e). Scale bars represent 100pA and 20ms.
(h) Stimulus response curve showing the variation in synaptic amplitude of a medial LSO cell in response to minimal stimulus. The grey bar represents the noise level.
(i) Stimulus-response plot showing the increase in amplitude of the synaptic response of the medial LSO cell with increasing stimulus amplitude.

occurred in small steps that were not statistically significant between each consecutive age points (p value at different ages: E 18 vs P 1 = 0.05; P 1 vs P 2-3 = 0.09, P 2-3 vs P 5-6 = 0.79). After P 5-6, the single input strength showed a significantly large increase where each input was strengthened by 4 fold to 423.2 ± 114.8 pA (n=17) (P 5-6 vs P 9-13, p = 0.014; Mann-Whitney test) (E 18 to P 13: p = 0.014, Kruskal-Wallis test) (Fig. 3.3 b).

Thus the increase in strength of single MNTB inputs to medial LSO cells in pre-hearing stages occurs in two phases. The strength of single inputs increases significantly from E 18 to P 2-3. Then a second phase of significant increase in the strength of the single inputs occurs between P 5-6 and P 9-13.

3.2.3 Functional elimination of synaptic inputs precedes the strengthening of the inputs in the medial MNTB-LSO circuit.

The functional refinement in the medial part of the circuit during the pre-hearing period was quantitatively assessed from the maximal stimulation response amplitudes and the bootstrapped convergence ratios at the ages E 18, P 1, P 2-3, P 5-6, and P 9-13.

Examination of the maximal evoked synaptic responses of the medial LSO cells revealed that the cumulative medial MNTB input significantly increased from E 18 to P 1 to P 2-3 (Fig. 3.4 c; Table 3.2, row: Medial). The p values for comparison between different ages were: E 18 vs P 1 = 0.0015 (Mann-Whitney test); P 1 vs P

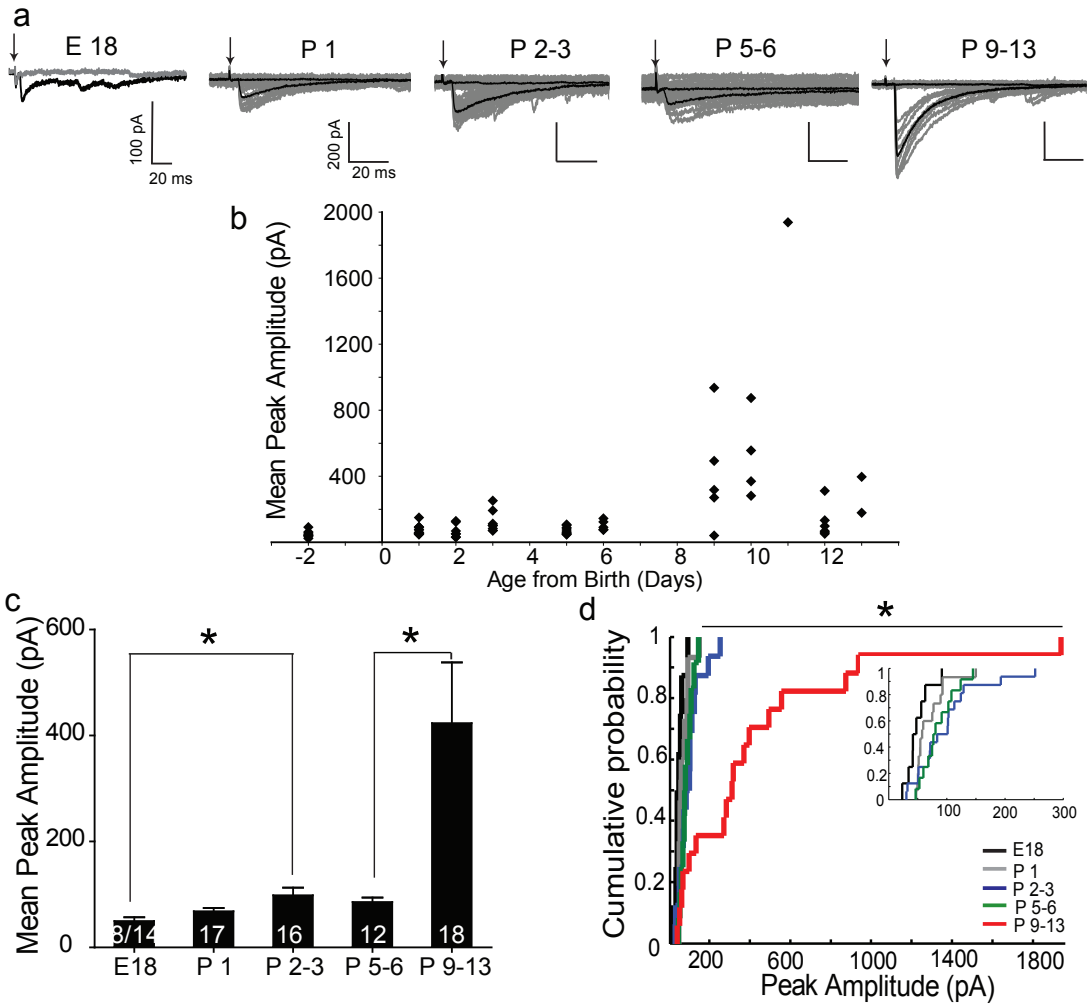

Figure 3.3: **Developmental increase in synaptic amplitudes of medial LSO neurons in response to minimal stimulation**

(a) Example traces of minimal stimulation responses of postsynaptic medial LSO cells at different ages (Grey: single traces, Black- average traces of 20-40 responses). Scale bars: 100pA, 20ms (E18); 200pA, 20ms for P1 to P13.

(b) Plot of mean peak amplitudes at each postnatal day.

(c) Population data of the mean peak amplitudes of synaptic responses of medial LSO cells to minimal stimulation at developmental time points of E 18 (49.64 $\pm$ 7.36 pA n=8), P 1 (68.15 $\pm$ 6.38 pA n=17), P 2-3 (98.28 $\pm$ 14.48 pA n=16), P 5-6 (85.63 $\pm$ 8.52 pA n=12), P 9-13 (423.2 $\pm$ 114.8 pA n=17) (p value = 0.0001; Kruskal-Wallis test). Error bars represent SEM.

(d) Cumulative probability histograms for single fiber responses at different age points. (E 18 vs P1: p value = 0.05; P 1 vs P 2-3: p value= 0.08, P 2-3 vs P 5-6: p value= 0.98, P 5-6 vs P 9-13: p value= 0.002; P 2-3 vs P 9-13: p value= 0.0009, P 1 vs P 9-13: p value=0.0003 Kolmogorov-Smirnov test). Inset shows E 18 to P 5-6 age groups in more detail.

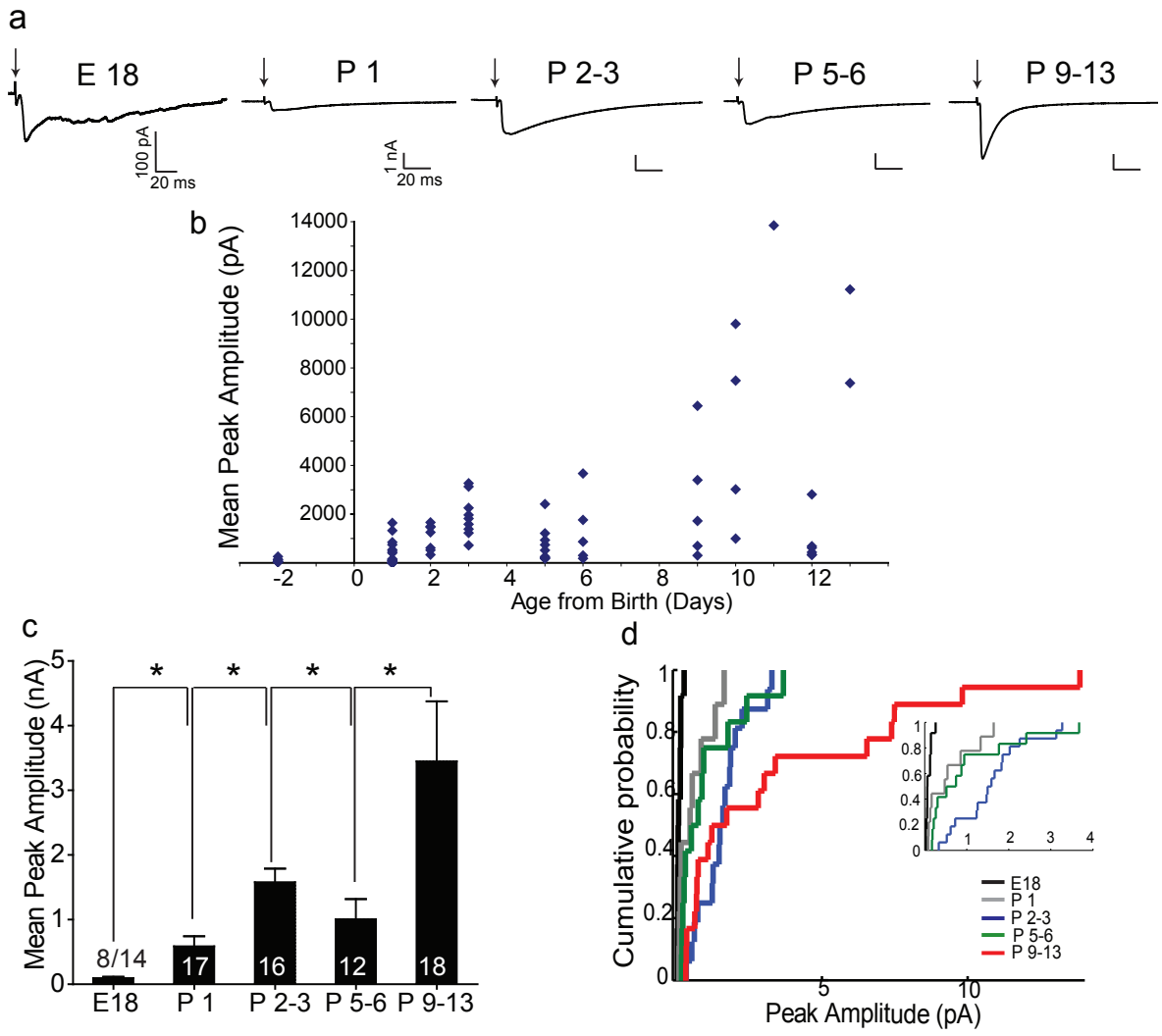

Figure 3.4: **Development of synaptic amplitudes of medial LSO cells in response to maximal stimulation**

(a) Example traces of maximal stimulation responses of postsynaptic medial LSO cells at different ages (Grey: single traces, black: average of 10 traces). Scale bars: 100pA, 20ms for E 18; 1nA, 20ms for P 1 to P 13.

(b) Plot of mean peak amplitudes at each postnatal day.

(c) Population data of the maximal synaptic responses of medial LSO cells at developmental time points of E 18 (0.10 ± 0.02 nA n=12), P 1 (0.59 ± 0.16 nA n=11), P 2-3 (1.58 ± 0.21 nA n=16), P 5-6 (1.01 ± 0.31 nA n=12), P 9-13 (3.45 ± 0.93 nA n=18) (p value ¡ 0.0001; Kruskal-Wallis test). Error bars represent SEM.

(d) Cumulative probability histograms for maximal synaptic responses at different age points. (E 18 vs P 1: p value = 0.04; P 1 vs P 2-3: p value= 0.04; P 2-3 vs P 5-6: p value= 0.04; P 5-6 vs P 9-13: p value= 0.12; P 2-3 vs P 9-13: p value= 0.32; Kolmogorov-Smirnov test). Inset shows E 18 to P 5-6 age groups in more detail.

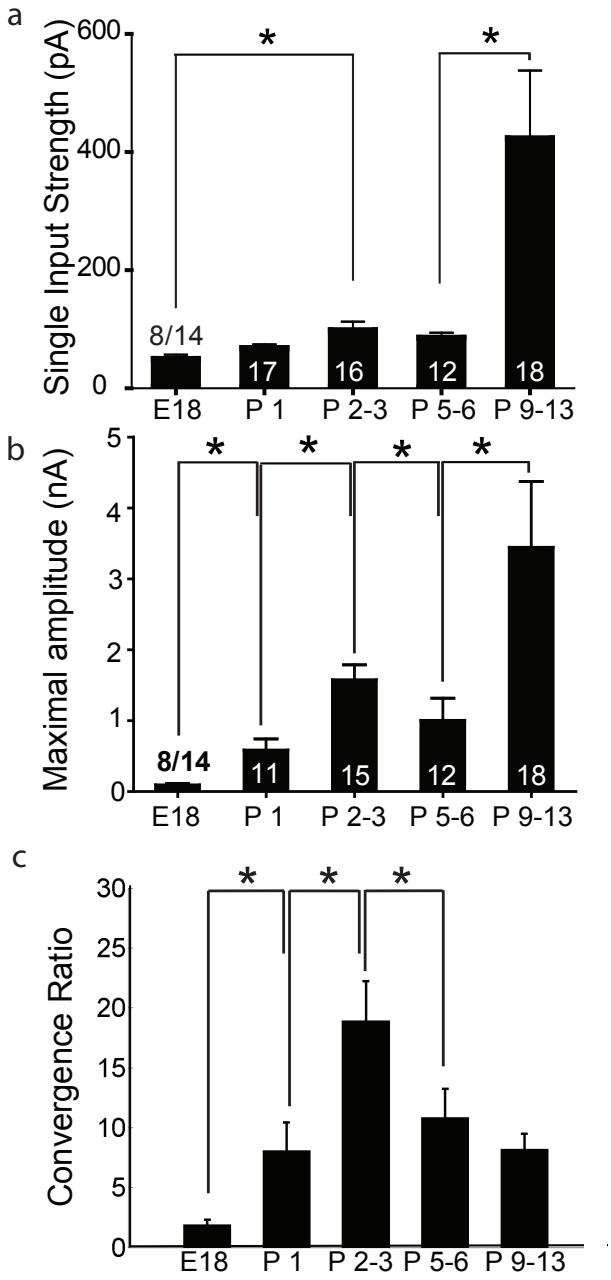

Figure 3.5: **Functional elimination of synaptic inputs precedes strengthening of single inputs in medial part of LSO**
(a) Population data of minimal stimulation responses (strength of single MNTB inputs) of medial LSO cells from E 18 to P 9-13. Error bars represent SEM.
(b) Population data of maximal stimulation responses of medial LSO cells from E 18 to P 9-13. Error bars represent SEM.
(c) Population data of convergence ratio of medial LSO cells from E 18 to P 9-13 estimated by bootstrap analysis (E 18 vs P 1: p value = 0.002; P 1 vs P 2-3: p value = 0.002; P 2-3 vs P 5-6: p value = 0.001; P 5-6 vs P 9-13: p value = 0.16; Permutation test). Error bars represent standard deviations.

Table 3.2: **Summary of the maximal stimulation response amplitude at different ages.** The p values represent comparisons between medial and lateral LSO cells.

Position	E 18	P 1	P 2-3	P 5-6	P 9-13
Medial	0.10 ± 0.03 nA (n=8 of 14)	0.59 ± 0.16 nA (n=11)	1.58 ± 0.21 nA (n=16)	1.01 ± 0.31 nA, (n=12)	3.45 ± 0.93 nA (n=18)
Lateral	0.06 ± 0.01 nA (n=4 of 17)	0.32 ± 0.09 nA (n=10)	0.89 ± 0.17 nA (n=23)	0.67 ± 0.20 nA (n=10)	2.03 ± 0.58 nA (n=18)
P Values	0.3 (Mann-Whitney test)	0.16 (Students t test)	**0.01** (Students t test)	0.48 (Mann-Whitney test)	0.24 (Mann-Whitney test)

Table 3.3: **Summary of the convergence ratios at different ages.** The p values represent comparisons between medial and lateral LSO cells.

Position	E 18	P 1	P 2-3	P 5-6	P 9-13
Medial	2:1	9:1	19:1	11:1	9:1
Lateral	1:1	5:1	10:1	6:1	7:1
P Values		**0.002** (Permutation test)	**0.001** (Permutation test)	0.18 (Permutation test)	0.06 (Permutation test)

2-3 = 0.002 (Students t-test). After P 2-3, however, a significant decrease was noted in the maximal input at P 5-6 (p value = 0.048; Mann-Whitney test) (Fig. 3.4). The maximal amplitude then increased between P 5-6 and P 9-13 (p value = 0.03; Mann-Whitney test).

Similarly, the convergence ratios, estimated from the minimal and maximal stimulation data at the different ages showed that the convergence ratio increased from E 18 to P 1 to P 2-3 as shown in the table (Table 3.3, row: Medial; Fig. 3.5) (p values: E 18 vs P 1 = 0.001; P 1 vs P 2-3 = 0.002; Permutation test). Then the ratio decreased significantly between P 2-3 and P 5-6 (p value: P 2-3 vs P 5-6 = 0.001; Permutation test). After P 5-6, the convergence ratio stayed constant until at least P 13 (p value: P 5-6 vs P 9-13 = 0.16).

These data together suggest that weak synaptic inputs are gradually added from E 18 until the circuit reaches its peak convergence at P 2-3. Then between P 2-3 and P 5-6 most of the synaptic inputs are functionally eliminated or silenced so that only a few are active at P 5-6 and onwards. These data are in agreement with the focal uncaging study (Kim and Kandler, 2003), where the input map area of the MNTB in rats shows a sharp decrease (almost 50 %) by P 8, a week before hearing onset in rats. Similarly I found that the functional elimination of medial MNTB inputs in mice is also complete a week before hearing onset (by P 5-6). This study further shows that single MNTB inputs then strengthen significantly after P 5-6 (Fig 3.3). These results together suggest that in the developing MNTB LSO circuit, elimination of inputs precedes their strengthening.

3.2.4 Lateral MNTB-LSO inputs also strengthen between E 18 and P 9-13.

The minimal stimulation responses of lateral LSO cells were recorded at the ages E

18, P 1, P 2-3, P 5-6, and P 9-13. At E 18, only 4 cells out of 17 cells recorded showed any response to MNTB stimulation. Due to the small number of data points at E 18, a statistical test to compare the minimal synaptic response amplitudes between age groups could not be performed on this dataset. Thus I examined the increase in strength of fibers between P 1 to P 9-13. The single input strength gradually increased from P 1 to P 9-13 (p value= 0.04, Mann-Whitney test) but the increments between consecutive age groups were not statistically significant (p values at different ages: P 1 vs P 2-3 = 0.73; P 2-3 vs P 5-6 = 0.24, P 5-6 vs P 9-13 = 0.20, Mann-Whitney test) (Fig 3.6). The single input strength in the lateral LSO at P 9-13 was 3 fold of that at P 1 and matched the strength of medial inputs of age P 9-13 (Table 1, p value = 0.31; Mann-Whitney test).

The above data shows that like the medial inputs, the lateral inputs also strengthen significantly between E18 and P 9-13 (Fig. 3.6). The strengths of single inputs to the lateral LSO become equivalent to the medial inputs by P 9-13 (Fig 3.8 a). However, while the medial cells follow a two-step mode of strengthening, the lateral inputs show a more gradual increase in strength in the pre-hearing stages of development.

3.2.5 Lateral MNTB-LSO connections do not show functional refinement in the pre-hearing stages of development.

The maximal evoked synaptic amplitude for the lateral LSO cells showed a gradual but significant increase between E 18 and P 9-13 (Table 3.2, row: Lateral; Fig. 3.7). Due to the low number of datapoints, we did not include the E 18 dataset in the

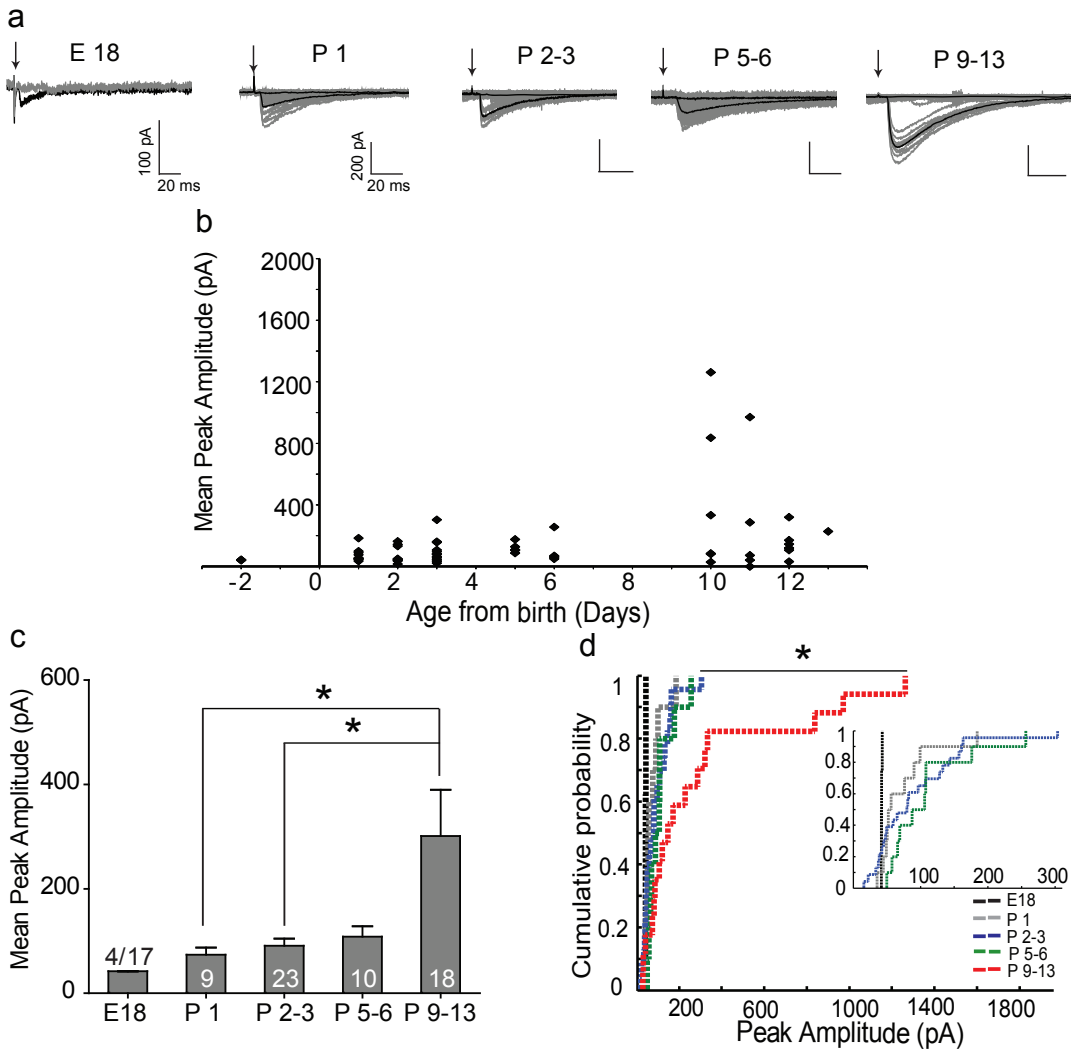

Figure 3.6: **Developmental increase in synaptic amplitudes of lateral LSO neurons in response to minimal stimulation**

(a) Example traces of minimal stimulation responses of postsynaptic lateral LSO cells at different ages (grey: single traces, black: average of 20-40 traces). Scale bars: 100pA, 20ms (E18); 200pA, 20ms (P1- P13).

(b) Plot of mean peak amplitudes at each postnatal day.

(c) Population data of the mean peak amplitudes of synaptic responses of lateral LSO cells to minimal stimulation at developmental time points of E 18 (42.05 $\pm$ 0.27 pA n=4), P 1 (73.66 $\pm$ 13.89 pA n=10), P 2-3 (90.80 $\pm$ 13.72 pA n=23), P 5-6 (108.3 $\pm$ 20.07 pA n=10), P 9-13 (301.1 $\pm$ 88.65 pA n=18) (p value= 0.01; Kruskal-Wallis test). Error bars represent SEM.

(d) Cumulative probability histograms for single fiber responses at different age points. (P1 vs P 2-3: p value= 0.72, P 2-3 vs P 5-6: p value=0.18, P 5-6 vs P 9-13: p value= 0.23; P 2-3 vs P 9-13: pvalue= 0.04; Kolmogorov-Smirnov test). Inset shows E 18 to P 5-6 age groups in more detail.

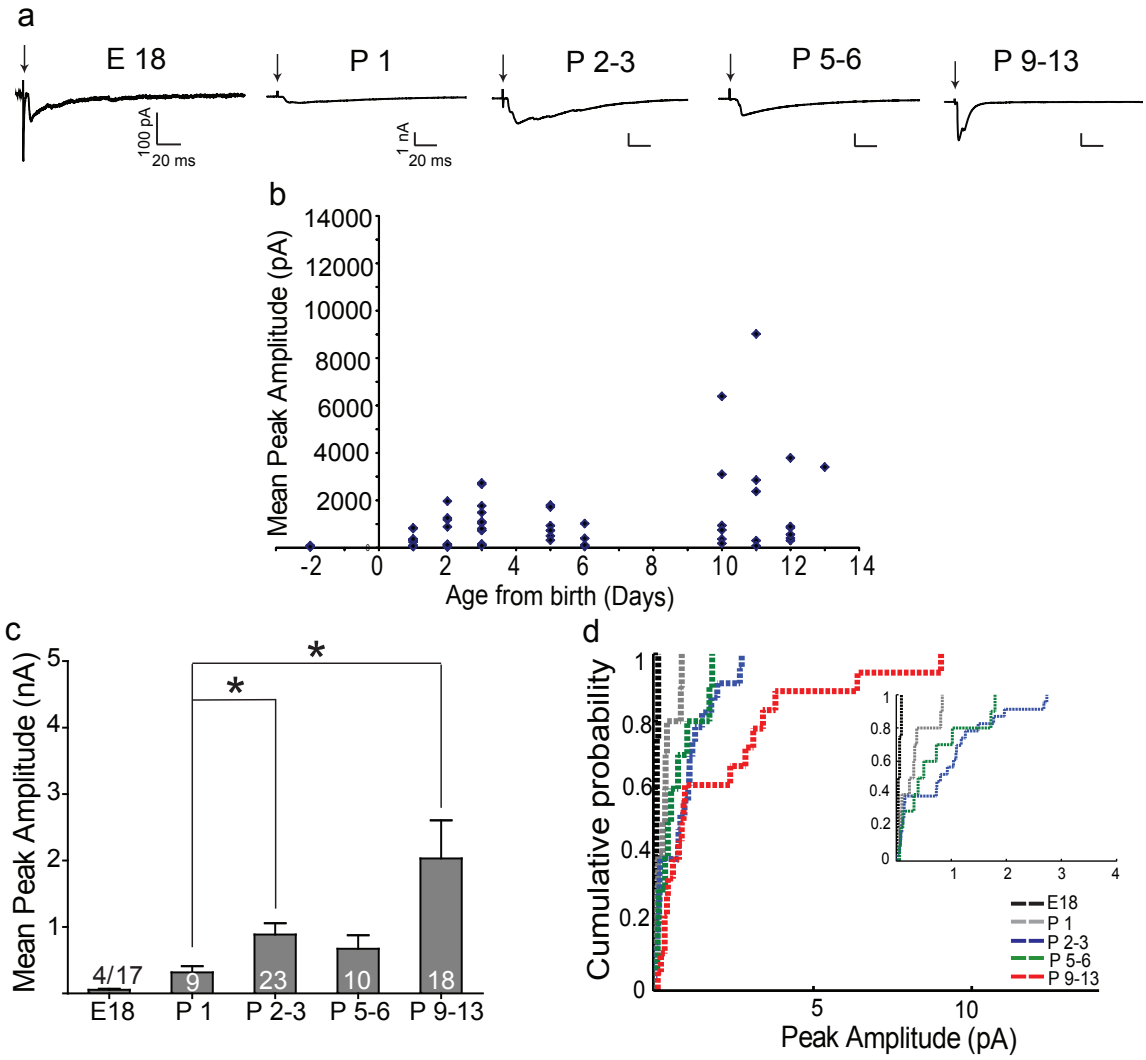

Figure 3.7: **Development of synaptic amplitudes of lateral LSO cells in response to maximal stimulation**

(a) Example traces of maximal synaptic responses of postsynaptic lateral LSO cells at different developmental time points (grey: single traces, black average of 10 traces). Scale bars: 100pA, 20ms for E18; 1nA, 20ms for P1 to P13.

(b) Plot of mean peak amplitudes at each postnatal day.

(c) Population data of the maximal synaptic responses of lateral LSO cells at developmental time points of E 18 (0.06 ± 0.01 nA n=4), P 1 (0.32 ± 0.09 nA n=10), P 2-3 (0.89 ± 0.17 nA n=23), P 5-6 (0.67 ± 0.20 nA n=10), P 9-13 (2.03 ± 0.58 nA n=18) (p value = 0.002; Kruskal-Wallis test). Error bars represent SEM.

(d) Cumulative probability histograms for maximal synaptic responses at different age points. (P 1 vs P 2-3: p value=0.06; P 2-3 vs P 5-6: p value= 0.44; P 5-6 vs P 9-13: p value= 0.22; P 2-3 vs P 9-13: p value= 0.16; Kolmogorov-Smirnov test). Inset shows E 18 to P 5-6 age groups in more detail.

statistical comparison of maximal amplitudes with the other age groups. The maximal amplitude of lateral cells increased significantly between P 1 and P 2-3 (p value = 0.04; Students t test). From P 2-3 to P 9-13 the maximal amplitude for the lateral cells stayed consistent (Table 3.2, row: Lateral; Fig. 3.7) (p value: P 2-3 vs P 5-6= 0.47, Students t test; P 5-6 vs P 9-13= 0.10, Mann-Whitney test).

The convergence ratios of the lateral LSO cells stayed constant between ages P 1 to P 9-13 as shown in Table 3.3 (row: Lateral) (p value= 0.27; Kruskal-Wallis test). The above data together suggest that the lateral MNTB-LSO circuit lacks functional elimination between the ages E 18 and P 9-13. The convergence of MNTB inputs on to the lateral cells stays constant from P 1 until hearing onset.

3.2.6 Functional elimination and strengthening of MNTB inputs are independent processes.

A comparison of the minimal stimulation amplitudes of medial and lateral parts of the MNTB LSO circuit shows that both medial and lateral single inputs strengthen almost 3-4 fold between E 18 and P 9-13. As a result, at P 9-13, both medial and lateral inputs are of equivalent strength (Table 3.1, p value = 0.31; Mann-Whitney test; Fig 3.8a). Thus strengthening occurs throughout the entire LSO to a similar degree. The significantly large phase of strengthening occurs between P 5-6 and P 9-13 for the medial MNTB-LSO connections.

Comparing the maximal stimulation responses between the medial and lateral LSO cells we found that at P 1 the amplitudes were not significantly different (Table

3.2, p value=0.16, Students t test). However, at P 2-3, the maximal response in the lateral cells was 60% lower than that in the medial cells. This may result from dendritic filtering of synaptic currents from a distal arrangement of synapses. Such arrangement of synapses would also lead to longer rise times corresponding to smaller synaptic amplitudes. The mean rise times for synaptic responses of the medial (1.2 ± 0.14 ms n=10) and lateral cells (1.3 ± 0.15 ms n=15) were not significantly different from each other (p value = 0.38, Mann-Whitney test; Fig 3.8). There was also no correlation between the rise times and the minimal synaptic amplitudes for medial as well as lateral cells at P 2-3 (medial: R^2= 0.11; p value = 0.27; lateral: R^2=0.002; p value = 0.88, Fig 3.8 c, d) showing absence of dendritic filtering. The mean input resistance (at P 2-3: Medial cells: 789.1 ± 117.0 MOhm, n=10; Lateral cells: 640.7 ± 94.09 MOhm, n=19; p value = 0.14, Mann Whitney test) was also similar for both medial and lateral cells (Fig 3.9 a). Thus the lower maximal response of lateral cells could only be explained by the presence of fewer numbers of weak inputs. The maximal amplitudes were not significantly different between the medial and lateral cells at the other ages.

From a comparison of the convergence ratios of medial and lateral cells, we observed two main differences. First, the convergence ratios for the lateral cells were significantly smaller than that of the medial cells at ages P 1 and P 2-3 (Table 3.3, row: p value, Fig 3.8c) suggesting that fewer active inputs contacted lateral LSO cells, compared to the medial cells at these ages. Secondly, in contrast to the signif-

icant decrease in the convergence ratio of medial cells between P 2-3 and P 5-6, the convergence ratio for the lateral cells did not change significantly between P 2-3, P 5-6, and P 9-13 (Table 3.3, Fig. 3.8c). This suggested a distinct lack of functional elimination of the lateral MNTB-LSO connections between the ages P 2-3 and P 9-13. Thus the lateral part of the MNTB-LSO circuit did not show the peak in convergence at P 2-3 and the later significant functional elimination of inputs before P 5-6 that is characteristic of the medial LSO cells (Fig 3.8 c).

From the above data it is clear that, while the MNTB-LSO connections show functional elimination followed by strengthening of inputs between E 18 and P 13, the lateral inputs show strengthening of inputs even in the absence of any significant functional elimination between these ages (Fig 3.8 a, c). Thus the functional elimination of inputs does not seem to be a pre-requisite for the strengthening of the remaining inputs. This suggests that the processes of strengthening and functional elimination are independent of one another.

3.2.7 Proportion of LSO cells expressing I_H current changes with age.

Morphologically seven different types of neurons have been described in the rat LSO (Rietzel and Friauf, 1998) but functionally the LSO cells can be classified into LSO principal neurons and lateral olivocochlear (LOC) neurons. The LSO principal neurons can be further classified into single firing and multiple firing neurons (Barnes-Davies et al., 2004). In rats, the single spiking and the multiple spiking principal neu-

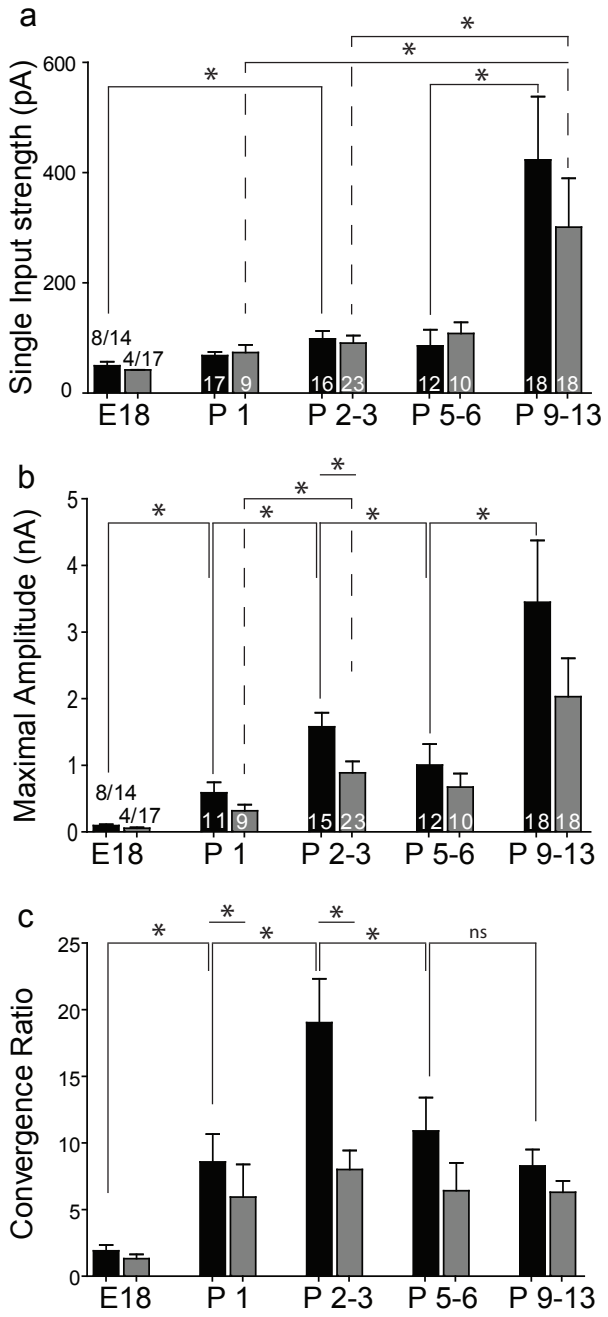

Figure 3.8: **Strengthening of single inputs to lateral LSO occurs even in the absence of functional elimination of inputs**
(a) Population data of minimal stimulation responses (strength of single MNTB inputs) of medial (black bars) and lateral (grey bars) LSO cells at different ages (E 18 to P 9-13). Error bars represent SEM.
(b) Population data of maximal stimulation responses (strength of all MNTB inputs) of medial (black bars) and lateral (grey bars) LSO cells at different ages (E 18 to P 9-13). Error bars represent SEM.
(c) Population data of convergence ratio of medial (black bars) and lateral (grey bars) LSO cells at different ages (E 18 to P 9-13) estimated by bootstrap analysis (E 18 vs P 1: p = 0.001; P 1 vs P 2-3: p = 0.10; P 2-3 vs P 5-6: p = 0.18; P 5-6 vs P 9-13: p = 0.92; Permutation test). Error bars are standard deviations.

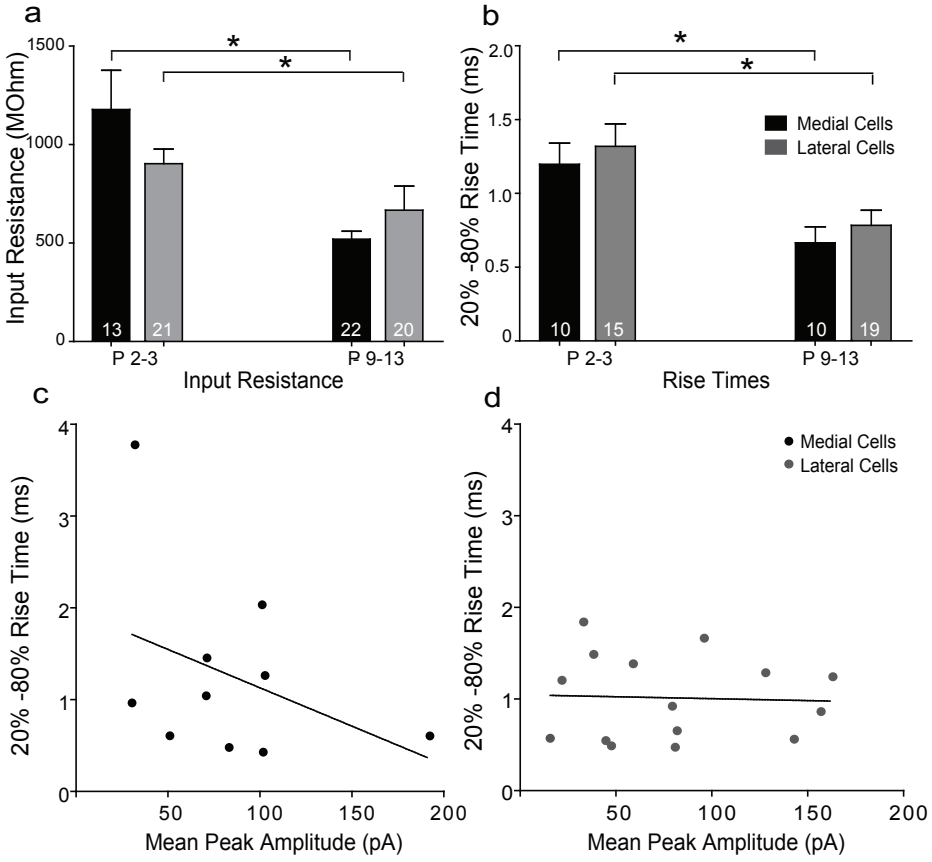

Figure 3.9: **Intrinsic and synaptic properties of the medial and lateral LSO cells are similar over the first two postnatal weeks**
(a) Population data of input resistance of medial (black bar) and lateral (grey bar) LSO cells at P 2-3 (medial: 1178 ± 198.7 MOhm n=13; lateral: 902.8 ± 74.47 MOhm n = 21; p value= 0.14, Mann-Whitney test) and P 9-13 (medial: 519.6 ± 40.23 MOhm n = 22; lateral: 667.0 ± 122.4 MOhm n = 20; p value=0.79, Mann-Whitney test) developmental time points.
(b) Population data for the rise times of the maximal synaptic responses of medial (black) and lateral (grey) LSO cells at P 2-3 (medial: 1.20 ± 0.14 ms n = 10; lateral: 1.32 ± 0.15 ms n = 15; p value = 0.39, Mann-Whitney test) and P 9-13 (medial: 0.67 ± 0.11 ms n = 10; lateral: 0.79 ± 0.10 ms n = 19; p value= 0.3, Mann-Whitney test).
(c) Plot of minimal stimulation amplitude against 20-80% rise time for medial cells at P 2-3. Black line= Linear regression fit, R^2= 0.11, p value = 0.27.
(d) Plot of minimal stimulation amplitude against 20-80% rise time for lateral cells at P 2-3. Black line= Linear regression fit, R^2= 0.001, p value = 0.88.

rons are distributed in a gradient along the tonotopic axis of LSO (Barnes-Davies et al., 2004). However no such organization is evident for LSO principal neurons and LOC neurons. In mice, they seem to be distributed evenly throughout the LSO (Sterenborg et al., 2010). The presence or absence of I_H or hyperpolarization activated cation current has been used in some studies to differentiate between LSO principal neurons and LOC neurons. I_H is a mixed inward Na^+-K^+ current activated at hyperpolarized potentials and influences the resting membrane potential and the excitability of the cell (Pape, 1996; Chen, 1997; Shaikh and Finlayson, 2003). According to some studies, in 9-19 day old mice, the presence of HCN1 channel mediated ZD-7288 sensitive I_H current (Leao et al., 2006) and onset (chopper) firing properties denoted LSO principal neurons, while the absence of I_H and delayed firing properties correlated with the LOC neurons (Sterenborg et al., 2010; Fujino et al., 1997). There was no difference in the I_H current between the single firing and the multiple firing LSO principal neurons in 24-29 day old rats (Barnes-Davies et al., 2004) or 12-14 day old mice (Leao et al., 2006). However in one previous report, the magnitude of I_H has been shown to be larger in lateral LSO cells compared to medial LSO cells in P 17 gerbils (Hassfurth et al., 2009).

While the presence or absence of I_H has been thoroughly investigated in rodents post hearing onset, little is known about the development of I_H in the LSO in the first two weeks of postnatal development. Due to the uniform distribution (Sterenborg et al., 2010) and lack of distinct morphological features to distinguish between differ-

ent functional classes of LSO cells, I recorded from LSO cells both with and without I_H between the ages P 1 to P 13. Assuming non-biased sampling, I separated the cells at each age group, post-hoc, on the basis of presence or absence of I_H to investigate the ontogeny of the development of I_H in the LSO cells. I found that the proportion of LSO cells showing the presence of I_H increased from E 18 to P 13. In the medial cells, the proportion of I_H positive cells increased from 20% to almost 80% between P 1 and P 5-6. However, for the lateral cells, the proportion of I_H positive cells was still less than 40% at P 5-6 and became 80% only at P 9-13. Thus it seems that the I_H current develops in LSO cells over time in the first two postnatal weeks. The development of I_H seems to occur earlier in the medial LSO cells (by P 5-6) compared to the lateral cells (by P 9-13).

According to previous studies in 18-21 day old mice, dendritic I_H can modulate the integration of postsynaptic potentials leading to a lesser degree of summation of simultaneous inputs (Leao et al., 2011). Thus the presence of I_H in a subset of the cells may lead to an underestimation of the postsynaptic response amplitudes in those cells. Since the proportion of I_H positive cells also vary with age, this might lead to an underestimation of mean response amplitudes at some ages but not others. So I redistributed my dataset between ages P 2 to P 13 to compare the synaptic amplitudes between the I_H positive and I_H negative cells. Since the percentage of I_H positive cells varied over ages, there were not enough data points for statistical comparison between I_H positive and negative cells at any of the age groups except

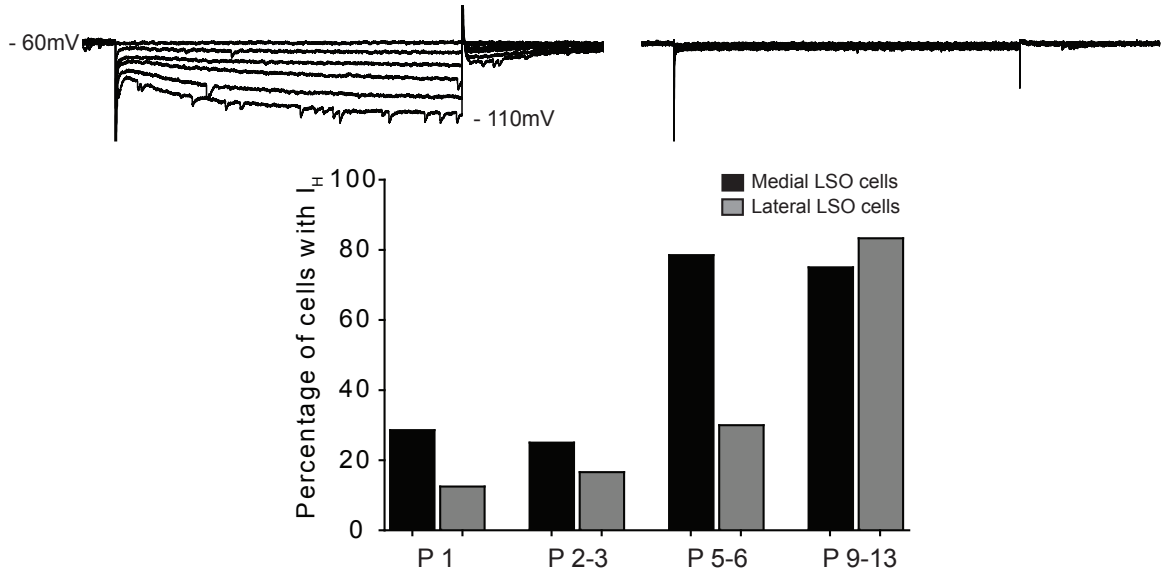

Figure 3.10: **Percentage of I_H positive LSO cells at different ages**
(Top) Voltage clamp traces showing presence (left) and absence (right) of I_H current. (Bottom) Population data of percentage of medial (black bars) and lateral (grey bars) LSO cells at different ages (P 1 to P 9-13) that show the presence of I_H.

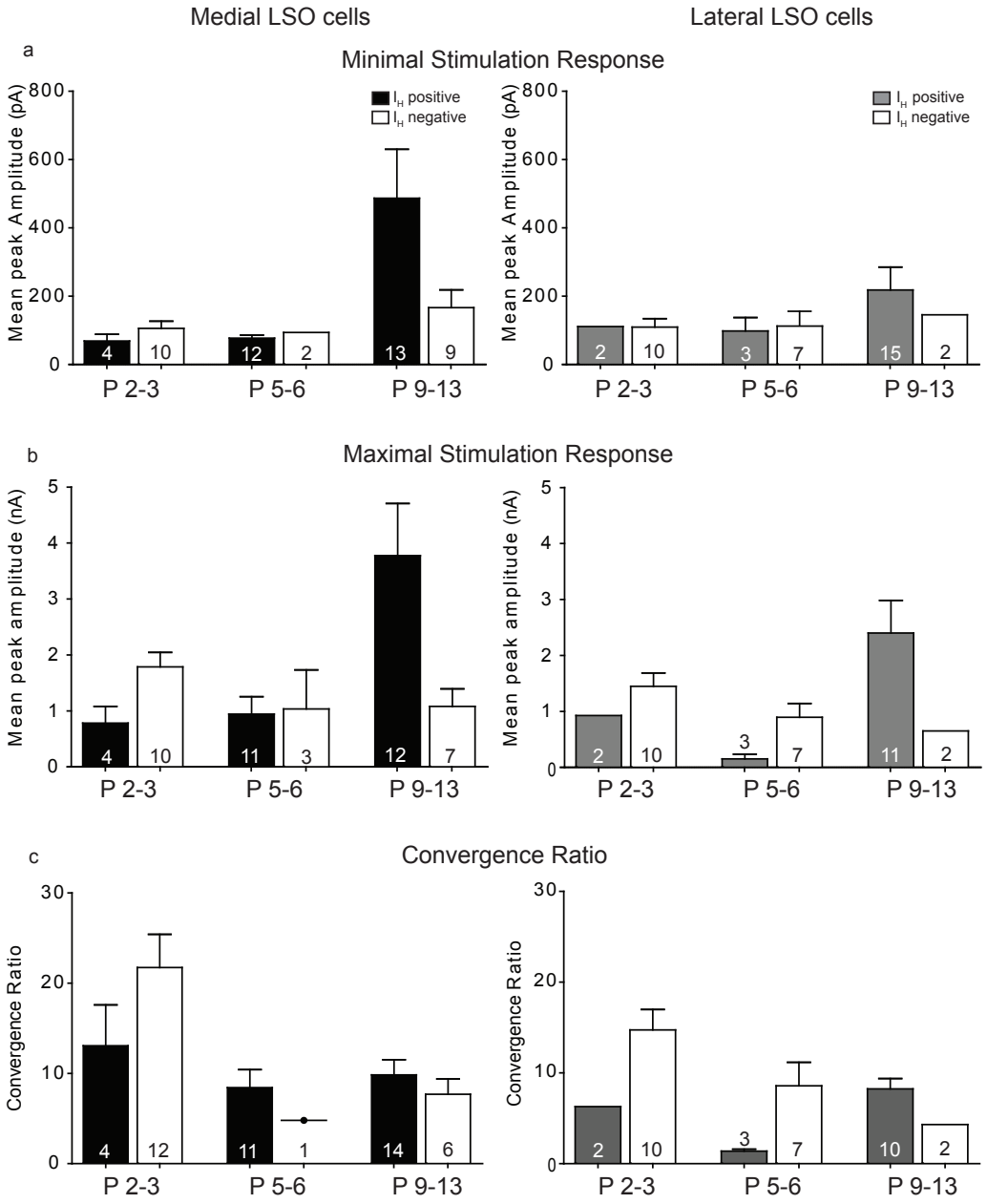

Figure 3.11: **Comparison of stimulation response amplitudes and convergence ratios of I_H positive and negative cells at different ages**
(a) Population data of minimal stimulation responses of medial (left, black bars) and lateral (right, grey bars) LSO cells at different ages (P 2-3 to P 9-13). Error bars represent SEM.
(b) Population data of maximal stimulation responses of medial (left, black bars) and lateral (right, grey bars) LSO cells at different ages (P 2-3 to P 9-13). Error bars represent SEM.
(c) Population data of convergence ratio of medial (left, black bars) and lateral (right, grey bars) LSO cells at different ages (P 2-3 to P 9-13). Error bars represent SEM.

for the medial cells of age P 9-13. At this age the minimal response amplitudes for I_H positive cells (486.9 ± 143.2 pA, n=13) were similar to that of I_H negative cells (166.5 ± 51.88, n=9) (p value= 0.07, Mann-Whitney test). I also did not find any significant differences in the maximal amplitudes at this age (I_H positive = 3.776 ± 0.93 nA, n= 12, I_H negative = 1.08 ± 0.31 nA, n=7, p value= 0.07, Mann-Whitney test). The convergence ratios were also not significantly different between these cells (I_H positive = 10:1, I_H negative = 8:1, p value= 0.45).

Thus from the above data it is evident that I_H current develops in LSO cells gradually within the first two weeks of development. The proportion of I_H positive cells reaches a majority in the medial part of the LSO by P 5-6 but does so in the lateral part only by P 9-13. However, the presence of I_H does not seem to cause significant differences in the estimation of the minimal and maximal synaptic response amplitudes at least at P 9-13.

3.2.8 Age dependent changes in synaptic properties do not seem to cause disparity between inputs of similar strength

The minimal and maximal stimulation data suggest that the disparity in strength of the medial MNTB inputs does not seem to play an important role in the functional elimination during the early postnatal development. A possible alternative may be that the synchronicity of the inputs may be one of the deciding factors regarding the elimination or retention of a given input. If this were true, the 20% - 80% rise times of the minimal and maximal synaptic responses would change with age reflecting the

change in synchronicity of the inputs.

A closer examination of the 20% - 80% rise times of the minimal and maximal synaptic response amplitudes at the ages P 2-3, P 5-6 and P 9-13 revealed that, while there was no significant difference in the rise times for minimal responses between the ages P 2-3 and P 5-6, the rise times for the maximal amplitudes differed significantly between these ages. The rise time of the maximal response increased significantly from P 2-3 to P 5-6 (Table 3.4, Fig 3.12 a, c). After P 5-6, both the minimal and maximal rise times decreased significantly (p value = 0.01, ANOVA). The same trend was observed in the lateral cells too (p value = 0.001, ANOVA, Fig. 3.12 b).

One possible reason behind the significant increase in the mean maximal but not the minimal rise time may be a desynchronization of the different input fibers, presumably due to different degrees of myelination at different ages. Different degrees of expression of myelin associated glycoprotein (MAG) in the developing LSO at different postnatal ages has been suggested by some studies (Hafidi et al., 1996). If this were true then the differences in conduction velocities of the differentially myelinated fibers would be reflected in the differences in the latencies of the minimal responses. The mean latencies of minimal responses did not differ significantly between P 2-3 and P 5-6 in the medial cells (p value = 0.23, Student's t test, Fig. 3.12 d). The mean latencies of the minimal responses for the lateral cells also did not differ at different ages (Fig 3.12 e). The latencies of the minimal and maximal responses in the lateral cells were significantly higher than the medial cells at all ages presumably

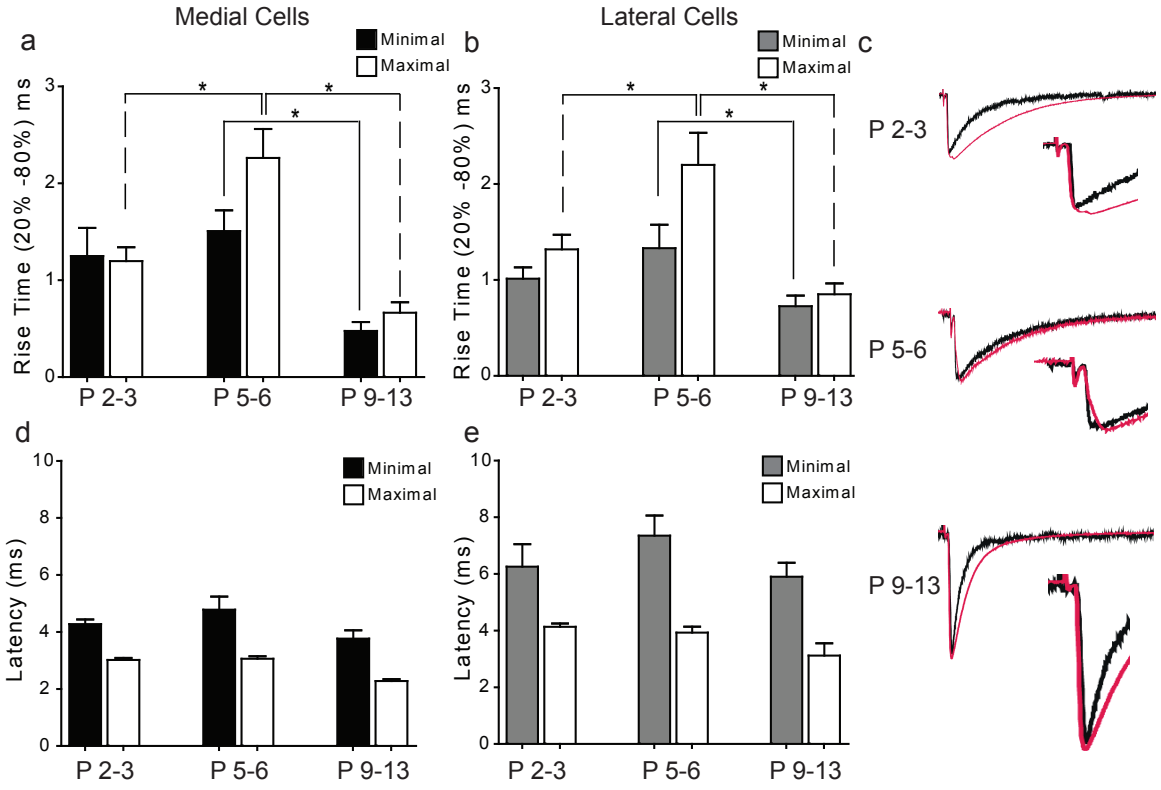

Figure 3.12: **Rise times of maximal synaptic responses change significantly between P 2 and P 13**

(a, b) Population data of rise times of minimal and maximal stimulation responses (strength of single MNTB inputs) of medial (black bars) and lateral (grey bars) LSO cells at different ages (P 2-3 to P 9-13). Error bars represent SEM.

(c) Average of ten traces of scaled minimal (black trace) and maximal (red trace) stimulation responses of medial cells at different ages (P 2-3, P 5-6, and P 9-13). Error bars represent SEM.

(d, e) Population data of latencies of minimal and maximal synaptic responses of medial (black bars) and lateral (grey bars) LSO cells at different ages (P 2 to P 13). Error bars represent SEM.

Table 3.4: **Summary of the rise times of synaptic responses of LSO cells at different ages.** The p values represent comparisons between medial and lateral LSO cells.

	Position	P 2-3	P 5-6	P 9-13
Minimal	Medial	1.25 ± 0.3 ms (n=11)	1.51 ± 0.21 ms (n=10)	0.48 ± 0.09 ms (n=11)
	Lateral	1.01 ± 0.12 ms (n=15)	1.33 ± 0.24 ms (n=10)	0.72 ± 0.11 ms (n=6)
P values		0.41 (Student's t test)	0.59 (Student's t test)	0.06 (Mann-Whitney test)
Maximal	Medial	1.20 ± 0.14 ms (n=10)	2.26 ± 0.30 ms (n=9)	0.67 ± 0.11 ms (n=10)
	Lateral	1.31 ± 0.15 ms (n=15)	2.2 ± 0.33 ms (n=10)	0.85 ± 0.11 ms (n=16)
P values		0.39 (Mann-Whitney test)	0.89 (Student's t test)	0.10 (Mann-Whitney test)

due to longer distance between the stimulation electrode and the recorded cell (Table 3.5).

Table 3.5: **Summary of the latencies of synaptic responses of LSO cells at different ages.** The p values represent comparisons between medial and lateral LSO cells.

	Position	P 2-3	P 5-6	P 9-13
Minimal	Medial	4.28 ± 0.16 ms (n=16)	4.78 ± 0.46 ms (n=11)	3.76 ± 0.30 ms (n=22)
	Lateral	6.25 ± 0.79 ms (n=16)	7.36 ± 0.71 ms (n=10)	5.9 ± 0.50 ms (n=5)
P values		**0.02 (Student's t test)**	**0.005 (Mann-Whitney test)**	**0.003 (Student's t test)**
Maximal	Medial	1.20 ± 0.14 ms (n=10)	2.26 ± 0.30 ms (n=9)	0.67 ± 0.11 ms (n=10)
	Lateral	4.13 ± 0.11 ms (n=16)	3.93 ± 0.21 ms (n=10)	3.12 ± 0.43 ms (n=5)
P values		**<0.001 (Student's t test)**	**0.006 (Student's t test)**	**0.002 (Student's t test)**

I also measured the decay kinetics of the minimal and maximal responses in medial as well as lateral cells by fitting single exponentials to the decay of the synaptic responses. The decay constants decrease significantly over the first two postnatal weeks. The decay constant for minimal responses in both medial and lateral cells decreased significantly between P 5-6 and P 9-13 (medial cells: p value < 0.001, Student's t test, lateral cells: 0.03, Student's t test, Fig 3.13 a, b). The higher decay

constants for minimal responses at P 2-3 and P 5-6 suggests that at these ages the synaptic response is a mixture of GABAergic and Glycinergic response (Nabekura et al., 2003; Jonas et al., 1998). However after P 5-6, the glycinergic component increases as reflected in the small decay constant more similar to purely glycinergic responses (Nabekura et al., 2003; Jonas et al., 1998; Kandler and Friauf, 1995b). For both medial and lateral cells, the decay constant for maximal responses decreased significantly between P 2-3, P 5-6 and P 9-13 (medial cells: p value < 0.001, ANOVA, lateral cells: p value < 0.001, ANOVA, Fig 3.13 a, b). The significantly high decay constant for the maximal response compared to the minimal response in the P 2-3 medial LSO cells also suggest the possible activation of extrasynaptic receptors by spilled over GABA/glycine.

To investigate whether differences in the release probability in the MNTB inputs may be one possible way of causing disparity among different inputs of the same strength, I measured the paired pulse ratio of both medial and lateral inputs at the different age points. The paired pulse ratios did not show any significant difference between the ages (medial cells: p value $= 0.21$, ANOVA, lateral cells: p value $= 0.70$, ANOVA, Fig 3.13 c). There was also no tonotopy specific differences in the paired pulse ratios at any of the ages (Table 3.7).

All the above data together show that the differences in the rise time of the minimal and maximal synaptic responses, latencies of the responses, decay kinetics of the responses or the probability of release are not sufficient to explain the strengthen-

ing independent functional elimination process in the pre-hearing development of the LSO.

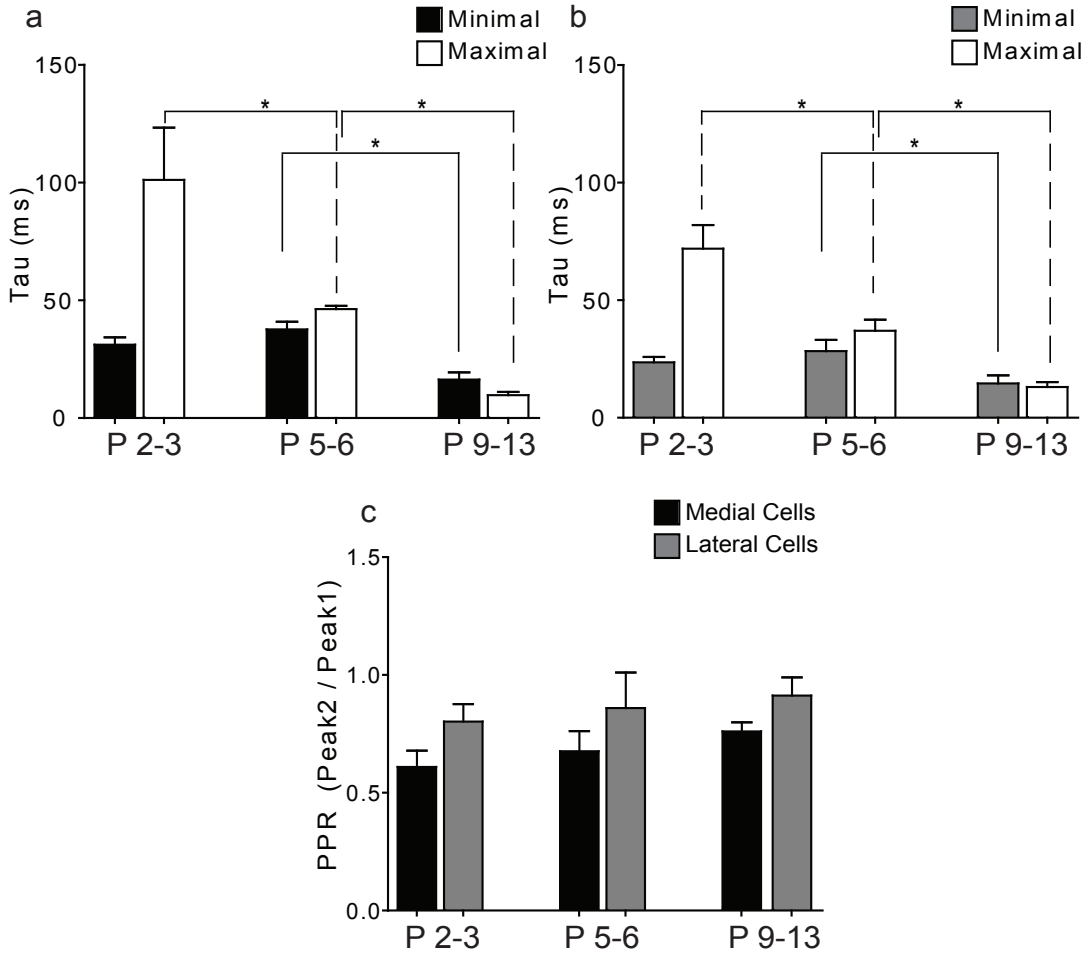

Figure 3.13: **Decay constants and paired pulse ratios of medial and lateral LSO cells between ages P 2 and P 13**
(a, b) Population data of decay constants of minimal and maximal stimulation responses (strength of single MNTB inputs) of medial (black bars) and lateral (grey bars) LSO cells at different ages (P 2-3 to P 9-13). Error bars represent SEM.
(c) Population data of paired pulse ratio of medial (black bars) and lateral (grey bars) LSO cells at different ages (P 2 to P 13). Error bars represent SEM.

Table 3.6: **Summary of the decay constants of synaptic responses of LSO cells at different ages.** The p values represent comparisons between medial and lateral LSO cells.

	Position	P 2-3	P 5-6	P 9-13
Minimal	Medial	31.13 ± 3.15 (n=16)	37.68 ± 3.23 (n=14)	9.72 ± 1.4 (n=19)
	Lateral	23.58 ± 2.3 (n=11)	28.35 ± 4.75 (n=11)	14.62 ± 3.41 (n=11)
P values		0.09 (Student's t test)	**0.02 (Mann-Whitney test)**	0.19 (Mann-Whitney test)
Maximal	Medial	101.2 ± 22.16 (n=16)	46.27 ± 1.37 (n=12)	16.34 ± 3.08 (n=15)
	Lateral	71.92 ± 10.02 (n=16)	36.98 ± 4.69 (n=11)	13.04 ± 2.13 (n=17)
P values		0.36 (Mann-Whitney test)	0.06 (Student's t test)	0.37 (Student's t test)

Table 3.7: **Summary of the paired pulse ratios of synaptic responses of LSO cells at different ages.** The p values represent comparisons between medial and lateral LSO cells.

	Position	P 2-3	P 5-6	P 9-13
PPR	Medial	0.61 ± 0.07 (n=11)	0.68 ± 0.09 (n=11)	0.76 ± 0.04 (n=17)
	Lateral	0.80 ± 0.07 (n=10)	0.86 ± 0.15 (n=7)	0.91 ± 0.08 (n=9)
P values		0.07 (Student's t test)	0.27 (Student's t test)	0.06 (Student's t test)

3.3 Discussion:

In the present study, I have shown that, in the medial part of the MNTB-LSO circuit, the strength of single inputs increase in two steps: between E18 to P 2-3 and again between P 5-6 and P 9-13. While the increase is gradual between E18 and P 2-3, the input strengths show a significantly large increase after P 5-6, indicating that the significant phase of strengthening occurs only after P 5-6. However the number of inputs converging onto single medial LSO cells increase from E18 until P 2-3 but then decrease before P 5-6, suggesting significant functional elimination of synaptic inputs between P 2-3 and P 5-6. Thus the elimination of synaptic inputs precedes the significant strengthening phase of the medial MNTB inputs. To the best of my knowledge, this is the first report of such a phenomenon in the synaptic refinement of inhibitory synapses.

From the previous studies of excitatory circuits like neuromuscular junction, visual cortex and cerebellar circuits (Purves and Lichtman, 1983; Colman et al., 1997; Hashimoto and Kano, 2003; Shatz, 1990; Katz and Shatz, 1996), it is evident that the disparity in the strengths of inputs determines which ones are likely to be selectively maintained (Hashimoto and Kano, 2003). The weaker synapses are subsequently eliminated (Purves and Lichtman, 1983). In these circuits, increase in synaptic strength always precedes synaptic elimination. As an exception, the elimination of the excitatory inputs from the principal sensory trigeminal nucleus (PrV) to the ventral posteromedial nucleus (VPm) of the somatosensory thalamus was shown to

be independent of their AMPAR dependant strengthening (Wang et al., 2011). In this study I showed that not only the elimination of medial MNTB inputs occurs before strengthening, in the lateral part, strengthening of inputs occurs even in the absence of elimination. These results suggest the lack of interdependence between the two processes.

Spontaneous bursts of ATP driven spike trains generated in the pre-hearing cochlear inner hair cells (IHC) have been hypothesized to provide structured activity patterns to guide the synaptic refinement in the downstream auditory nuclei in the absence of external stimulus (Tritsch and Bergles, 2010; Tritsch et al., 2007). The spontaneous cochlear activity, which is correlated in the nearby (tonotopically similar) cells, is transmitted to the functionally connected downstream auditory nuclei during the first two postnatal weeks (Kandler and Friauf, 1995a; Kotak and Sanes, 1995; Jones et al., 2001, 2007; Tritsch and Bergles, 2010). The spontaneous firing patterns transmitted from the cochlea shapes the firing of central auditory neurons like the MNTB principal neurons (Tritsch and Bergles, 2010). The activity is random at first, but later transforms into bursts, with the frequency of bursts peaking at P 8-10 in mice (Tritsch and Bergles, 2010). This period coincides with the strengthening phase that I observe in the MNTB-LSO connections irrespective of their position along the tonotopic axis. The spiking activity of MNTB neurons also change from tonic to phasic at P 4-6 (Hoffpauir et al., 2010). The number of calyceal inputs to each MNTB neurons also reduces to one by P 4 (Hoffpauir et al., 2010), possibly

leading to increased synchronicity of the tonotopically similar MNTB inputs to the LSO. Thus, the increase in frequency and synchronicity in the spontaneous activity driven MNTB activity may help to strengthen the MNTB inputs between P 5-6 and P 9-13.

The differences in the pre-hearing refinement of the medial versus the lateral part of the circuit may result from the developmental timeline of the different parts of the cochlea. In addition to becoming spontaneously active, the immature cochlea also develops structurally during the first two postnatal weeks. The structural changes in the high frequency region (base) of the cochlea precede the changes in the low frequency region (apex) (Sato et al., 1999; Lim and Rueda, 1992). This may lead to a base (high) to apex (low) gradient of activity patterns that might be important in guiding tonotopic refinement of the connections in the downstream auditory pathway (Tritsch and Bergles, 2010). From our results, the convergence ratio of the lateral cells at P 2-3 is significantly lower than that of the medial cells of this age and resembles the convergence ratio of medial cells at P 1. This suggests that there may be a medial (high) to lateral (low) gradient in the increase of convergence in the MNTB-LSO circuit.

However the peak of convergence seen in medial cells at P 2-3 is absent in the lateral cells even at later ages. This may be influenced by the local changes in the LSO cells like the excitatory to inhibitory switch of GABA/Glycine. As seen in many brain areas (spinal cord: (Todd et al., 1996; Wu et al., 1992; Ma et al., 1992) ;

brainstem: (Kandler and Friauf, 1995a; Frech et al., 1999; Kraushaar and Backus, 2002; Singer et al., 1998); hippocampus: (Ito and Cherubini, 1991; Cherubini et al., 1991); cerebral cortex: (Flint et al., 1998)), GABA/glycine undergo a switch from their perinatal depolarizing state to adult-like hyperpolarizing state at P 4-8 in rats and P 3 or P 6 in mice (rats: P 4-5: (Löhrke et al., 2005), P 5-8: (Ehrlich et al., 1999), P 8: (Kandler and Friauf, 1995a); mice: P 3 (Kullmann and Kandler, 2001) P 6 (Poulopoulos et al., 2009). The functional elimination of inputs in the developing rat MNTB-LSO circuit has been shown to be complete by P 8 (Kim and Kandler, 2003). The present study shows that the functional elimination of the medial inputs in mice LSO occurs mainly between P 3 and P 5 which precisely correlates with change of the chloride reversal potential in mice LSO cells from depolarizing to hyperpolarizing (Kullmann and Kandler, 2001). Thus in both rats and mice, the elimination phase seems to be tightly coupled with the change in polarity of GABA/Glycine.

Thus the pre-hearing refinement in the LSO may be influenced by both the upstream cochlea generated spontaneous activity as well as the local change in polarity of GABA/Glycine. The early spontaneous activity of the basal cochlea and the excitatory phase of GABA/glycine may help the medial MNTB inputs proliferate, leading to a high convergence ratio at P 2-3. The lateral MNTB inputs lag behind, probably due to lack of early activity in the underdeveloped apical cochlea, showing low convergence at P 2-3. The hyperpolarization shift of GABA/Glycine (at P 4-8) may act as "brakes" to the proliferation and cause rapid elimination of inappropriate connections

by physiological processes like LTD (Chang et al., 2003). Thus the medial inputs with high convergence at P 2-3 show significant elimination between P 2-3 and P 5-6. Furthermore, in the presence of hyperpolarizing action of GABA/Glycine, the lateral inputs cannot proliferate anymore after P 2-3 (even in presence of activity of the apical cochlea), thus showing low convergence throughout the developmental period. Controversy exists whether or not a medio-lateral gradient is present in the timing of chloride shift within the LSO (Kotak et al., 1998; Löhrke et al., 2005; Ehrlich et al., 1999). However, the interpretation of our results would remain the same regardless of the presence or absence of such a gradient. Then in the hyperpolarization phase, the increased frequency and synchronization of the bursts of spontaneous cochlear activity may facilitate the strengthening of the maintained MNTB inputs.

In conclusion, this study elucidates that the elimination of inputs precedes their strengthening in the MNTB-LSO circuit. While significant strengthening of inputs occurs only after P 5-6, elimination of inputs occurs between P 2-3 and P 5-6. The presence of strengthening of inputs in the lateral part of the circuit even in the absence of the elimination phase suggests that the two processes are independent of each other and may be influenced by separate mechanisms.

Chapter 4

Role of Glutamate co-release in the pre-hearing strengthening of MNTB-LSO projections

4.1 Introduction

Classically, the identity of a neuron is determined using Dale's principle. According to this principle, each neuron is assumed to release the same neurotransmitter from all its terminals regardless of the identity of the postsynaptic target (Eccles,1964). This principle, however, has been misinterpreted widely into the rule of thumb of "one neuron, one neurotransmitter". But over the years, various studies have gathered evidence that invalidates this oversimplified point of view. For example, co-release of GABA and Glycine has been described in the spinal cord (Jonas et al., 1998), dorsal cochlear nucleus (Juiz et al., 1996) as well as the auditory brainstem (Kotak et al., 1998). Release of GABA and acetylcholine has been shown in retinal starburst amacrine cells (Zheng et al., 2004). However, the MNTB-LSO circuit was the first place where a GABA/Glycinergic synapse was shown to release a third fast neurotransmitter, glutamate (Gillespie et al., 2005). While the release of GABA and glutamate from the same terminal had been shown before in case of hippocampal mossy fibers (Sandler and Smith, 1991), this was the first time that the release of three major neurotransmitters from the same terminal, with seemingly opposing physiological functions, was reported.

Glutamate co-release in the MNTB-LSO circuit

Pharmacological interventions of whole cell recordings of LSO cells in the first two postnatal weeks revealed that the MNTB-LSO synapses also released glutamate in

addition to GABA and glycine (Gillespie et al., 2005). The glutamate release from the MNTB terminals is mediated by the glutamate transporter VGlut-3, which is co-expressed with VGAT (vesicular GABA transporter) (Gillespie et al., 2005) in the developing MNTB terminals. VGlut-3 (or *Slc17a8*) was first identified by sequence homology to the more abundant forms of glutamate transporters VGlut1 and VGlut2. But VGlut-3 was always found to be expressed in terminals which were classically "non-glutamatergic" (Seal and Edwards, 2006; Schäfer et al., 2002; Somogyi et al., 2004; Herzog et al., 2004; Gras et al., 2002). Thus it was hypothesized to be responsible for glutamate release from non-glutamatergic terminals. Glutamate released from these MNTB terminals activate postsynaptic AMPA receptors (AMPARs) as well as GluN2B containing NMDA receptors (NMDARs) on LSO cells (Case and Gillespie, 2011).

VGlut-3 mediated glutamate co-release is well studied in the medial part of the MNTB-LSO circuit. Glutamate is released by the medial MNTB terminals transiently during the first two postnatal weeks (predominantly in the first postnatal week) (Gillespie et al., 2005). This released glutamate activates mostly AMPARs early in development, but switches to more NMDARs mediated response in the postsynaptic LSO cells in the second postnatal week (Case and Gillespie, 2011). Activation of both AMPARs and NMDARs may induce activity-dependent changes in the postsynaptic cell. The timing of this transient glutamate release seems to be well correlated with major developmental changes in this circuit. The peak of glutamate co-release in

the first postnatal week (Gillespie et al., 2005; Case and Gillespie, 2011) coincides with the depolarizing phase of the inhibitory neurotransmitters GABA and glycine in this circuit (Kullmann and Kandler, 2001; Kandler and Friauf, 1995a; Ehrlich et al., 1999; Löhrke et al., 2005). The depolarizing action of GABA and glycine during this period is due to high intracellular chloride concentration in the LSO cells (Ehrlich et al., 1999; Löhrke et al., 2005). In the first postnatal week, the intracellular chloride concentration is high due to low membrane expression of KCC2 transporters that extrude chloride ions from the cell (Balakrishnan et al., 2003). Due to this high intracellular chloride, GABA and glycine causes chloride ions to flow out from the cells when the ligand dependent ion channels are activated. This causes depolarization of the LSO cell (Kullmann and Kandler, 2001). Such depolarization by GABA and glycine can lead to action potentials in the LSO cells (Kullmann and Kandler, 2001) and may facilitate removal of the magnesium block from the postsynaptic GluN2B containing NMDARs (expressed in the P 3 to P 9 rat LSO) (Case and Gillespie, 2011). The glutamate released from the MNTB terminals may then activate these unblocked NMDARs and lead to influx of Ca^{++} ions into the postsynaptic cells, in addition to the calcium influx caused by depolarizing GABA and Glycine (Kullmann et al., 2002). This calcium influx due to activation of NMDARs may activate many synaptic plasticity mechanisms that can occur during the developmental period of a circuit (Malenka and Bear, 2004). The NMDAR (GluN2B) mediated glutamatergic response gradually diminish after P 9 while the AMPAR mediated component remains

small throughout the first two postnatal weeks (Case and Gillespie, 2011). The exact mechanism and factors affecting the developmental changes in the glutamatergic component is still not well understood.

Role of glutamate release on refinement

The role of glutamate release in the developing medial MNTB-LSO circuit has been extensively studied (Noh et al., 2010). The period of glutamate release in this circuit coincides with the period when the circuit undergoes massive postnatal refinement (Gillespie et al., 2005). The glutamate released from the VGlut-3 containing MNTB synapses was found to be crucial for the proper refinement and strengthening of medial MNTB inputs during the first two postnatal weeks (Noh et al., 2010).

Glutamate co-release did not influence the initial formation of the MNTB-LSO synapses. This was evident from the strength and number of the MNTB inputs in *vglut3-/-* animals at P 1-2. The strength of the MNTB inputs in *vglut3-/-* animals was similar to the strength of the inputs of wild type animals of the same age. The initial strength of the inputs then increased by almost 8 fold in the wild type animals in the first two weeks of development. In *vglut3-/-* animals the increase in strength was only two fold (Noh et al., 2010). Thus the VGlut-3 mediated glutamate co-release plays an important role in the proper strengthening of the MNTB-LSO connections. It was also noted that there was a 17% decrease in the quantal content of the MNTB inputs of the *vglut3-/-* mice. But the overwhelming 50% reduction in strength suggested that the lack of glutamate co-release caused impairments in addition of new release

sites during development (Noh et al., 2010; Kim and Kandler, 2010).

During the first two weeks of postnatal development, the MNTB-LSO projections undergo extensive functional refinement, mediated by functional silencing of inputs, leading to a decrease in convergence of inputs to single LSO cells. At early postnatal ages (P 1-2) the number of inputs converging on to single LSO cells was similar for both wild type and *vglut3-/-* animals (19:1 for wild type and 18:1 for knockout). But at the end of two postnatal weeks, the convergence ratio of *vglut3-/-* mice (13:1) was almost twice of that of the wild type animals at this age (7:1) (Noh et al., 2010). This showed that the functional elimination of inputs that occurs in the first two weeks of development in the wild type mice (19:1 at P 1-2 to 7:1 at P 9-12) does not occur in the absence of glutamate co-release (18:1 at P 1-2 to 13:1 at P 9-12). In correlation to the functional loss of connections over the first two weeks, the broad tonotopic input map in the MNTB also undergoes almost a 50% reduction in area as the maps become sharper and more precise from P 1-2 to P 9-12 (Kim and Kandler, 2003). But in the absence of glutamate co-release, this refinement in the tonotopic map area was also impaired (Noh et al., 2010). The tonotopic input map in the MNTB of P 9-12 *vglut3-/-* animals was only 15% smaller than the map at P 1-2. This lack of reduction in the input map area indicated a substantial decrease in the precision of the tonotopic map at hearing onset (Noh et al., 2010).

Possible role of glutamate in the lateral part of MNTB-LSO circuit

From the detailed studies of the medial MNTB-LSO circuit, it is clear that VGlut-3 mediated transient glutamate co-release, during the first two weeks of development, is crucial for the proper strengthening of medial MNTB inputs and refinement of the tonotopic map. However it is not known whether glutamate co-release plays a similar role in the lateral part of the circuit. The lateral MNTB-LSO inputs, as already shown, undergo strengthening similar to the medial inputs. So I hypothesized that the lack of glutamate co-release would have a strong effect on the strengthening of the lateral MNTB inputs similar to that of the medial cells. However, functional elimination of inputs in the lateral MNTB-LSO projections is absent in wild type mice and the convergence ratios of the lateral LSO cells are low even at P 2-3. I hypothesized that the low convergence ratios seen in lateral LSO cells at P 2-3 may be due to a higher glutamatergic effect on the lateral connections. So I expected to see a higher convergence ratio in the lateral LSO cells at P 2-3 in the absence of glutamate co-release. This study of the effects of lack of glutamate co-release on the lateral MNTB-LSO connections would help to tease apart its role in strengthening of inputs or their functional elimination in greater detail.

4.2 Results

4.2.1 VGlut-3 is expressed in the lateral MNTB-LSO projections during development

To examine the role of glutamate co-release in the lateral MNTB-LSO projections, the first step was to determine whether glutamate was being released in the lateral connections. VGlut-3 has been shown to be expressed profusely in the medial and lateral MNTB-LSO projections in rats (Gillespie et al., 2005). To determine whether VGlut-3 was also expressed in the lateral MNTB-LSO projections in mice, DAB immunohistochemistry using antibodies against VGlut-3 was done in brainstem sections from mice (Kristy Cihil). Figure 4.1 shows sections of the auditory brainstem stained immunohistochemically for VGlut-3 expression in mice LSO at different ages (P 1, P 5 and P 15).

Robust staining of VGlut-3 was seen in the superior paraolivary nucleus (SPON) in addition to the LSO at the ages P 1 and P 5 but not at P 15 (Fig. 4.1, Bottom panel). There was no expression of VGlut-3 visible in the MNTB at any of the time points of investigation (Fig 4.1, Bottom, MNTB). The VGlut-3 expression in SPON was high at P 1 and P 5 but then gradually decreased after P 5 such that at P 15, the level of VGlut-3 staining matched the background levels. In the LSO, the expression of VGlut-3 showed a medio-lateral gradient. While the lateral part of the LSO was heavily stained for VGlut-3 expression, the medial part showed almost negligible levels of VGlut-3 expression. The staining in the lateral part of the LSO

seemed to be higher than the medial part throughout the first two postnatal weeks (Fig 4.1). However at P 15, the expression levels of the medial and lateral parts of LSO did not seem to be significantly different from that of a nonspecific region above the LSO.

The above data suggests that VGlut-3 is expressed transiently in the LSO during the early stages of development. However, the cell bodies in the MNTB do not show any expression of VGlut-3 in these first two postnatal weeks. The expression level of VGlut-3 in the neuronal terminals in the LSO as well as SPON is high at P 1 and P 5, then decreases significantly. During the first two postnatal weeks, VGlut-3 expression in the LSO showed a medio-lateral gradient of expression such that the lateral LSO was always stained darker than the medial part. Thus the above data confirms the expression of VGlut-3 in the LSO in mice (similar to rats (Gillespie et al., 2005)), and also shows a medio-lateral gradient of VGlut-3 expression in the developing LSO.

4.2.2 Glutamate co-release in the lateral MNTB-LSO circuit

From the immunohistochemistry data, it is evident that there is high level of VGlut-3 expression in the terminals in the lateral LSO transiently during the first week of development. However, the identity of the terminals is still not clear. To ascertain that glutamate was being released from the lateral MNTB projections, I pharmacologically isolated the glutamatergic component of the MNTB synaptic input. The proportion of the maximal synaptic current amplitude that was pharmaco-

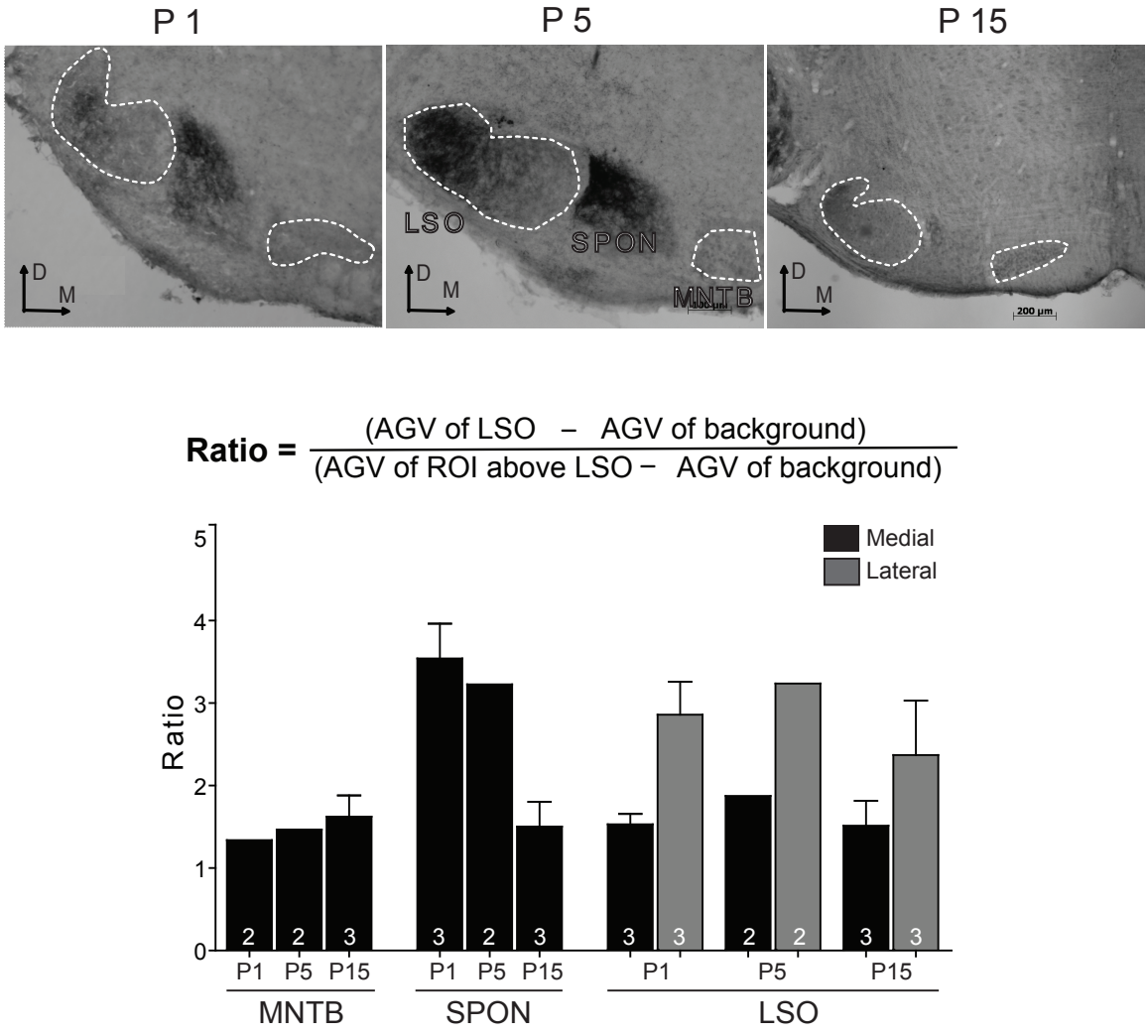

Figure 4.1: **VGlut-3 is expressed in the MNTB-LSO circuit in a medio-lateral gradient**
(Top) DAB stained sections of auditory brainstem of wildtype mice at different ages (immunostaining by Kristy Cihil).
(Bottom) Barplot showing age dependent differences in intensity of VGlut-3 staining in the MNTB, SPON, and LSO (black bars: medial LSO, grey bars: lateral LSO).

logically blocked by adding glutamate receptor blockers CNQX and APV estimated the glutamatergic component of the MNTB transmission.

From the pharmacological manipulations, I found that at the early postnatal days of P 2-3, the medial LSO cells received 12.6±2.8% (n=5) of glutamatergic input. The lateral cells also received a similar percentage of glutamate (14.02±1.9% ; n=6) at this age. After two weeks, around hearing onset, the glutamatergic component on to the medial cells became 8.2±2.1% (n=9) (p value = 0.23, Student's t test). The glutamatergic component to the lateral cells showed a significant decrease in the two weeks to become 6.6±2.2% (n=8) at P9-13 (p value = 0.03, Student's t test).

From the above data it is clear that glutamate co-release occurs in both the medial and lateral MNTB-LSO projections during the first two weeks of development. In the lateral MNTB-LSO projections, the glutamatergic component showed a significant decrease within the first two weeks of development.

4.2.3 Lateral MNTB-LSO connections strengthen in absence of glutamate co-release

From previous studies it is well known that the glutamate co-release in the medial MNTB-LSO circuit is essential for the strengthening of single MNTB inputs (Noh et al., 2010). Without the glutamate co-release, in the first two postnatal weeks, each medial MNTB input strengthens to only 2 fold instead of the characteristic 8 fold increase in the wild type mice. To test whether similar changes occur in the lateral LSO cells, I recorded the synaptic responses of both the medial and lateral LSO cells

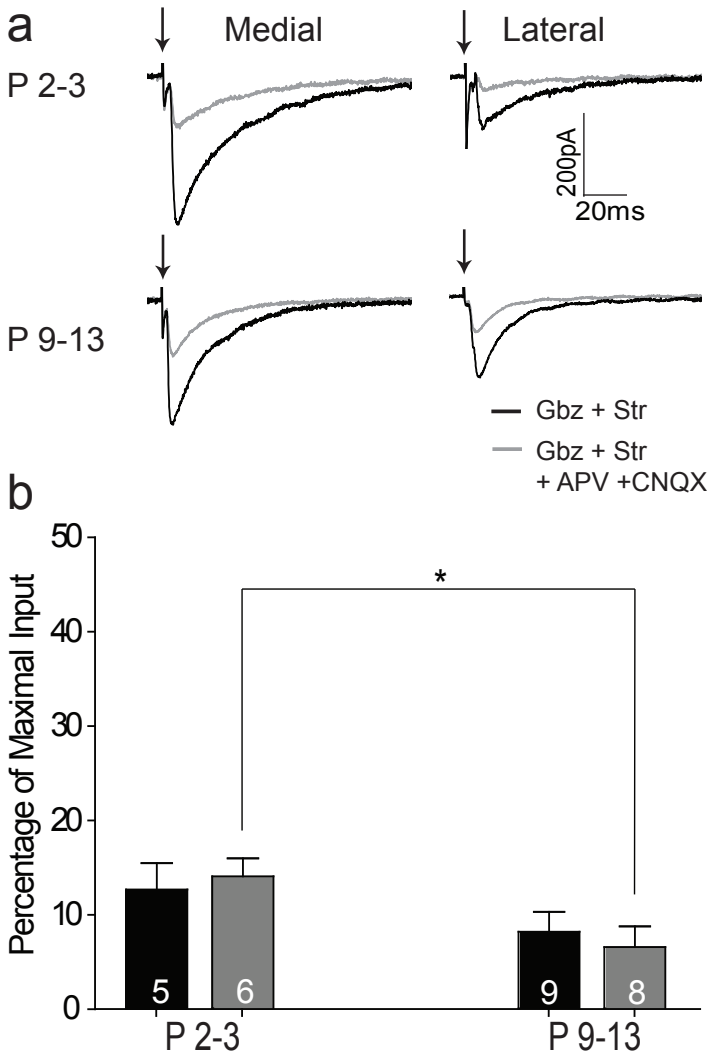

Figure 4.2: **Transient glutamatergic transmission in the medial and lateral MNTB-LSO projections**
(a) Average example traces before (black) and after (grey) pharmacological block of glutamate receptors in medial and lateral LSO cells .
(b) Population data showing the mean peak amplitude of glutamatergic transmission in medial and lateral LSO in response to maximal MNTB stimulation at different ages.

of *vglut3-/-* mice to minimal MNTB stimulation.

Similar to the previous study, the lack of glutamate co-release does not seem to influence for the initial strength of the medial MNTB-LSO synaptic inputs in my study. The amplitudes of minimal synaptic responses of medial cells of wild type and *vglut3-/-* animals at P 2-3, were not significantly different from each other (See Table 4.1). Then at P 9-13, the single input (minimal) response strength of the medial cells of wild type animals increased by 4 fold showing strengthening of synaptic inputs in the first two weeks . But the minimal synaptic response of the medial cells of the *vglut3-/-* animals did not increase significantly in the first two weeks (p value = 0.13, Mann-Whitney test). This distinct lack of strengthening of the medial MNTB-LSO connections showed that the presence of glutamate co-release is important for strengthening of the connections similar to previous studies (Noh et al., 2010).

For the lateral cells, at P 2-3, the minimal synaptic responses of wild type and *vglut3-/-* animals were not significantly different from each other. This showed that like medial cells, the lack of glutamate co-release did not affect the initial strength of the lateral MNTB-LSO synapses. Then at P 9-13, the strength of the lateral cells increased by almost 3 fold (See Table 4.1) showing developmental strengthening of the synaptic inputs. The lateral LSO cells of *vglut3-/-* animals also showed a similar significant increase in strength at P 9-13 (p value = 0.03, Student's t test). The strengths of single inputs of the lateral cells of the wild type and *vglut3-/-* animals were not significantly different from each other at P 9-13 (Table 4.1). This shows that

the strengthening of single inputs in the lateral MNTB-LSO circuit was not affected by glutamate co-release. This result was contrary to the effect of glutamate co-release seen in the medial cells.

Table 4.1: **Summary of minimal stimulation response amplitudes at different ages for wild type and *vglut3-/-* animals.** The p values represent comparisons between wild type and VG3KO LSO cells.

Genotype	Medial P 2-3	Medial P 9-13	Lateral P 2-3	Lateral P 9-13
vglu3 +/+	98.3 ± 14.5 pA (n=16)	423.2 ± 114.8 pA (n=17)	90.80 ± 13.7 pA (n= 23)	301.1 ± 88.7 pA (n=17)
vglu3 -/-	82.6 ± 16.7 pA (n= 9)	188.6 ± 83.7 (n= 11)	63.1 ± 12.3 pA (n= 7)	274.3 ± 70.1 pA (n=10)
P Values	0.55 (Mann-Whitney test)	0.09 (Mann-Whitney test)	0.29 (Student's t test)	0.54 (Mann-Whitney test)

Since glutamate co-release is crucial for strengthening of the medial part of the circuit (Noh et al., 2010), it was hypothesized that the lateral part of the circuit would also closely follow the model. The lack of the effect of glutamate on the strengthening in the lateral LSO cells is surprising and counter-intuitive. However this observation suggests that the process of strengthening in the lateral part of the LSO may follow a different underlying mechanism. The above data together suggests that the underlying mechanisms of strengthening of MNTB inputs vary along the tonotopic axis. While the medial MNTB projections strengthen by a glutamate dependent mechanism, the lateral projections strengthen in a glutamate independent manner.

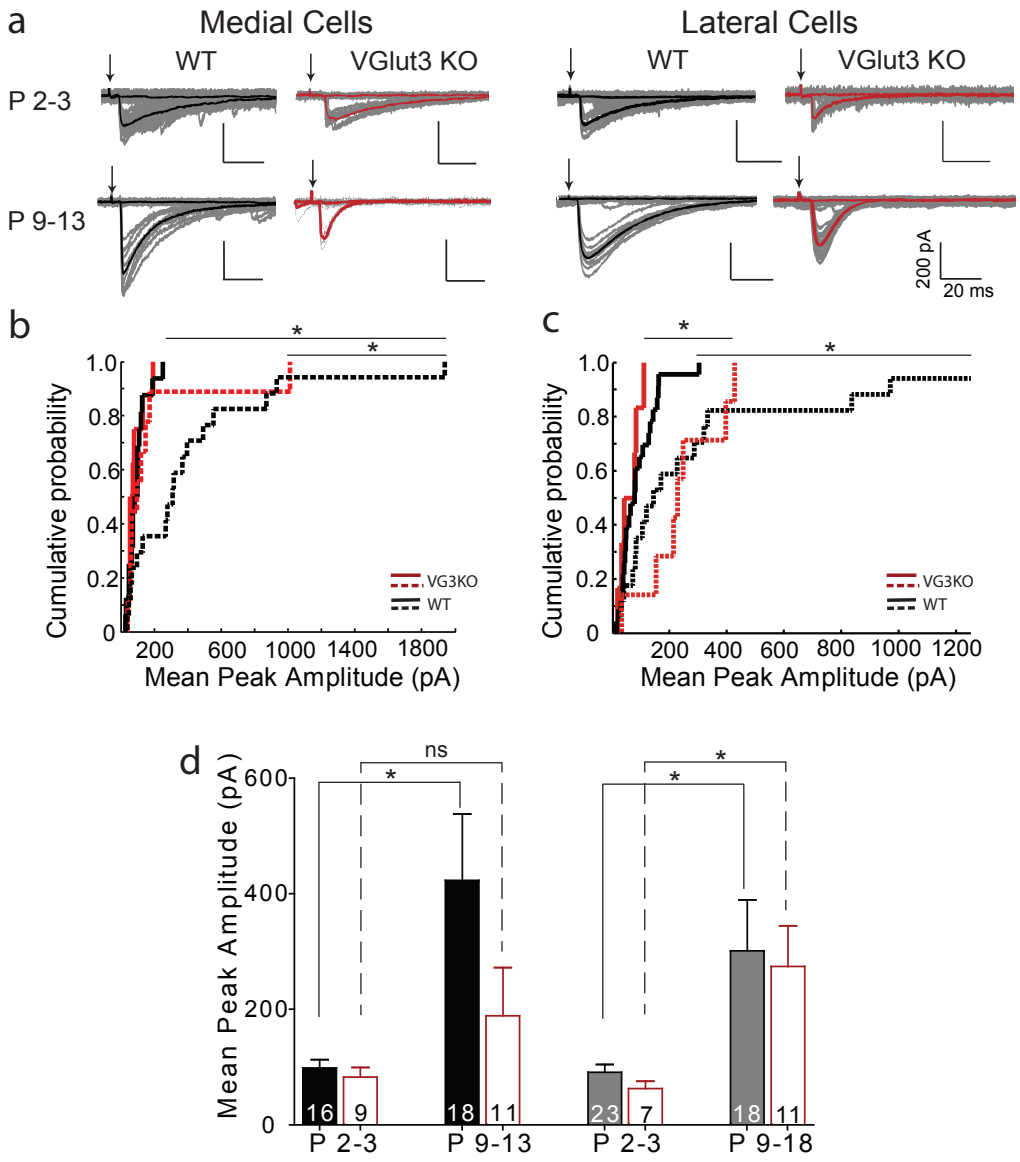

Figure 4.3: **Minimal stimulation responses of medial and lateral MNTB-LSO projections in wildtype and *vglut3-/-* mice**
(a) Average(black) and raw(grey) traces in medial and lateral LSO cells of WT and VG3KO animals at different ages.
(b) Cumulative probability distribution of minimal amplitudes of medial cells of WT and VG3KO animals at different ages.(Medial: P 2-3= 0.58, P 9-13= 0.04, KS test)
(c) Cumulative probability distribution of minimal amplitudes of lateral cells of WT and VG3KO animals at different ages.(Lateral: P 2-3= 0.88, P 9-13= 0.97, KS test)
(d) Population data showing the mean peak amplitude in medial and lateral LSO in response to minimal MNTB stimulation at different ages.

4.2.4 Convergence ratios in the lateral MNTB-LSO circuit do not change in the absence of glutamate co-release

The medial LSO cells show a phase of significant functional elimination of synaptic inputs during the first two postnatal weeks leading to sharpening of the tonotopic map of the MNTB-LSO circuit (Kim and Kandler, 2003; Noh et al., 2010). In the absence of the glutamate co-release, this process of functional elimination is impaired leading to high convergence ratios in the *vglut3-/-* medial cells (Noh et al., 2010).

In this study, at P 2-3, the mean peak amplitude of the maximal synaptic response of the medial cells in *vglut3-/-* animals was significantly smaller than that of wild type animals (See Table 4.2). In *vglut3-/-* animals, the maximal amplitude then significantly increased between P 2-3 and P 9-13 (p value = 0.02, Student's t test). At P 9-13, the maximal amplitude did not differ between wild type and *vglut3-/-* animals (See Table 4.2). However, the convergence ratio of medial LSO cells for *vglut3-/-* animals at P 9-13 was significantly higher (Table 4.3) than that of wild type animals showing a lack of functional elimination in these animals. Thus in agreement to previous reports (Noh et al., 2010), my data also shows that the lack of the glutamatergic component significantly affects the normal refinement of the medial LSO cells.

The lateral LSO cells, however, do not show this phase of functional elimination during the first two postnatal weeks (Chapter 3). The number of inputs converging on to each lateral LSO cell, even at P 2-3, is much lower than the number of inputs contacting the medial LSO cells at this age. At P 2-3, the expression of VGlut-3

was also much higher in the lateral LSO than the medial LSO. So I hypothesized that higher levels of glutamate release might be the underlying cause for the low convergence ratio of lateral cells at this age. Thus in the absence of the glutamatergic input, I expected to see a higher convergence ratio in the lateral cells at P 2-3.

For lateral cells, the maximal synaptic responses at P 2-3 in wildtype and *vglut3-/-* animals were not significantly different from each other (See Table 4.2). The maximal amplitude for *vglut3-/-* lateral cells then significantly increased between P 2-3 and P 9-13 (p value = 0.005, Mann-Whitney test) such that at P 9-13, it did not differ from the maximal amplitude for the wild type animals. Similarly when I examined the convergence ratios for the lateral cells, I did not find any significant difference between the wildtype and *vglut3-/-* cells at any of the tested age points (See Table 4.3)

Thus the above data together suggests that the glutamate co-release does not seem to play any significant role in determining the convergence of MNTB inputs on to single LSO cells in the lateral part of the circuit. Even though the expression of VGlut-3 shows a medio-lateral gradient along the tonotopic axis, the higher levels of VGlut-3 expression in the lateral part of LSO does not seem to reflect any major role of glutamate co-release in the strengthening or elimination of lateral MNTB-LSO projections.

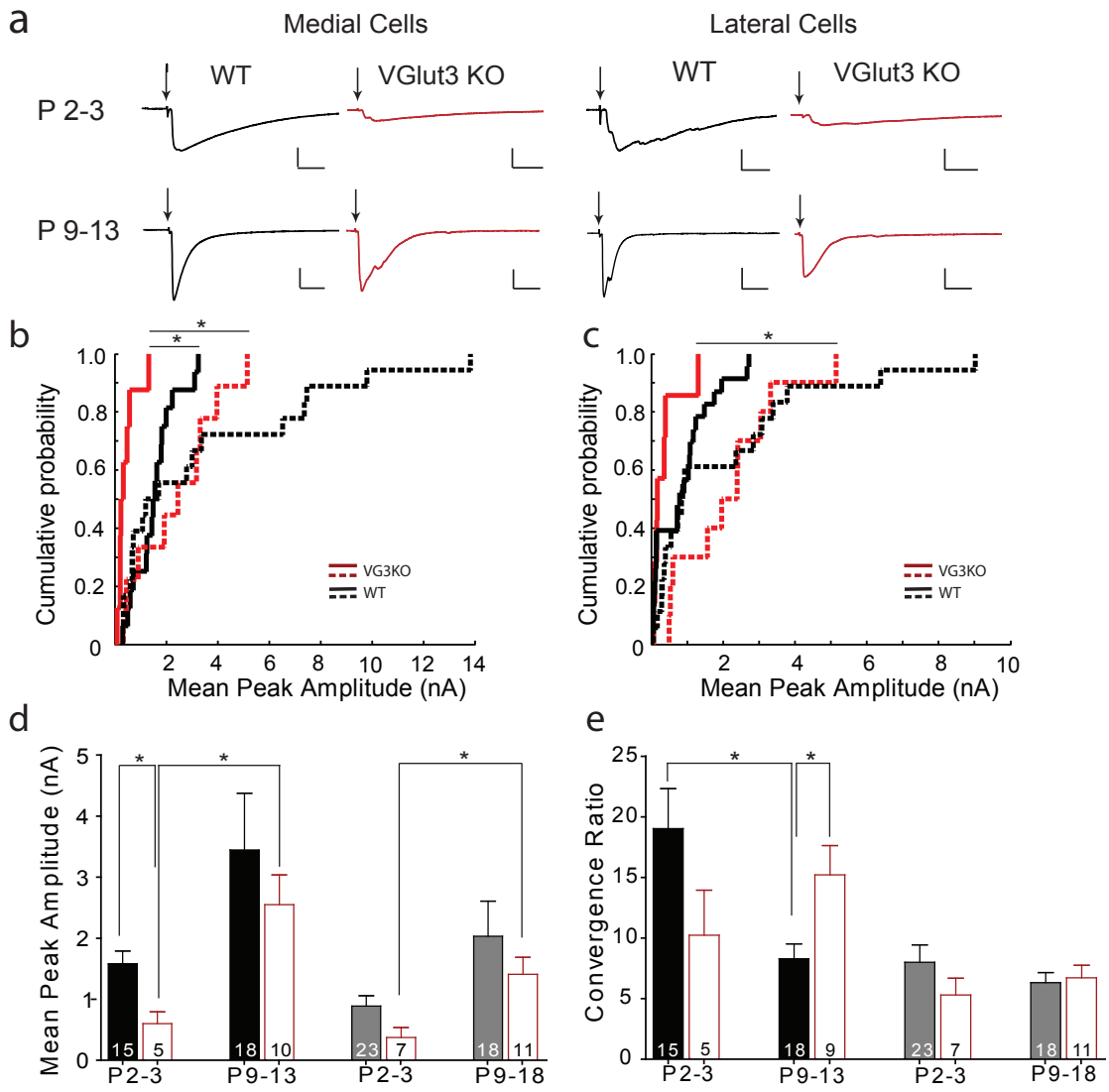

Figure 4.4: **Maximal stimulation responses of medial and lateral MNTB-LSO projections in wildtype and *vglut3-/-* mice**
(a) Average(black) and raw(grey) traces in medial and lateral LSO cells of WT and VG3KO animals at different ages.
(b) Cumulative probability distribution of maximal amplitudes of medial cells of WT and VG3KO animals at different ages.(Medial: P 2-3= 0.002, P 9-13= 0.67, KS test)
(c) Cumulative probability distribution of maximal amplitudes of lateral cells of WT and VG3KO animals at different ages. (Lateral: P 2-3= 0.13, P 9-13= 0.39, KS test)
(d) Population data showing the mean peak amplitude in medial and lateral LSO in response to maximal MNTB stimulation at different ages.
(e) Population data for convergence ratio of medial and lateral LSO cells of WT and VG3KO animals at different ages.

Table 4.2: **Summary of maximal stimulation response amplitudes at different ages for wild type and *vglut3-/-* animals.** The p values represent comparisons between wild type and VG3KO LSO cells.

Genotype	Medial P 2-3	Medial P 9-13	Lateral P 2-3	Lateral P 9-13
vglu3 +/+	1.58± 0.21 nA (n=16)	3.45 ± 0.93 nA (n=18)	0.89±0.17 nA (n= 23)	2.03± 0.58 nA (n=18)
vglu3 -/-	0.60 ± 0.20 nA (n= 5)	2.5 ± 0.5 nA (n= 10)	0.37 ± 0.17 nA (n= 7)	1.41 ± 0.28 nA (n=11)
P Values	**0.02 (Student's t test)**	0.71 (Mann-Whitney test)	0.35 (Mann-Whitney test)	0.83 (Mann-Whitney test)

Table 4.3: **Summary of convergence ratios at different ages for wild type and VG3KO.** The p values represent comparisons between wild type and VG3KO LSO cells.

Genotype	Medial P 2-3	Medial P 9-13	Lateral P 2-3	Lateral P 9-13
vglu3 +/+	19:1	8:1	8:1	6:1
vglu3 -/-	10:1	15:1	6:1	7:1
P Values	0.16	**0.008**	0.33	0.76

4.3 Discussion

From previous studies it has been shown that the glutamate co-release from the MNTB inputs is crucial for the proper strengthening and refinement of the MNTB-LSO connections (Noh et al., 2010). From my present study using *vglut3-/-* mice, it is evident that the role of glutamate co-release in the refinement of the MNTB-LSO circuit varies in a tonotopy specific manner. Though glutamate is co-released in both the medial and the lateral parts of the circuit, it seems to execute very different functions along the tonotopic axis. While glutamate is essential for the

functional elimination and strengthening of medial MNTB inputs during the first two weeks of development, it seems to be non-essential for the strengthening of lateral inputs in the MNTB-LSO circuit. The exact function of the glutamate co-release in the lateral part of the circuit would need further detailed investigations. My study further showed a significant decrease in the maximal synaptic response of the medial LSO cells even at P 2-3, suggesting possible deficits in circuit formation. Since the previous report (Noh et al., 2010) did not show this difference, a possible explanation for my observation may be worsening of circuit formation in the knockout mice with advanced generations (genetic drift) (Specht and Schoepfer, 2001).

In the medial MNTB-LSO connections, it is hypothesized that GABA and glycine, which are depolarizing at the early postnatal ages, help to depolarize the postsynaptic LSO cell and may release the magnesium block of the postsynaptic NMDARs. The co-released glutamate may then cause homosynaptic activation of the NMDARs leading to calcium influx into the LSO cell. This NMDAR mediated calcium influx may help in plasticity mechanisms in the MNTB-LSO synapses. The lack of glutamate co-release in the medial cells may cause loss of such plasticity mechanisms, which is reflected in the deficits in the strengthening of the medial MNTB-LSO projections. However, the lack of any effect of glutamate loss in the lateral MNTB-LSO projections suggest that these inputs strengthen using a glutamate independent mechanism. A closer examination of the changes in the strength of medial MNTB inputs in *vglut3-/-* mice show a 2 fold increase in the first two postnatal weeks, even in the absence of

glutamate co-release (Noh et al., 2010). This observation also suggests the possibility of the presence of a glutamate independent mechanism of strengthening. Thus it seems that while the medial MNTB inputs strengthen by a glutamate dependent as well as a glutamate independent process, the lateral inputs strengthen only using the glutamate independent mechanism.

Repeated bursts of activity have been suggested to be a possible mechanism which helps in strengthening of inhibitory inputs in the rat hippocampus (Gubellini et al., 2001). Spontaneous cochlear activity during the pre-hearing stages may provide synaptic activity to the downstream nuclei of the auditory pathway (Tritsch et al., 2007). This spontaneous but patterned activity is thought to be important for guiding the developmental changes that happen in the downstream nuclei (Tritsch et al., 2010; Tritsch and Bergles, 2010). Thus repeated firing of the MNTB neurons in response to spontaneous activity coming from the cochlea maybe a candidate mechanism helping in the strengthening of the lateral MNTB-LSO projections. However, in *vglut3-/-* mice, the inner hair cells in the cochlea are unable to release glutamate (Seal et al., 2008), which may impair spontaneous activity in the cochlea. However, the lack of such cochlear spontaneous activity does not underlie the lack of strengthening observed in the medial cells of *vglut3-/-* animals as evident from the normal strengthening of medial connections in Pachanga or *otoferlin -/-* mice (Noh et al., 2010). So it seems improbable that cochlear spontaneous activity underlies the normal strengthening of the lateral connections in the *vglut3-/-* animals.

Spontaneous firing from the spiral ganglion cells (SGC) may be another candidate mechanism which may help in strengthening of the lateral MNTB-LSO connections. The spiral ganglion cells are spontaneously active at P 2-3 and the pattern of activity transform into bursting at around P 5 (Tritsch and Bergles, 2010). This spontaneous activity causes the activation of the MNTB neurons during the first two postnatal weeks (Tritsch et al., 2010; Tritsch and Bergles, 2010). Along with incoming activity, the MNTB neurons also undergo maturation of their cellular and physiological properties during this period (Hoffpauir et al., 2010). Between P 0-4, each MNTB neuron exhibits tonic firing properties in response to synaptic depolarization. After P 4 the MNTB neurons begin to fire in a phasic manner in response to synaptic input and by P 6 almost 100% of the MNTB activity is phasic (Hoffpauir et al., 2010). Additionally the calyces providing synaptic input to the MNTB cells also transform from multi-innervation to mono-innervation during the first postnatal week such that by P 4 most MNTB neurons are mono innervated (Holcomb et al., 2013; Hoffpauir et al., 2006). These observations suggest that there may be an increase in the synchrony of MNTB neuronal spiking after P 4. This synchronous phasic firing of MNTB inputs could help in strengthening the MNTB-LSO synapses in the lateral part of the circuit. Further detailed investigations would be necessary to elucidate how the lateral MNTB-LSO inputs strengthen. But from the above results it is clear that glutamate co-release from the MNTB terminals does not seem to play a critical role in the process of pre-hearing strengthening of lateral MNTB-LSO inputs.

Chapter 5

Role of GABA co-release in the pre-hearing refinement in the MNTB-LSO circuit

5.1 Introduction

GABA: A fast inhibitory neurotransmitter

Gamma amino butyric acid (GABA) is one of the primary fast inhibitory neurotransmitters in the central nervous system (Galanopoulou, 2008; Ben-Ari et al., 2007). It is derived from the excitatory neurotransmitter glutamate as a result of a decarboxylation reaction by the enzymes GAD65 and GAD67 (Huang, 2009; Soghomonian and Martin, 1998). GABA can exert its effects by binding to the metabotropic $GABA_B$ receptors or to ionotropic $GABA_A$ or $GABA_C$ receptors (Bormann, 2000). Ionotropic $GABA_A$ receptors are permeable to chloride ions and to a lesser extent, bicarbonate ions while metabotropic G-protein coupled $GABA_B$ receptor activation causes changes in membrane conductance (Ben-Ari et al., 2007).

The fast inhibitory activity of GABAergic transmission mainly occurs via postsynaptic $GABA_A$Rs which are heteropentameric chloride channels with several subunit classes (Huang, 2009; Michels and Moss, 2007). The subunit composition of $GABA_A$Rs vary extensively with age and tissue (Fritschy et al., 1994; Sieghart et al., 1999). Most of the postsynaptic receptors are composed of two α , two β , and one γ subunit (McKernan and Whiting, 1996). In the mammalian brain, there are 19 different genes (α 1-6, β 1-3, γ 1-3, δ , ϵ, ρ 1-3, π) encoding different subunits which assemble to form functional receptors of various subunit combinations (Mohler et al., 1998; Olsen and Sieghart, 2009; Sarto-Jackson and Sieghart, 2008). The presence of an α and a β subunit has been shown to be essential for the expression of functional

$GABA_A$Rs (Mohler et al., 1998). In the immature brain, $\alpha 2$ subunit containing $GABA_A$Rs are most predominant which are later replaced by $\alpha 1$ subunit containing $GABA_A$Rs as the circuit matures to adult configuration (Fritschy et al., 1994). In contrast, staining for β 2,3 subunit is ubiquitous at all developmental stages (Fritschy et al., 1994).

Depolarizing-hyperpolarizing switch

In adult neurons, on ligand binding, the $GABA_A$ receptors open to allow influx of Cl^- into the cell causing hyperpolarization of the postsynaptic neuronal membrane preventing activation of the postsynaptic cell due to excitatory inputs. However, in the early stages of development, ionotropic GABA receptor activation mediates depolarizing currents resulting from chloride ion efflux, activating calcium sensitive signaling pathways that may cause synaptic changes in the postsynaptic cell (Huang, 2009; Galanopoulou, 2008; Ben-Ari et al., 2007; Leinekugel et al., 1995; Ben-Ari, 2002). The depolarizing nature of the GABAergic transmission in the early developmental stages is due to high levels of intracellular chloride maintained by high NKCC1 expression. The nature of GABAergic signaling changes from depolarizing to hyperpolarizing current during the course of development due to increased extrusion of intracellular chloride resulting from upregulation of KCC2 chloride transporter expression (Huang, 2009; Rivera et al., 2005). This change (depolarizing to hyperpolarizing) is found to be tightly correlated to the time course of the maturation of developing neurons. Thus the depolarizing action of GABA has been hypothesized

to be very important for proper maturation of neuronal circuits.

Study of the role of GABA in refinement

In certain inhibitory circuits (including the MNTB-LSO circuit in the auditory brainstem), transient co-release of two inhibitory neurotransmitters, GABA and Glycine, is seen during the early developmental stages (Jonas et al., 1998; Nabekura et al., 2003) even though after maturation of these circuits, the inhibitory transmission system switches to primarily glycinergic neurotransmission (Kotak et al., 1998; Korada and Schwartz, 1999). Hence the MNTB-LSO circuit is ideal for the study of the significance of such additional GABAergic signaling during development and would help to elucidate the role of GABAergic signaling in the maturation of inhibitory neuronal synapses.

In the adult animal, the MNTB-LSO inhibitory circuit is predominantly glycinergic. But in the earliest postnatal stages, GABA is the primary neurotransmitter in this circuit. As the GABAergic component declines from postnatal day 1 (P 1) to postnatal day 14 (P 14) (Fig 5.1, 5.2 bottom panel), the glycinergic component gradually grows stronger such that after P 14 the circuit becomes mainly glycinergic (Kotak et al., 1998; Korada and Schwartz, 1999). This change in the nature of inhibitory transmission in the MNTB-LSO circuitry is reflected in the decrease in GABA containing terminals as seen by a decrease in staining for GAD65 and $\beta 2/3$ subunit containing $GABA_A$Rs while gephyrin and GlyR immunoreactivity increases (Kotak et al., 1998). The transient duration of GABA co-release also coincides with

the stage of functional refinement of the MNTB-LSO circuit. During this period (P 1 to P 14) functional silencing of inputs and strengthening of maintained inputs occur, thus narrowing and refining the tonotopic arrangement of the MNTB projections to the LSO cells. This produces 2-fold sharper tonotopic specificity equivalent to that found in adult (Kim and Kandler, 2003). Thus it seems likely that the transient GABAergic signaling may play a key role in the maturation of this inhibitory circuit.

The role of GABAergic neurotransmission has been demonstrated in the process of refinement of excitatory as well as inhibitory circuits in different brain areas. GABAergic signaling is known to be crucial for the proper refinement of the excitatory climbing fiber- Purkinje cell (CF-PC) circuit in the cerebellum (Nakayama et al., 2012). In the cerebellum, the Purkinje cell receives robust $GABA_A$ receptor mediated somatic inhibition from the molecular layer interneurons. The proper strength of this heterosynaptic inhibition is crucial for the elimination of supernumerary synapses of climbing fibers on to single Purkinje cells that occurs between P 10 and P 16. In the cerebellum, at P 5-9, each Purkinje cell (PC) receives numerous excitatory climbing fibers. During P 10-12 one of these climbing fibers (CF) become stronger than the others and causes large influxes of calcium into the postsynaptic PC via P/Q type voltage gated calcium channels (VDCCs). As the disparity in strengths of climbing fibers emerges, the PC receives inhibitory GABAergic input from basket cells and stellate cells in the molecular layer as well as recurrent projections from PCs. The GABAergic input, specifically from the basket cells, inhibits the small

calcium influxes from the weak climbing fibers and this may help in depressing them (Nakayama et al., 2012). In absence of this Gad67 dependent GABAergic input, even weak climbing fibers generate enough calcium response in the PC to survive, leading to multiple innervation in the mature CF-PC circuit.

The requirement of proper GABAergic signaling has also been elucidated in shaping the innervation patterns present in the inhibitory circuits in the visual cortex. In the visual cortex, the pyramidal cells receive extensive perisomatic inhibitory innervation from the basket interneurons. This perisomatic innervation is highly dependent on neuronal activity as evident by its significant retardation upon blocking of activity by tetrodotoxin application (Chattopadhyaya et al., 2004, 2007). Neuronal activity regulates Gad67 mediated GABA synthesis in the basket cell synapses by regulating levels of Gad67 expression and activity (Chattopadhyaya et al., 2007). Low GABA release in the basket cell synapses has been implicated in the impaired regulation of the GABAergic axonal and synaptic morphogenesis in these inhibitory circuits.

In view of the above evidences of the major role of GABA in the synaptic organization of excitatory as well as inhibitory circuits, the presence of transient GABAergic neurotransmission in the MNTB-LSO circuit during the period of its pre-hearing refinement (Fig 5.1) suggests a regulatory role of GABA in the process of refinement in this circuit. One way to investigate the role of GABAergic signaling in the MNTB-LSO circuit is to quantify the effects of the absence of GABAergic signaling on the refinement of this circuit. But GABAergic transmission has been shown to be very

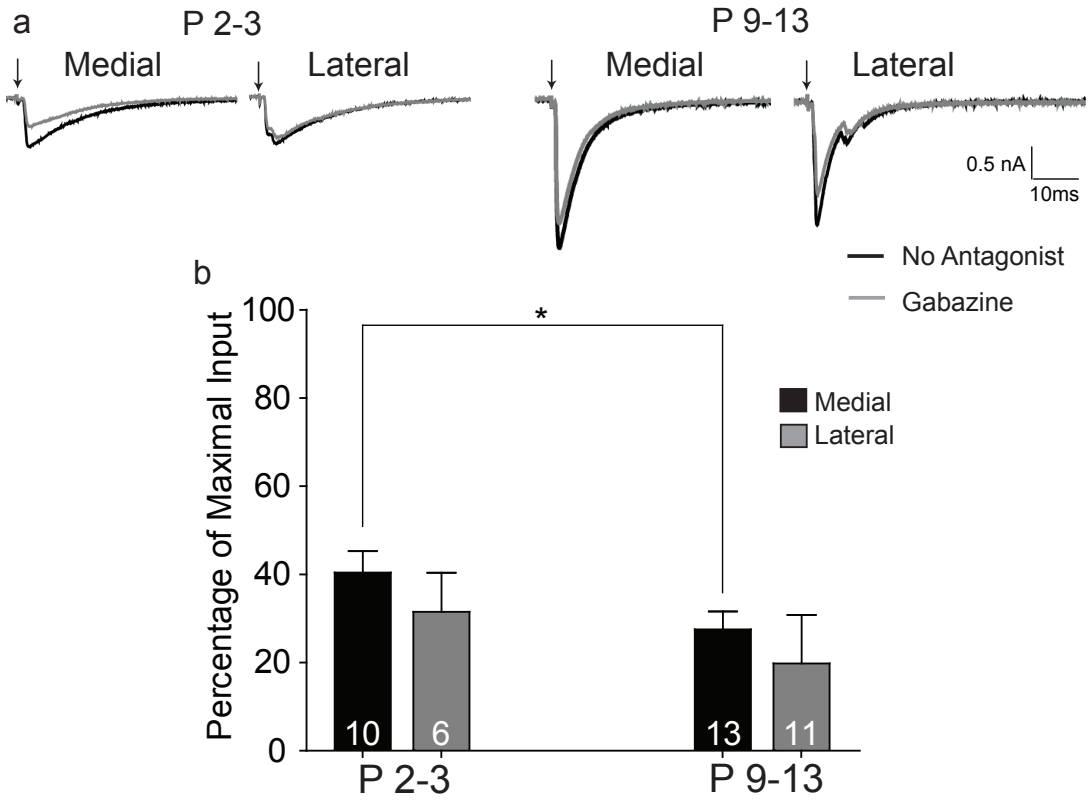

Figure 5.1: **Transient GABAergic transmission in the medial and lateral MNTB-LSO projections**
(a) Average example traces before (black) and after (grey) pharmacological block of $GABA_A$ receptors in medial and lateral LSO cells .
(b) Population data showing the mean peak amplitude of GABAergic transmission in medial and lateral LSO in response to maximal MNTB stimulation at different ages.

important for the early stages of the development of the nervous system (Ben-Ari et al., 2007). Gad67 mediated GABA synthesis constitutes almost 90% of GABA production in the developing neurons (Asada et al., 1997). Gad65 mediated GABA synthesis is restricted to more mature nerve terminals and is recruited only during enhanced synaptic activity (Dupuy and Houser, 1996; Namchuk et al., 1997; Kaufman et al., 1991). Global knockout of GABA transmission (GAD67 knockouts) in the brain causes lethality at birth by causing birth defects like cleft palate (Asada et al., 1997). However no other structural abnormalities are found in the gross histology of the brains of these knockout animals (Asada et al., 1997). This indicates that GABA transmission may be more important for proper functioning of neurons and their synapses than their initial formation. Thus to study the role of GABA in the neonatal brain but avoid lethality at birth, transgenic mice with conditional or tissue specific knockout of GABA transmission in the brain are required. Thus to study the role of GABA in the refinement of the MNTB-LSO circuit, it would be helpful to have GABA transmission knocked out specifically in this circuit. In this study, I have used three approaches to knockout GABAergic transmission in the MNTB-LSO circuit which are discussed in the result section below. The conditional LSO specific knockout animals were then used for electrophysiology and immunohistochemistry experiments to elucidate the role of GABA in the developmental refinement of the MNTB-LSO circuit.

5.2 Results

5.2.1 Conditional knockout of GABAergic transmission in MNTB-LSO circuit using Sert-Cre mice

Global knockouts of GABAergic signaling lead to lethal phenotypes. Thus to study the role of GABA in the developmental refinement of the MNTB-LSO circuit, it was important to create conditional LSO specific $GABA_AR$ knockouts by LSO specific expression of Cre and targeting the $\beta 3$ subunit of the $GABA_AR$ in the LSO.

Conditional knockout of $GABA_AR$ $\beta 3$ subunit in LSO cells is possible using mice in which the exon 3 of the $\beta 3$ subunit is flanked by LoxP sites (floxed) (Ferguson et al., 2007). Genetic breeding of such floxed mice with strains of mice expressing Cre enzyme in an LSO specific manner will result in LSO specific knockout of $GABA_AR$ $\beta 3$ subunit in the progeny. LSO cells are known to accumulate serotonin, another important neurotrophic neurotransmitter, with the help of expression of serotonin transporters during the first two postnatal weeks (Thompson, 2008; Thompson and Thompson, 2009a,b). Mice strains expressing Cre enzyme under the serotonin promoter have been developed (Zhuang et al., 2005). These mice (Sert-Cre mice) produce Cre enzyme only in cells that express serotonin transporters. Thus a part of the progeny of a cross between the floxed $GABA_AR$ $\beta 3$ mice and Sert-Cre mice will lack $GABA_AR$ $\beta 3$ subunits in the neuronal cell populations that express serotonin transporters. In the auditory system, LSO is known to express high levels of serotonin transporter during P 1 - P 14, and hence should

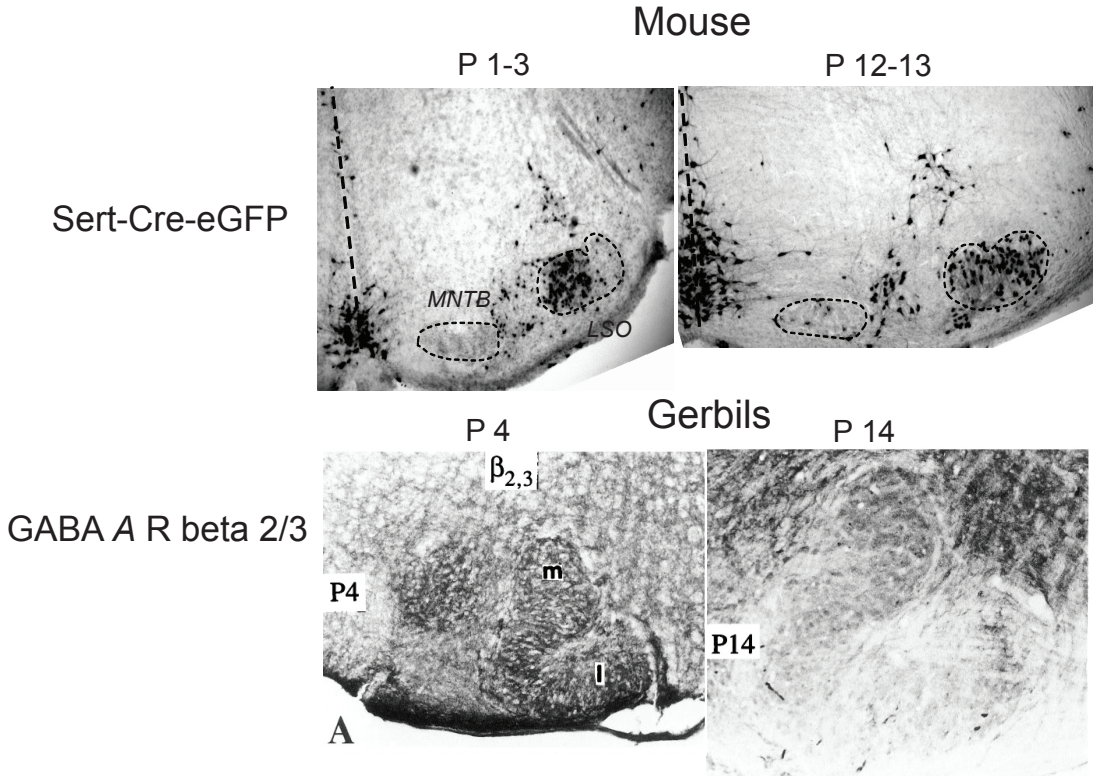

Figure 5.2: **Expression of eGFP in the LSO under the promoter for serotonin transporter**
(Top panel) DAB stained brainstem sections of Sert-Cre-eGFP mice showing expression of Sert-Cre at different ages (Kandler lab, unpublished data). Darkly stained cells are GFP positive.
(Bottom panel) DAB stained sections of gerbil LSO showing expression of $GABA_AR$ $\beta 2/3$ subunit at different ages (modified from Kotak et al, 1998). Dark staining represents $GABA_AR$ $\beta 2/3$ subunit expression.

be affected by Cre expression under the serotonin transporter promoter (Thompson, 2008). Thus in these mice, LSO cells will lack the $GABA_AR$ during the precise period when the GABA transmission is most abundant in the MNTB-LSO circuit. Other serotonergic cells in other parts of brain may also have $GABA_AR$ $\beta 3$ subunits knocked out but they are not expected to influence the results of my investigation. To identify the cells lacking $GABA_AR$ $\beta 3$ subunits, a floxed $GABA_AR$ mouse carrying a marker gene is needed for the crosses. To generate $GABA_ARKO$ mice with a reporter, the floxed $GABA_AR$ mice were crossed with Rosa-tomato (Gt(ROSA)26Sor$^{tm4(ACTB-tdTomato,-EGFP)Luo}$/J)(Jaxson Mice) mice which carries floxed td-Tomato reporter gene. A part of the progeny of such a cross was expected to carry the floxed $GABA_AR$ $\beta 3$ gene as well as the floxed *tdTomato* and *eGFP* gene. When these mice were crossed to Sert-Cre mice, some of the progeny would have Cre expressing cells which have floxed out *td-Tomato* gene and floxed out $GABA_AR$ $\beta 3$ gene and were now expressing the *eGFP* gene (Fig 4.2 top panel).

However, I encountered difficulties in genotyping the floxed $GABA_AR$ mice. The inability to positively genotype the homozygous floxed $GABA_AR$ mice forced me to abandon this approach of creating the conditional knockouts for $GABA_AR$ in LSO.

5.2.2 Conditional knockout of GABAergic transmission in MNTB-LSO circuit using adenoviral injection in the IC

As an alternative approach to creating a $GABA_AR$ knockout using Mendelian

breeding, I used viral injection of adenovirus to express Cre directly in the LSO cells of the floxed $GABA_AR$ mice. Retrograde transport of recombinant adenovirus in the central nervous system has been shown in previous studies (Kuo et al., 1995). I took advantage of the retrograde transport of the adenovirus and injected the adenovirus carrying Cre and GFP into the Inferior Colliculus (IC). The retrograde transport of the virus facilitated uptake of the virus through the synapses of LSO cells projecting to the IC. The viral DNA was then transported to the nucleus of the LSO projection neurons and integrated into the rodent DNA. The expression of this viral genome by the LSO cell's own cellular machinery led to expression of Cre and GFP in the LSO cells that assimilated the virus. The Cre expression in the LSO cells of floxed $GABA_AR$ mice was hypothesized to cause excision of the floxed genome and cause knockout of the $GABA_AR$ $\beta 3$ subunit leading to $GABA_AR$ knockout. The cells expressing the adenoviral Cre were identified by their GFP expression seen as dark staining in the DAB stained slices.

Since the injections were done in P1 pups, their survival after the injection mostly depended on the nursing by the mother. The acceptance rate of injected pups by the mother was very low. Thus the survival rate of the injected pups was also very low. Different positions for injections within the IC were also tested so that maximum number of LSO cells would get labelled. I observed that small focal injections targeted towards the LSO projection area in the central nucleus of the IC did not label any LSO cells. So I injected the whole IC using a Hamilton syringe which caused a large area

of injury in the IC. The injury in the projection endings in the IC greatly facilitated the uptake of virus.

GFP expression was observed in retrogradely labeled cells within 3 days post injection. With the adenoviral injections in the IC, I found a few cells in the LSO that were positive for GFP expression (Fig 5.3). However, other auditory nuclei which are known to have more abundant projections to the IC were also found to be labeled. For example, we found intense labeling in the deep layer of dorsal cochlear nucleus (DCN) and anterior ventral cochlear nucleus(AVCN) as well as the dorsal nucleus of lateral leminscus (DNLL) (See Fig. 5.3).

LSO receives inhibitory input from the MNTB and direct excitatory synaptic input from the AVCN. The expression of GFP (and hence Cre) in the AVCN was not desirable because AVCN cells would also lose the GABAergic activity in their circuit. This may lead to aberrant synaptic activity in the AVCN-LSO projections causing undesired effects on the development and refinement of the MNTB-LSO projections. Such upstream effects on the refinement of the MNTB-LSO projections would complicate the interpretations of the changes in the refinement of the circuit due to loss of GABAergic component of the MNTB inputs. In view of these possible problems in circuit activity and extremely low yield of GFP positive LSO cells, the approach of adenoviral injections in the IC was abandoned.

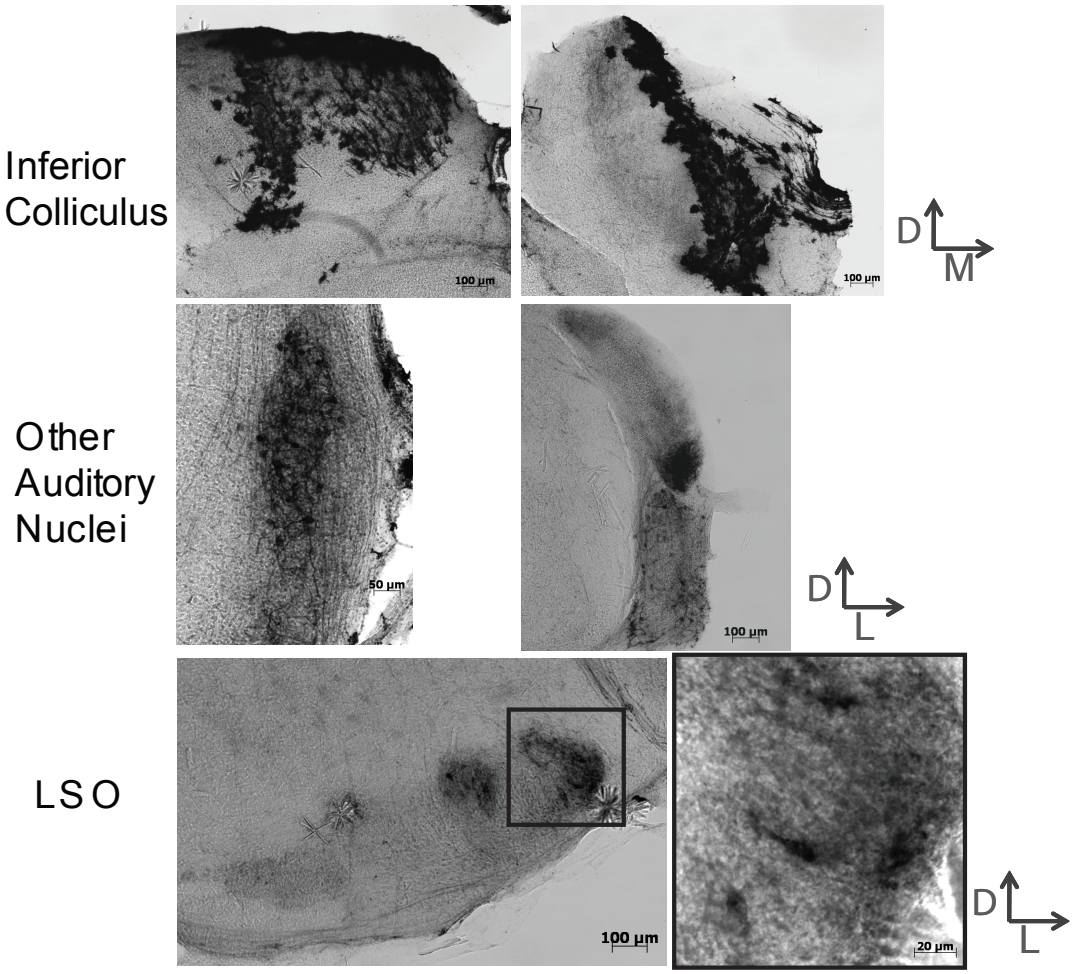

Figure 5.3: **Retrograde expression of eGFP in the LSO after injection of Ad-Cre virus in the IC at P 1**
DAB stained sections of different nuclei in the auditory brainstem of mice at different ages . The darkly stained cells in the different auditory nuclei are positive for GFP expression due to retrograde expression of the recombinant Adenovirus injected in the IC. The top panel shows the injection site in the central nucleus of the IC. The lower panels show GFP positive cells in different auditory nuclei upstream and downstream of LSO.

5.2.3 Conditional knockout of GABAergic transmission in the MNTB-LSO circuit using Vglut3-Cre and *gad1*$^{fl/fl}$ mice

To knockout the GABAergic component specifically in the LSO, a third approach was taken. A transgenic mouse graciously gifted by Dr. Rebecca Seal (University of Pittsburgh) showed expression of Cre recombinase under the promoter of the glutamate transporter VGlut-3. VGlut-3 is expressed in the GABA/glycinergic terminals of MNTB during the first two weeks of postnatal development (Gillespie et al., 2005; Noh et al., 2010). After crossing the VGlut-3-Cre mouse with a reporter mouse (Gt(ROSA)26Sor$^{tm4(ACTB-tdTomato)Luo}$/J), the progeny mice showed robust Cre expression in the MNTB cells which turned red due to expression of td-Tomato (See Fig. 5.4). Numerous tdTomato expressing projections, presumably of these Cre expressing MNTB neurons, were also found in the LSO.

Although the whole MNTB looked red due to expression of td-Tomato, there seemed to be a gradient of expression of Cre along the tonotopic axis of the MNTB. The lateral MNTB cells seemed to be expressing Cre (and hence td-Tomato) to a greater degree than the medial cells. This medial (low) to lateral (high) gradient of expression was also evident in the td-Tomato filled neuronal terminals in the LSO. The lateral part of the LSO showed greater td-Tomato expression than the darker medial part (Fig. 5.4). This pattern of expression was reminiscent of the VGlut-3 expression pattern in the LSO as seen by immunohistochemistry (Fig. 4.1).

Cre expression under VGlut-3 promoter was also noted in cells of DCN, cerebel-

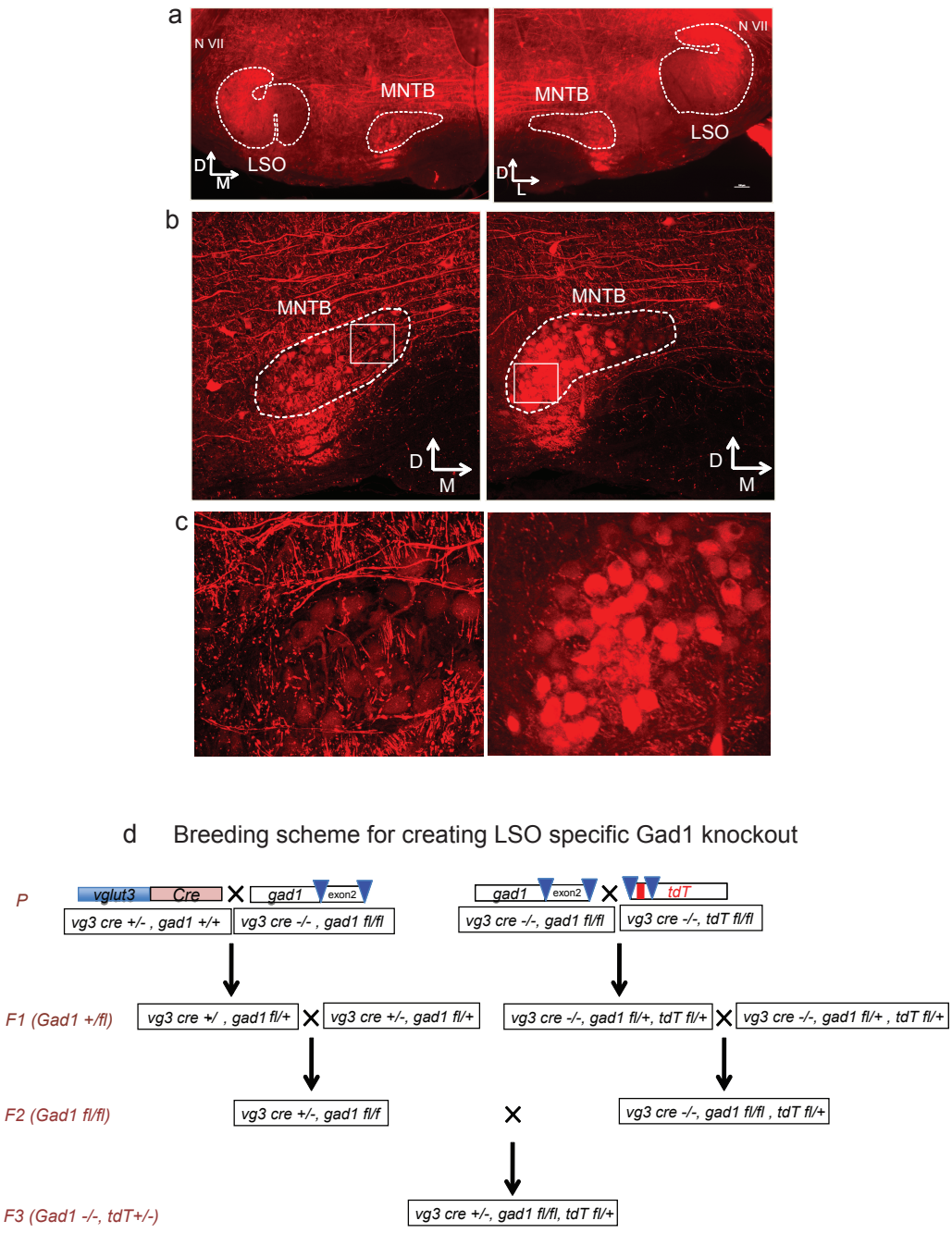

Figure 5.4: **LSO specific Gad1 knockout using VGlut3-Cre mice**
(a) Fluorescent sections of auditory brainstem of VGlut3-Cre-td-Tomato mice at P30 showing tdTomato expression in the MNTB and LSO.
(b) Higher magnification images of MNTB of VGlut3-Cre-td-Tomato mice showing medio-lateral gradient of tdTomato expression.
(c) 60X confocal images of MNTB cells in the white boxes in (b). Left: MNTB cells showing low expression of tdTomato, Right: MNTB cells showing higher expression of tdTomato.
(d) Schematic representation of the breeding scheme for creating LSO specific Gad1 knockout mice.

lum, and the serotonergic raphe. The IC also showed neuropil filled with fluorescent td-Tomato. However, the AVCN-LSO projections did not express the VGlut-3-Cre. No cells in the AVCN showed any td-Tomato expression. Thus this transgenic mouse expressing Cre under the VGlut-3 promoter was chosen to create a tissue specific conditional GABA knockout in the MNTB-LSO projections.

To create the conditional knockout of GABA in the MNTB-LSO projections from the presynaptic MNTB terminals, we needed a mouse where the genes for GABA producing enzymes were floxed. We obtained a transgenic mouse from Dr. Richard Palmiter (Janelia farm) which had loxP sequences flanking the exon 2 of the *gad1* (Gad67 enzyme) gene (Chattopadhyaya et al., 2007). Thus, when crossed with the VGlut3-Cre mouse, 50% of the progeny would would express Cre in the MNTB effectively floxing out the *gad1* gene leading to a deletion of Gad1 or Gad67 enzyme in the MNTB cells. For easy identification of Cre expressing animals, a reporter gene was included while breeding the VGlut3-Cre mice with the *gad1* $^{flox/flox}$ mice. The complex breeding scheme of creating the triple transgenic is shown in Fig. 5.4 (d).

5.2.4 GABAergic transmission is intact in the medial MNTB-LSO circuit of *gad1-/-* (Gad1KO) mice

From the breeding scheme mentioned in Fig 5.4 (d), I obtained transgenic animals which were genotypically Cre positive, homozygous for floxed *gad1* gene (*gad1-/-*) and tdTomato positive. To test if the GABAergic component of the MNTB input was deleted or decreased, I recorded maximal synaptic responses of the LSO cells to

MNTB stimulation before and after addition of the $GABA_AR$ blocker SR95530 (also known as Gabazine). I recorded the Gabazine sensitive component of the MNTB input in the medial LSO cells for both wildtype and the Cre +ve animals at P 2-3 and P 9-13 age points. I found no significant difference in the percentage of the maximal synaptic response that was Gabazine sensitive in wildtype and Cre +ve animals. The gabazine sensitive components in the medial LSO cells of different ages are summarized in Table 1 and Figure 5.5.

The decay constant of a GABAergic synaptic response is much longer than that of a purely glycinergic response (Nabekura et al., 2003). The decay constant of the synaptic response in LSO is much longer at P 2-3 when the synapses are primarily GABAergic. Gradually as the synapses become primarily glycinergic, at P 9-12, the decay constants of the responses become much shorter. So if there is any change in the proportion of GABA and glycine in the MNTB-LSO projections, it should be reflected in the decay constants of the maximal responses. I analyzed the decay constants of the maximal synaptic responses of the medial LSO cells in the wildtype and Gad1KO mice at P 2-3 and P 9-13. At P 2-3, the decay constant (tau) of the maximal response in the wild type animals was 101.2 ± 22.16 (n=12). The tau of Gad1KO animals was found to be 43.20 ± 4.779 (n=6). However the littermates of the transgenic *gad1 fl/fl* mice which were Cre -ve (hence with wildtype expression of Gad1) also showed a decay constant of 37.87 ± 14.70 (n=2). Thus it seems that the low decay constant is not specific to the Cre+ve animals and hence probably does

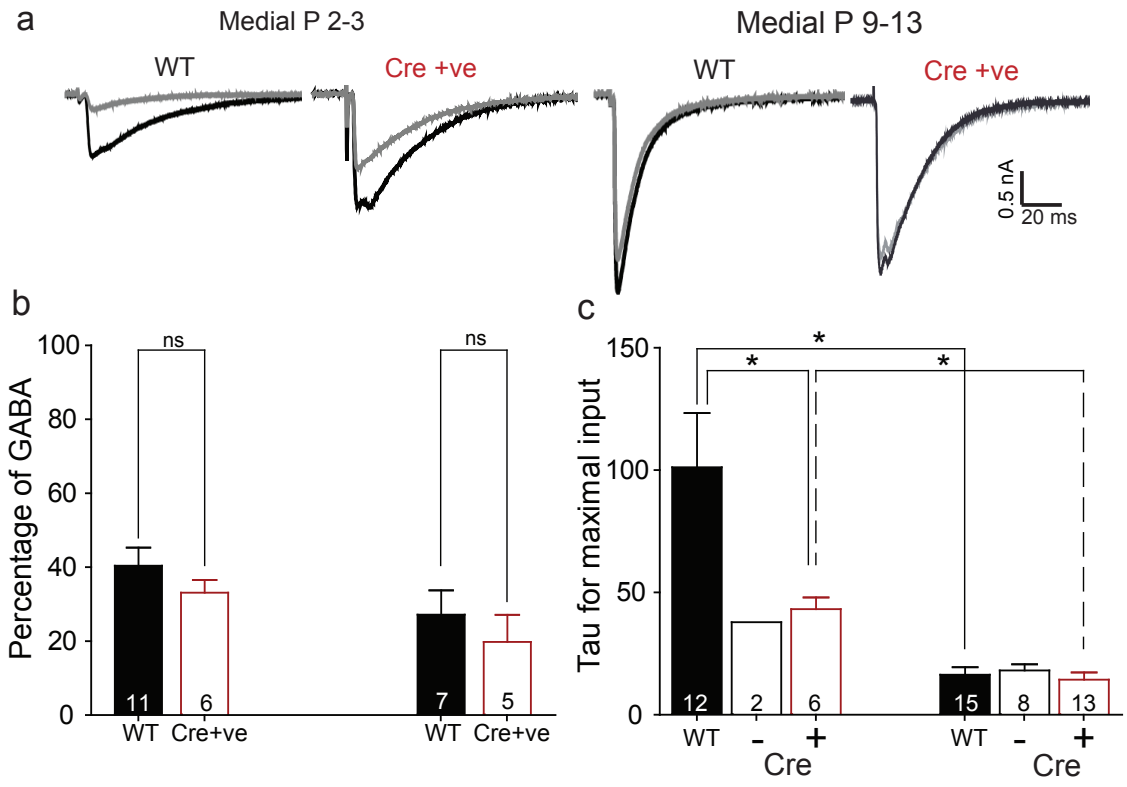

Figure 5.5: **GABAergic transmission is unchanged in the medial MNTB-LSO projections in *gad1-/-* mice**
(a) Average traces of synaptic responses of medial LSO cells for maximal MNTB stimulation.
(b) Population data of Gabazine sensitive component of the maximal synaptic response of medial LSO cells of wildtype and Gad1KO animals.
(c) Decay constants of maximal responses of medial LSO cells of wild type, Cre-ve and Cre+ve animals at different ages.

not correlate to any change in composition of the synaptic input. At P 9-13, the decay constant of the maximal synaptic input for the wild type animals was 16.34 ± 3.081 (n=15) which was not significantly different from the decay constant for Gad1KO animals (14.33 ± 3.007 , n=13, p value= 0.64, Mann-Whitney test). Since there was no significant difference in the kinetics of the maximal synaptic responses of medial LSO cells between Cre -ve (wildtype expression of Gad1) and Cre +ve (Gad1KO) animals at P 2-3, the observed difference between the decay constants of wildtype animals and Cre +ve or Cre-ve animals is attributed to a difference in strain. Thus there was no indication of decrease in Gad1 evident from examining the decay constants.

Thus it is evident that even though the obtained transgenic mice progeny shows the presence of the genes for VGlut-3-Cre and floxed *gad1* alleles, phenotypically the release of GABA is not altered in these mice. Such absence of phenotype can be seen if there is compensation for GABA production by the over expression of Gad2 (Gad65) enzyme. Since GABA is a very important neurotrophic molecule which is essential for the proper development of the brain, the loss of Gad1 enzyme may have been compensated for in the surviving members of the litter. Thus from the recording experiments it was clear that there was no significant loss of GABAergic component of the MNTB input to the medial LSO in the genotypically Gad1 knockout (Gad1KO)

Table 5.1: **Summary of Gabazine sensitive component of medial MNTB-LSO projections at different ages for wild type and Gad1-/- animals.** The p values represent comparisons between wild type and Gad1-/- LSO cells.

Genotype	Medial P2-3	Medial P9-13
Gad1 +/+	40.39 ± 4.894% (n=11)	27.14 ± 6.59% (n=6)
Gad1 -/-	33.12 ± 3.40% (n=7)	19.79 ± 7.33% (n=5)
P Values	0.29 (Student's t test)	0.53 (Mann-Whitney test)

mice.

5.2.5 Medial MNTB inputs strengthen normally in the *gad1-/-* mice

The strengths of single MNTB inputs are known to increase by almost 4 fold during the first two weeks of development. The transient GABAergic input in the MNTB-LSO circuit before hearing onset is hypothesized to help in the pre-hearing strengthening of these MNTB inputs. It was unclear whether the Gad1KO animals showed any deficits in the strengthening of individual MNTB inputs. Even though there was no significant difference in the GABAergic component in the Gad1KO mice compared to the wildtype mice, I recorded the strengths of the single inputs in the medial MNTB-LSO projections as a part of the blind study. The strength of the single input was estimated from the synaptic amplitude of the postsynaptic LSO cell in response to minimal stimulation of the MNTB in wild type and Gad1KO animals of age P 9-13, i.e around hearing onset (Fig 5.6).

The minimal amplitude of the synaptic responses of medial LSO cells at P 9-13 in

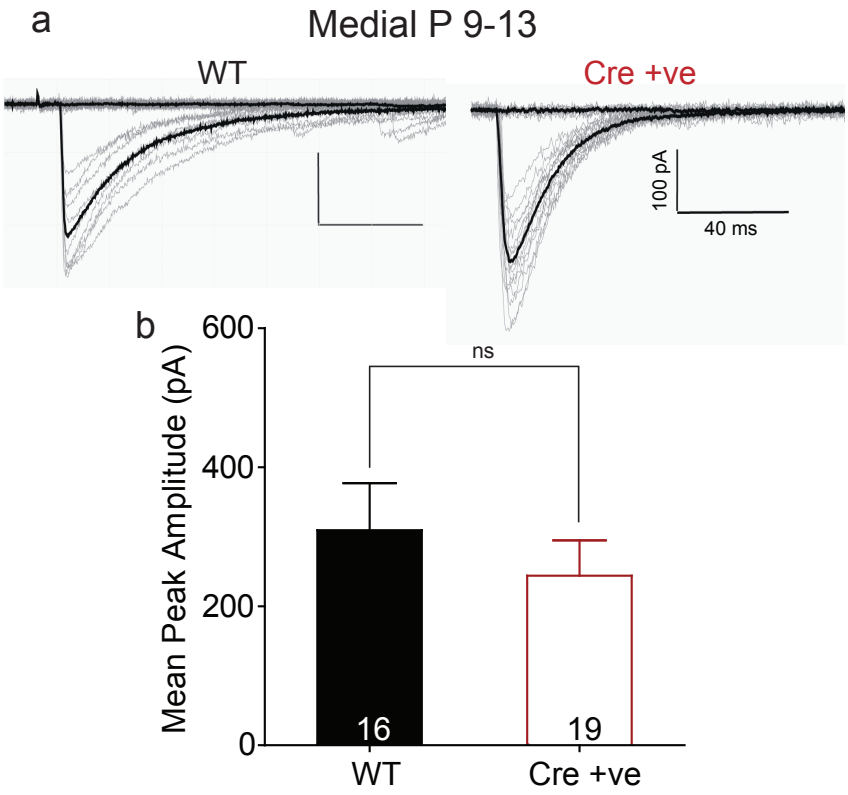

Figure 5.6: **Minimal stimulation responses of medial and lateral MNTB-LSO projections in wildtype and *gad1-/-* mice**
(a) Average example traces before (black) and after (grey) pharacological block of glutamate receptors in medial and lateral LSO cells .
(b) Population data showing the mean peak amplitude of glutamatergic transmission in medial and lateral LSO in response to maximal MNTB stimulation at different ages.

wild type animals was 309.2 ± 67.76 pA (n=17). The minimal synaptic responses in the medial LSO cells of Gad1KO animals was 244.0 ± 50.76 (n=19). Thus there was no significant difference in the amplitudes of the single input responses in the medial MNTB-LSO projections (p value= 0.65, Mann-Whitney test) (Fig 5.6).

There was no difference in the strengths of single MNTB inputs to the medial LSO cells between the wildtype and Gad1KO animals. Since there was no difference in the GABAergic component of the MNTB input between the wildtype and Gad1KO cells, the role of GABA in the strengthening of MNTB inputs in the first two postnatal weeks remains inconclusive from these experiments. Future studies with a transgenic animal with significantly reduced GABAergic signaling in the MNTB-LSO circuit will be required to address the role of the transient GABAergic signaling in the refinement of the MNTB-LSO circuit during pre-hearing ages.

5.2.6 Maximal input or the convergence ratio in the medial MNTB-LSO circuit is not different in *gad1-/-* mice

The peak amplitude of the synaptic response of the LSO cells to maximal MNTB stimulation gives an estimate of the cumulative input of all the MNTB inputs on to a single LSO cell. The peak amplitude of the maximal synaptic response in wild type animals increases from 1.5 nA at P 2-3 to approximately 3nA at P 9-13. This increase in synaptic amplitude is commensurate with the increase in the strength of each synaptic input that occurs during the first two postnatal weeks. The ratio between the minimal synaptic response and the maximal synaptic response gives an

estimate of the number of MNTB inputs that converge on to a single LSO cell. The convergence ratio of medial MNTB-LSO projections in wildtype animals is 19:1 at P 2-3 but become 9:1 by the time of hearing onset. This decrease in convergence ratio occurs due to functional elimination of synaptic inputs and is crucial for proper refinement of the MNTB input map to the LSO.

Table 5.2: **Summary of maximal synaptic amplitudes of the medial LSO cells of wild type and Gad1-/- animals.** The p values represent comparisons between wild type and Gad1-/- LSO cells.

Genotype	Medial P2-3	Medial P9-13
Gad1 +/+	2.19 ± 0.49 nA (n=12)	2.97 ± 0.78 (n=16)
Gad1 -/-	1.56 ± 0.49 nA (n=7)	2.64 ± 0.61 nA (n=16)
P Values	0.42 (Mann-Whitney test)	0.83 (Mann-Whitney test)

Table 5.2 summarizes the maximal synaptic amplitudes recorded from the medial LSO cells of wildtype and Gad1KO mice at P 2-3 and P 9-13. I observed that the maximal amplitude increased from P 2-3 to P 9-13 in both wildtype and Gad1KO animals (Fig. 5.7a,b). There was no significant difference in the mean peak amplitudes between the wildtype and Gad1KO animals at either of the ages. Thus from the data presented in the previous section and the present one together suggest that the strengthening of synaptic inputs occur in both wildtype and the genotypic Gad1KO to a similar extent.

Furthermore, the convergence ratios were calculated for medial LSO cells of wild

type and Gad1KO animals at P 9-13 . The convergence ratio of the wildtype animals was low (8.27 ± 1.24 (n=18)) at P 9-13 due to extensive functional elimination occurring between P 2-3 and P 5-6. The convergence ratio of the medial LSO cells of Gad1KO animals at the same age was also found to be 9.02± 1.83 (n=15) (Fig. 5.7c). So in both wildtype and Gad1KO animals the convergence ratios at P 9-13 were found to be low and approximately 9:1. Thus functional elimination occurred normally in both wild type and Gad1KO animals leading to low convergence ratios at P 9-13.

The above data together shows that the strengthening of individual inputs and functional elimination of inputs that occur in the wildtype MNTB-LSO projections was not altered in the Gad1KO animals. Since alterations in the levels of GABA release were not observed in the Gad1KO animals, the role of GABA in the strengthening and elimination of synaptic inputs during pre-hearing refinement can neither be confirmed nor denied conclusively.

5.2.7 No change in Gad1 expression in the LSO of *gad1-/-* mice

The electrophysiology experiments of the auditory brainstem of *gad1-/-* mice showed that there was no significant difference in the Gabazine sensitive component of the medial MNTB inputs compared to the wild type mice. There was also no difference in the strengthening and functional elimination in the medial MNTB-LSO circuit in the *gad1-/-* mice. All the above information suggested that the *gad1-/-*

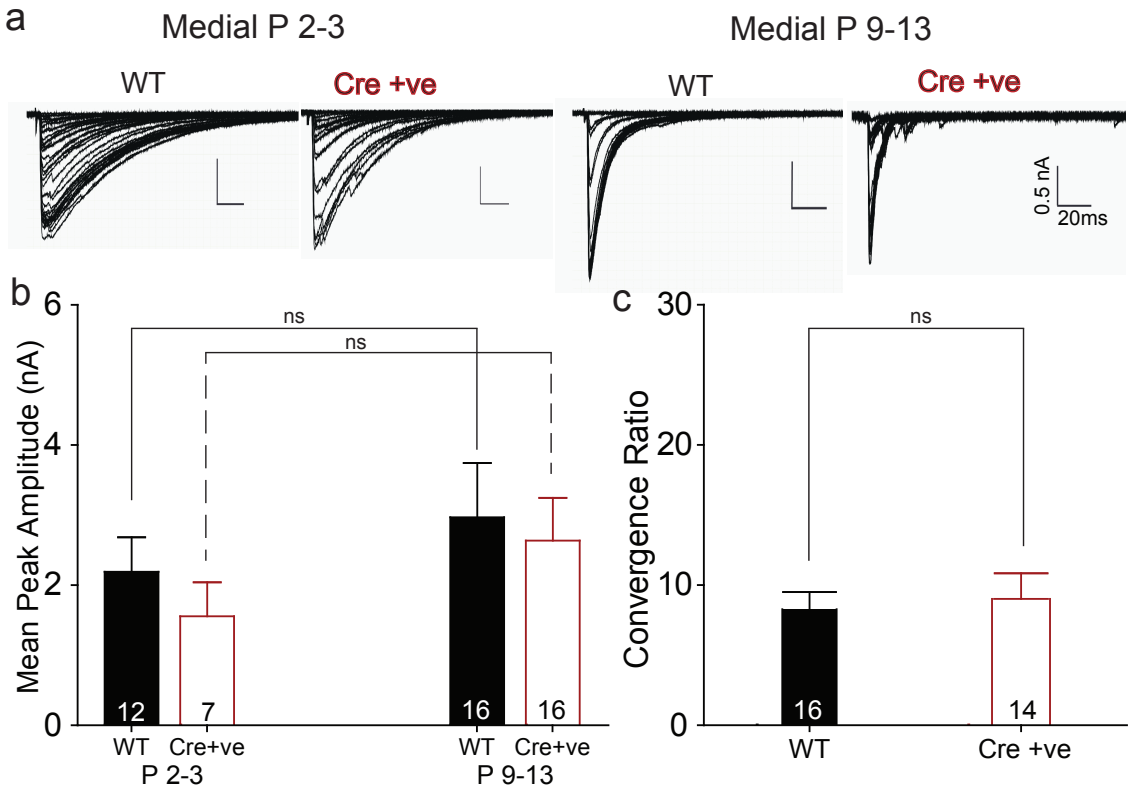

Figure 5.7: **Maximal stimulation responses of medial and lateral MNTB-LSO projections in wildtype and *gad1-/-* mice**
(a) Average example traces of maximal stimulation responses of medial LSO cells in wildtype and *gad1-/-* mice at different ages.
(b) Population data showing the mean peak amplitudes of in medial LSO in response to maximal MNTB stimulation at different ages.
(c) Population data showing the convergence ratios of medial LSO cells in wildtype and *gad1-/-* mice at P9-13.

mice, though genotypically a knockout, did not show a phenotype of knockout of Gad1 production in the MNTB cells. To confirm this observation, brainstem sections from *gad1-/-* mice were subjected to immunofluorescence using antibodies against the Gad1 enzyme (antibodies graciously gifted by Dr. Rebecca Seal, University of Pittsburgh).

Wildtype animals and *gad1-/-* mice expressing a reporter gene tdTomato were perfused and their brains were fixed in 4% PFA and sectioned carefully. The sections were then stained with antibodies against Gad1 enzyme (Fig 5.8 a, b). The red fluorescence was due to tdTomato expression in the cells expressing Cre recombinase. The green fluorescence was due to Gad1 staining.

Firstly, I found only a few tdTomato expressing cells in the lateral MNTB. This suggested that the MNTB cells were not expressing Cre recombinase in the *gad1-/-* animals. Since tdTomato expressing cells had been found in the MNTB of the VGlut-3-Cre animals (Fig 5.4), it is possible that the MNTB specific Cre expression was lost in the subsequent generations of breeding. The VGlut-3 directed Cre expression was however preserved in the other parts of the brain like cerebellum, and the serotonergic raphe as evident from the tdTomato expression in the respective cells in the brain sections.

Secondly, the Gad1 staining for the specific antibody used seemed to label the terminals of neurons instead of the cytoplasm of the whole neuron. Thus I did not see any Gad1 labeled cell bodies in the MNTB. So I analyzed the intensity of the

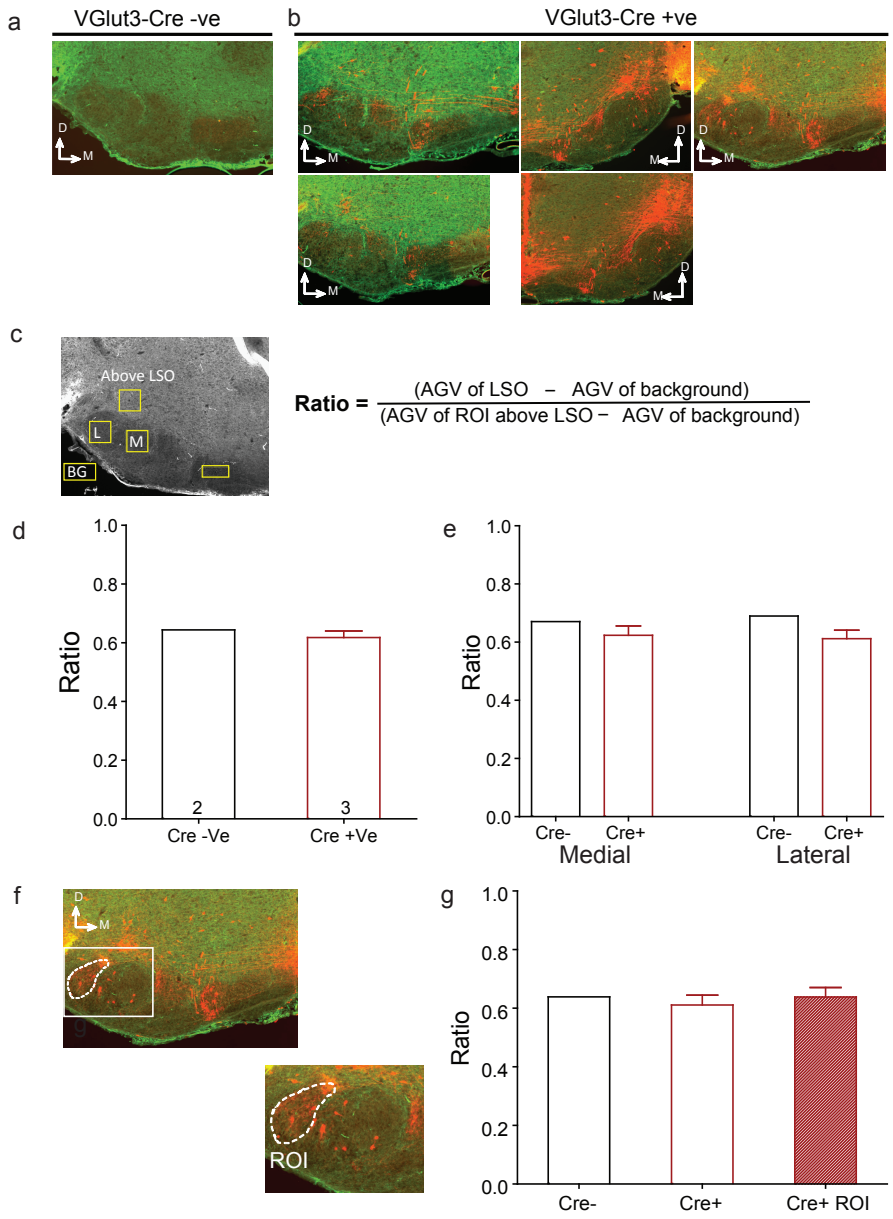

Figure 5.8: **Fluorescent immunolabelled images of P5 *gad1-/-* and wildtype mice stained for Gad1 expression**
(a) Fluorescent sections of auditory brainstem of P5 wildtype mice .
(b) Fluorescent sections of auditory brainstem of P5 *gad1-/-* mice.
(c) Grayscale image of the fluorescent section showing the selection of region of interest (ROI) for absolute grey value (AGV) measurements. The formula on the right is used to estimate the normalized relative grey values (RGV) of the ROI.
(d) Barplot showing differences in intensity of Gad1 staining in the whole LSO in wildtype (Cre -ve) and *gad1-/-* mice (Cre +ve) mice.
(e) Barplot showing differences in intensity of Gad1 staining along the tonotopic axis in the LSO in wildtype (Cre -ve) and *gad1-/-* mice (Cre +ve) mice.
(f) Selection of the most lateral part of LSO as ROI. (g) Comparision of the grey values in the selected ROI in the most lateral part of LSO with the rest of the LSO in Cre +ve and Cre -ve animals.

fluorescent labeling in the neuron terminals present in the LSO of wildtype and *gad1-/-* animals. I outlined regions of interest as shown in Fig 5.8c both in and outside the LSO and calculated the relative grey values (RGV) of the regions of interest. Then I normalized the fluorescence intensity of Gad1 staining in the LSO to the intensity of a region of interest outside the LSO to control for nonspecific staining. The normalized RGVs were then compared between wildtype and Cre+ve animals.

The mean normalized RGVs of the whole LSO was not different between wildtype (black bar) and Cre +ve *gad1-/-* animals (red bar). I also calculated the normalized RGVs of the medial and lateral parts of the LSO separately. I did not see any significant difference in Gad1 staining along the tonotopic axis of the LSO (Fig 5.8 e). A closer look at the LSO revealed a greater number of tdTomato expressing terminals in the most lateral part of the LSO. So I selectively outlined the area of the lateral LSO showing high intensity of tdTomato fluorescence and calculated the intensity of Gad1 staining in this restricted region of interest (ROI) (Fig 5.8 f,g). There was no significant difference in the Gad1 staining intensity in the restricted ROI as compared to the rest of the LSO in wild type (Cre-ve) and *gad1-/-* (Cre+ve) animals.

The above results together suggest that there was a loss of MNTB specific expression of Cre recombinase under the VGlut-3 promoter. The VGlut-3 promoter directed Cre expression was however intact in other parts of the brain like the cerebellum and the serotonergic raphe in the brainstem. I also observed no difference in the fluores-

cence intensities of Gad1 enzyme staining in the wild type and *gad1-/-* LSO. This suggests that the lack of alteration in the Gabazine sensitive component as seen from electrophysiology results is not due to a compensation of GABA production by Gad65 enzyme. The lack of a GABA knockout effect is due to the presence of native levels of Gad1 enzyme in the *gad1-/-* animals in the MNTB. Thus the immunofluorescence study conclusively proves that the Gad1 enzyme could not be knocked out successfully in the MNTB in the *gad1-/-* animal. Though the presence of Cre recombinase gene was confirmed in the *gad1-/-* animals from the tdTomato expression, it was evident that this phenotype was lost from the MNTB specifically.

5.3 Discussion

In the present study I attempted to knockout GABAergic neurotransmission in the MNTB-LSO circuit to elucidate the role of GABA in the pre-hearing refinement of this circuit. I used transgenic mice which expressed Cre under the VGlut-3 promoter in cells containing homozygous floxed *gad1* alleles and a reporter gene *tdTomato* in specific cell populations. Unfortunately, the cells in the MNTB did not show expression of Cre recombinase and hence there was no deletion of the floxed *gad1* gene. This lack of deletion of *gad1* gene was evident in the unaltered expression of Gad1 enzyme (Fig 5.8) and also in the unaltered Gabazine sensitive component of the maximal MNTB input to the LSO cells (Fig. 5.5). There was also no discernible change in the pre-hearing strengthening and functional elimination of synaptic inputs

that is characteristic in the medial MNTB-LSO circuit.

After its discovery as a principal inhibitory neurotransmitter, GABA has been implicated in various aspects of neuronal development. The trophic role of GABA is undeniable in cell proliferation, growth cone formation, migration and synapse formation. Gad65 (Gad2) and Gad67 (Gad1) are the two enzymes that control production of GABA in the neurons. While Gad65 is restricted to more mature neuronal terminals, the major component of GABA in the developing brain is synthesized by Gad67. Thus, it is comprehensible that any perturbation in the Gad67 levels is not well tolerated in the brain. Universal Gad67KO show lethal phenotype (Asada et al., 1997). In the VGlut-3-Cre mice, expression of Cre recombinase was evident in the MNTB. However, when crossed with the floxed *gad1* animals, the Cre expression phenotype was specifically lost in the MNTB but not from the other parts of the brain like cerebellum or raphe. This may be due to the survival of only those littermates who could keep the GABAergic input intact in the MNTB during development. The littermates in which there was Cre expression in the MNTB leading to knockout of Gad1 expression may not have survived.

This observation points to an even more important role of GABA in the developmental stages of the MNTB-LSO circuit than previously envisioned. The MNTB in the embryo originates from the basal plate of the neural tube (Marrs et al., 2013). Specifically, rhombomere 4 and 5 (r4 and r5) contribute to the origin of the MNTB and the rest of SOC (Marrs et al., 2013). Embryonic fate mapping studies have

revealed that r5 may also have a critical role in suppressing high frequency firing in r6, r7, r8 post-otic segments during embryonic development. The r6, r7, r8 segments are capable of generating high frequency activity analogous to the fetal respiratory behavior by the age of E12. However the low frequency activity of r5 (and maybe r4 too) suppresses the high frequency firing of the post-otic segments until E15 (Borday et al., 2006). This low frequency activity at this early age is probably GABAergic, nicotinic or glycinergic as seen for activity in the embryonic spinal cord (Hanson and Landmesser, 2003). VGlut-3(*slc17a8*) RNA expression is present in the r4 and r5 as early as E13.5 (Allen Developing Mouse Brain Atlas). Thus it is possible that the *gad1* gene in the transgenic mice is floxed out as early as E13.5 due to expression of Cre recombinase under the VGlut-3 promoter. This may lead to downregulation of GABA levels in the r4 and r5 at E13.5 onwards. The lack of GABAergic activity in r4 and r5 may cause premature high frequency firing and pattern generation in the r6, r7, r8 segments. Although speculative, it is possible that the premature appearance of high frequency activity in these fetal pattern generator centers may have negative consequences on the survival of the animal leading to survival of only those littermates where the GABAergic transmission in the MNTB was intact.

Thus from the present study, using Cre positive $gad1^{fl/fl}$ animals, the role of GABA in the pre-hearing refinement of the MNTB-LSO circuit was inconclusive. Future studies using MNTB-LSO specific GABA knockouts would be necessary to pinpoint the function of the transient co-release of GABA in this circuit.

Chapter 6

Discussion

6.1 Different phases of refinement in the MNTB-LSO circuit

In rodents, hearing begins almost two weeks after birth (P 12 in mice (Ehret, 1976) and P 14 in rats (Uziel et al., 1981)). Thus the auditory brainstem undergoes a pre-hearing and post-hearing phase of development. Both the pre-hearing as well as post-hearing phases of development are important for mature circuit function. In the present study I have done fine-grained study of the course of refinement of the MNTB-LSO connections in their pre-hearing phase of development in both the high frequency sensitive as well as low frequency sensitive part of the circuit.

6.1.1 Pre-hearing refinement of the MNTB-LSO circuit

The pre-hearing development phase begins prenatally (Fig. 6.1). The pre-hearing development can be subdivided into three temporally segregated phases. The first phase or the proliferation phase occurs between E 18 and P 3. This phase coincides with the depolarizing phase of GABA/Glycine when the release of GABA or glycine can elicit prolonged depolarizations (Kandler and Friauf, 1995a) and action potentials in the LSO cells (Kullmann and Kandler, 2001) causing calcium influx into the cell (Kullmann et al., 2002). Weak MNTB inputs are gradually added leading to an increase in the convergence ratio of the MNTB-LSO connections.

The second phase or the functional elimination phase occurs between P 3 and P 5, as the GABA/ glycine responses begin to turn hyperpolarizing (Kullmann and Kandler, 2001; Ehrlich et al., 1999; Löhrke et al., 2005; Kandler and Friauf, 1995a).

This switch from depolarization to hyperpolarization probably acts as "brakes" to the proliferation phase. As GABA/glycine become hyperpolarizing, $GABA_B$ receptor mediated long term depression (LTD) mechanisms may become activated leading to silencing of inputs (Kotak and Sanes, 2000; Chang et al., 2003; Kotak et al., 2001). Such silencing of synaptic inputs between P 3 and P 5 is reflected in the significant decrease in convergence ratio during the functional elimination phase. Since the individual MNTB inputs are of similar strength at these ages, the underlying principle of selectively retaining few inputs while silencing the rest is not clear yet. This elimination phase results in almost 50% reduction in the MNTB input map to the LSO and possibly forms a template for later post-hearing refinement (Kim and Kandler, 2003).

The third phase of pre-hearing refinement is the strengthening phase (between P 6 and P 13) whereby each single MNTB input is strengthened significantly so that at hearing onset each MNTB input is 3-4 times stronger than that at P 2-3. This phase of strengthening occurs mostly in the hyperpolarizing phase of GABA/glycine response. The connections not only strengthen but also become more glycinergic (Kotak et al., 1998) as evident from their smaller decay constants (Jonas et al., 1998).

6.1.2 Post-hearing refinement of the MNTB-LSO circuit

After hearing onset at P 12-14, extensive pruning of MNTB axonal boutons is evident in the LSO (Sanes and Takács, 1993; Sanes et al., 1992a). This structural

refinement phase of MNTB axonal boutons is complimented with a decrease in dendritic arbor of the LSO cells (Sanes et al., 1992b; Sanes and Siverls, 1991). The temporal segregation of the functional elimination phase in the pre-hearing period from the post-hearing structural refinement phase suggests that the structural pruning phase is driven by sound-evoked activity (Sanes and Takács, 1993; Kapfer et al., 2002). Sensory activity also modulates different physiological properties of the LSO cells making them well equipped to function as mature circuits (Hassfurth et al., 2009; Ene et al., 2007) in adult animals.

6.2 Functional elimination of synaptic inputs and their strengthening are independent processes

A surprising observation in the present study was the presence of the elimination phase of inputs in the medial part of the developing MNTB-LSO circuit but not in the lateral part. In the medial part of the circuit, as mentioned above, the phase of significant functional elimination of synaptic inputs (between P 2-3 and P 5-6) preceded the phase of significant strengthening of the inputs (between P 5-6 and P 9-13). This suggests that the functional elimination phase may not be dependent on the change in strength of the inputs. This chronological arrangement of phases raises the question whether the strengthening phase is dependent on the elimination phase. However, the observation that significant strengthening of inputs occur in the lateral MNTB-LSO connections even in the absence of a preceding phase of functional elimination, suggests that the two phases are independent of one another. This shows

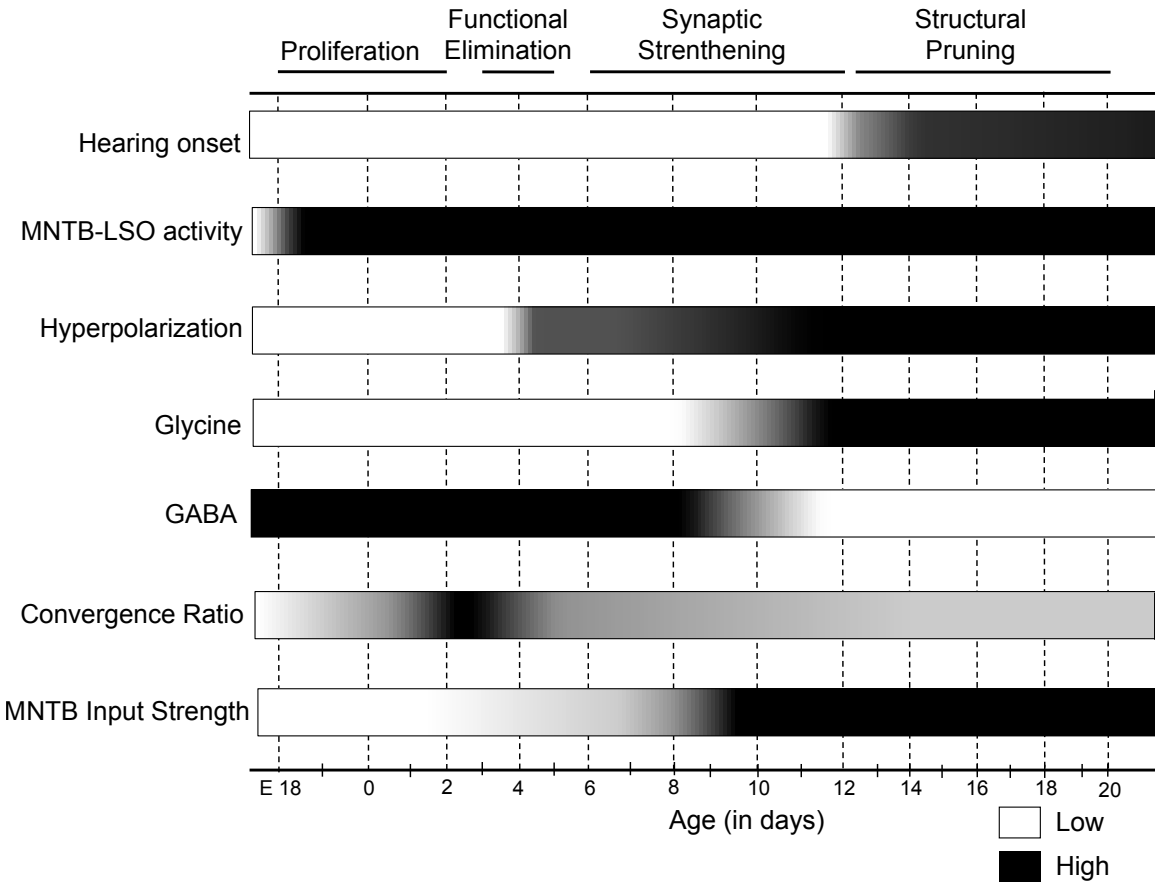

Figure 6.1: **Developmental changes in the MNTB-LSO circuit before and after hearing onset**

that the phase of elimination is not a pre-requisite for the proper strengthening of the retained inputs.

Spontaneous bursts of spike trains in the developing cochlea have been hypothesized to provide structured activity patterns that may guide the synaptic refinement in the downstream auditory nuclei (Tritsch and Bergles, 2010; Tritsch et al., 2007). This spontaneous activity coupled with the depolarizing GABA/glycine responses before P 3 in the medial part of the MNTB-LSO circuit may help in extensive proliferation of the synaptic inputs leading to very high convergence ratios. However, in addition to being spontaneously active, the immature cochlea also undergoes structural maturation in a base (high frequency) to apex (low frequency) gradient (Sato et al., 1999; Lim and Rueda, 1992). Thus the presence of spontaneous activity in the lateral LSO cells may lag behind the medial cells. Thus the lateral cells may experience spontaneous activity only after they have entered the hyperpolarizing phase of GABA/glycine and thus do not show the extensive proliferation phase and later elimination phase characteristic of the medial cells. The high frequency of spontaneous activity bursts driven by the cochlear inner hair cells (Tritsch and Bergles, 2010) as well as increase in the synchronization of the MNTB spiking due to the phasic firing of the mono-innervated MNTB neurons (Hoffpauir et al., 2010, 2006; Holcomb et al., 2013) after P 4, may then help in strengthening the retained MNTB inputs in both medial and lateral parts of the circuit to a similar degree.

From the above interpretation of data, it is clear that the functional elimination

phase and the strengthening phase of MNTB-LSO connections are two independent events with different possible underlying mechanisms.

6.3 Role of transient neurotransmitter co-release in the refinement of the MNTB-LSO circuit

Previous studies have shown the transient release of GABA (Kotak et al., 1998) and glutamate (Gillespie et al., 2005) in addition to glycine in the developing MNTB-LSO circuit during the first two postnatal weeks. The presence of two additional neurotransmitters exactly during the period when the circuit is undergoing numerous physiological changes suggests that they might play important roles in the these changes. In the present study I examined the role of glutamate and GABA co-release during this pre-hearing period of development.

According to previous reports, glutamate plays a critical role in the strengthening and functional elimination of medial MNTB-LSO inputs (Noh et al., 2010). In the absence of glutamate co-release during the first two postnatal weeks, the single medial MNTB inputs showed 2 fold instead of 8 fold increase in strength due to a reduction in quantal content as well as a lack of addition of release sites. The absence of glutamate co-release further impaired the functional elimination of medial MNTB-LSO connections during the first two postnatal weeks leading to high convergence ratios even at P 9-12 (Noh et al., 2010). In the present study I examined the role of glutamate in refinement and strengthening of both medial and lateral MNTB-LSO connections. My observations agree with previous reports that the lack of glutamate

co-release in the medial part of the circuit causes impairment of both strengthening and elimination of inputs. I also examined the effect of lack of glutamate co-release in the strengthening phase in the lateral LSO cells. The strengthening phase of the lateral MNTB-LSO connections did not seem to be affected by the absence of glutamate. Thus it seems that the process of strengthening in the lateral MNTB-LSO connections occurs in a glutamate-independent pathway. A closer examination of the medial cells shows that at least a two fold increase in the strength occurs even in the medial cells of *vglut3-/-* mice (Noh et al., 2010). Thus there seems to be a glutamate dependent as well as a glutamate independent process of strengthening. While the lateral cells seem to strengthen by only the glutamate independent process, the medial cells may undergo both the glutamate dependent and independent processes. Thus it is evident that the transient co-release of glutamate seems to play different roles in different parts of the same nucleus.

In this study I also attempted to study the role of transient GABA co-release in this circuit by using a conditional Gad1 knockout mouse. However, the study was inconclusive due to a lack of phenotype in the transgenic animal. Further investigation is necessary to ascertain the role of GABA in the developmental refinement of this circuit.

6.4 Role of the timing of the intracellular chloride shift in the refinement of the MNTB-LSO circuit

A distinguishing feature of inhibitory neurons is the shift of the GABA/glycinergic responses from depolarizing to hyperpolarizing due to a shift in the intracellular chloride concentration (Ben-Ari et al., 2012, 2007; Leinekugel et al., 1995). The present study suggests that the timing of the chloride shift may be important for the refinement of the MNTB-LSO circuit. A closer look at the timings of chloride shifts of major brain regions in rodents show a gradient of development. The earliest hyperpolarizing responses occur in the spinal cord (P 0- P 7) (Fellippa-Marques et al., 2000), followed by brainstem (Kullmann and Kandler, 2001; Ehrlich et al., 1999; Löhrke et al., 2005; Kandler and Friauf, 1995a), cerebellum (Brickley et al., 1996), and visual neocortex (P 3 - P 8) (Lin et al., 1994) then basal ganglia (P 10 - P 17) (Kyrozis et al., 2006) and finally neocortex including hippocampus (P 11- P 16) (Rivera et al., 1999; Marandi et al., 2002; Luhmann and Prince, 1991; Yamada et al., 2004). The timings of the chloride shifts in the different brain areas seem to reflect the relevance of these areas during the life of an organism eg. while the spinal cord reflexes are mature at birth, memory formation and cognitive abilities become relevant only later in life. It is also intriguing to notice that the chloride shift in the visual neocortex occurs along with the auditory brainstem rather than other parts of the neocortex. A possible explanation may be that hearing onset in rodents (P 12-P14) occurs right before eye opening (P 15) and thus both these circuits need to be

ready for maturity at similar times. Thus it seems that the timing of the chloride shift is correlated with the maturity of the circuits.

The timing of the chloride shift coupled with the base-apex gradient of structural maturity of the cochlea also seems to be a reason for the differences in the refinement in the medial versus the lateral MNTB-LSO circuit. The relevance of this difference is not yet clear and would require further studies in which the timing of the chloride shift is manipulated possibly using KCC2 knockout mice.

6.5 Refinement in the GABA/Glycinergic MNTB-LSO circuit differs from the refinement of model excitatory circuits

The detailed study of the MNTB-LSO circuit shows that neural circuit refinement is a common phenomenon between excitatory and inhibitory circuits. They share certain features like strengthening of few selected synaptic inputs in the MNTB-LSO circuit is analogous to the strengthening of the "winner" motor neuron in the neuromuscular junction (Colman et al., 1997) or that of one of the climbing fibers in the cerebellar circuit (Hashimoto et al., 2009). This strengthening occurs by increase in quantal content as well as addition of release sites (Kim and Kandler, 2003, 2010) as seen in retinogeniculate connections (Chen and Regehr, 2000). The structural pruning of synaptic inputs in the MNTB-LSO circuit after hearing onset is another feature that this inhibitory circuit has in common with other excitatory circuits like the neuromuscular junctions (Colman et al., 1997) and the cerebellar

circuit (Hashimoto et al., 2009).

However, the refinement of the MNTB-LSO circuit also differs from the refinement of excitatory circuits in various ways. First of all, the synaptic inputs in the MNTB-LSO circuit undergoes a period of silencing before the structural pruning while the synapses in the neuromuscular junction are functional until they are pruned (Balice-Gordon et al., 1993; Balice-Gordon and Lichtman, 1993; Purves and Lichtman, 1985). The period of synaptic silencing and synaptic pruning, in the MNTB-LSO circuit, is separated by a week, while in excitatory circuits, synaptic weakening is promptly followed by axonal pruning (Colman et al., 1997; Antonini et al., 1993).

Second of all, in the neuromuscular junction (Colman et al., 1997) or the cerebellar circuit (Hashimoto and Kano, 2005, 2003), one or a few of the synaptic inputs increase in strength (by an increase in quantal content or release probability) creating a disparity of strengths among the inputs which is thought to be key in selecting the inputs that are maintained. However from my study, it is clear that the silencing or functional elimination step occurs at a point when the inputs are still very weak. Significant strengthening of inputs occur after the completion of the functional elimination. Furthermore, in the lateral LSO cells it is evident that the synaptic strengthening step occurs even in the absence of the preceding functional elimination step showing the independence of the two processes.

Whether the above mentioned differences in the refinement of MNTB-LSO circuit and the excitatory circuits is true for all inhibitory circuits in the brain will

need further study. However given characteristic similarities between different inhibitory circuits like the depolarizing activity of GABA, the shift in intracellular chloride concentrations and the importance of intracellular calcium influx for plasticity mechanism, it seems highly likely that there would be substantial similarity between refinement of other inhibitory circuits and the MNTB-LSO circuit.

6.6 Evolutionary significance of the differential refinement in the MNTB-LSO circuit

The difference in the developmental refinement of the medial and the lateral parts of the same LSO nucleus is intriguing. What possible advantage could such a phenomenon impart to the survival of the animal? Most mouse vocalizations like mating calls (Maggio et al., 1983), same sex agonistic social calls (Gourbal et al., 2004), and pup separation calls (Branchi et al., 1998) all occur in the high frequency range. One possible reason for the evolution of the vocalizations specifically in the high frequency range could be that it provided better chances to avoid predators like birds whose auditory perception range is within the audible range (Dooling, 1982). Another reason for the dependence on higher frequencies could be that due to the smaller width of the mouse head, the ILD for high frequency sound becomes a more accurate cue for sound localization than ITDs of low frequency sound (Masterton et al., 2005), possibly leading to better chances of spotting and avoiding the predator. Thus it can be assumed that a mouse with an auditory brainstem wiring optimum for high frequency sound discrimination would be better equipped to avoid predators and have

better chances of survival.

The medio-lateral tonotopic map of the MNTB-LSO circuit is highly organized, so that the medial part of the circuit responds to high frequency sound stimulus and the lateral part of the circuit responds to low frequency sound stimulus (Friauf, 1992; Kandler and Friauf, 1993; Kil et al., 1995; Tsuchitani, 1977; Sanes et al., 1989; Sanes and Siverls, 1991). While the medial LSO cells rely only on interaural level difference (ILD) for sound source localization in the high frequency spectrum, the lateral LSO cells respond to ILD as well as interaural phase or time differences (IPD or ITD) for low frequency stimulus (Spitzer and Semple, 1995; Joris and Yin, 1995; Tollin and Yin, 2005). The lateral cells can respond to the ITD since the low frequency afferents from both the cochlear nucleus and the MNTB preserve the temporal fine structure of the incoming sound (Joris et al., 1994; Smith et al., 1998). The lateral LSO cells can also phase lock to low frequency ipsilateral stimulation (Tollin and Yin, 2005).

The pre-hearing changes in the medial LSO leads to a sharpening of the tonotopic map (Kim and Kandler, 2003) which probably forms a template helping in the structural pruning of the circuit guided by sound evoked activity. This pre-hearing refinement may be essential for proper convergence of the frequency specific excitatory and inhibitory inputs onto the same postsynaptic cell, preparing the circuit for mature function at hearing onset to ensure best chances of survival. Optimal wiring in the medial part of the LSO is probably a pre-requisite for the survival of a mouse with a later dependence on mostly ILDs of high frequency sound stimuli. Thus a mouse with

a more precise degree of discrimination and a wider range of high frequency sound source localization probably survived more often. The higher degree of refinement in the medial LSO is probably a reminder of this evolutionary advantage.

The lesser used low frequency sensitive lateral part of the LSO responds to ITDs similar to the MSO in animals specializing in low frequency hearing. In the MSO, subcellular reorganization of the glycinergic synapses occur after hearing onset (Kapfer et al., 2002) in contrast to the elaborate pre-hearing proliferation and functional elimination phases common in the LSO. Thus post hearing subcellular reorganization of the lateral MNTB-LSO connections may be more relevant for optimum low frequency sound source localizations by the lateral LSO. This may explain why extensive proliferation and functional elimination of inputs do not occur in the lateral LSO during pre-hearing development. Further investigation of the subcellular locations of the lateral MNTB-LSO synapses before and after hearing onset would be necessary to confirm this hypothesis.

Chapter 7

Future Work

7.1 Hypothetical model of pre-hearing changes in the MNTB-LSO circuit

Integrating all the physiological changes occurring in the MNTB-LSO circuit during the first two postnatal weeks, the following hypothetical model of the refinement can be constructed.

Proliferation phase: E 18 - P 2-3

Between E18 and P 2-3, GABA/glycine are depolarizing and excitatory along with glutamate. At this age, the MNTB receives sparse stimulation from the upstream auditory nuclei (possibly from the spiral ganglion cells and inner hair cells). Upon such sparse stimulation MNTB releases GABA/Glycine/Glutamate that activate $GABA_AR$, GlyR and AMPARs respectively. The cumulative depolarization from these receptors may cause magnesium release from NMDARs which are then activated by homosynaptically released glutamate. Under sparse stimulation, the released GABA/Glycine and glutamate may cause spatially restricted calcium influx (Kullmann and Kandler, 2008) into the cell which may lead to recruitment of receptors to the cell surface (Kneussel and Betz, 2000) and maintenance and addition of synapses. This calcium influx may also help in retrograde release of GABA from LSO cells (Magnusson et al., 2008) themselves leading to a retrograde trophic effect causing numerous MNTB inputs to make synapses on each LSO cells.

Elimination phase: P 2-3 - P 5-6

At around P 4, GABA/Glycine begins to turn hyperpolarizing. Thus the overwhelming depolarization induced by depolarizing GABA/Glycine is lost. But, GABA released from the MNTB may still act on $GABA_B$ receptors causing LTD due to calcium release from the intracellular stores. Such $GABA_BR$ mediated LTD may cause silencing of many MNTB inputs. The inadequate depolarization due to AMPAR activation by glutamate released from MNTB may not be sufficient for NMDAR activation anymore. However not knowing the exact plasticity mechanism recruited by glutamate in this circuit, it is hard to explain why lack of glutamate release from MNTB affects the elimination phase of the refinement in the medial part of this circuit.

Strengthening phase: P 5-6 - P 9-13

At P 2-3, high levels of GABA released due to activation of MNTB cells may activate $GABA_BRs$ leading to synaptic depression and hence inputs of low strength. Synaptic depression at these ages may also be facilitated by the presence of endocannabinoids (Chi and Kandler, 2012) as well as neurotrophin-TrkB (Kotak et al., 2001) signaling. At P 5-6, the MNTB activity becomes phasic and also stronger due to repeated bursting of upstream spontaneously active cells (spiral ganglion cells). Presence of high levels of GABA at P 5-6 may lead to low strength of the inputs due to $GABA_BR$ activation, creating the lag between elimination and strengthen-

ing. [Here high levels of GABA transmission has been assumed until P 9 (based on data from present study). The Gabazine sensitive component should be ascertained between ages P 3 and P 9 to support this assumption.] At P 9-13, as GABA levels diminish and glycine levels increase, the stronger MNTB activity (guided by repeated bursting of SGCs, frequency of bursting peaks at P 8 (Tritsch and Bergles, 2010)) may help in addition of release sites post synaptically leading to strengthening of inputs.

From the above model, the following hypotheses can be tested:

7.1.1 Role of GABA and $GABA_BR$ on strengthening and elimination of inputs

From the model of MNTB-LSO circuit refinement described above, I predict a major role of GABA and $GABA_BR$ mediated activity in the strengthening as well as elimination of the MNTB-LSO connections. The role of $GABA_BR$ activation may be addressed using a LSO specific or universal $GABA_BR$ knockout mouse. In $GABA_BR$ knockout mouse, at P 2-3, I would expect to see many strong connections (in the absence of LTD, each connection should become stronger prematurely). At P 5-6, I would expect absence of LTD mediated silencing of synapses leading to many strong connections at this age. At P 9-13, in the presence of low GABA, all the maintained strong synapses would become even stronger guided by patterned spontaneous activity.

Alternatively, in a wild type mouse, if the $GABA_BR$ activation is kept high by

injecting baclofen after P 3 until P 13, I would predict the presence of few weak connections at P 9-13 age point due to excessive depression of synapses by $GABA_BR$ mediated LTD.

The role of GABA may be assessed by knocking out GABA production specifically in the MNTB. This will decrease the cumulative depolarization of LSO at P 2-3 leading to failure to activate NMDARs even in the presence of glutamate. Additionally the $GABA_BR$ activation will also be absent. The retrograde release of GABA though intact, may not be activated due to low depolarization of postsynaptic LSO cells. So I would expect few weak connections at P 2-3. Then at P 5-6, due to lack of GABA mediated LTD, I would expect a lack of elimination as well as an immediate increase in strength guided by patterned spontaneous activity. In the absence of GABA, the lag between elimination and strengthening should be abolished.

To ascertain if there is a retrograde trophic release of GABA involved in the initial stages of circuit refinement (between E 18 and P 2-3), an LSO specific Gad1KO is needed. In an LSO specific Gad1KO, the retrograde trophic release of GABA would be absent even in the presence of high levels of depolarizations at the ages between E 18 and P 2-3. If we observe only few weak active MNTB inputs at P 2-3 in the absence of this putative retrograde GABA release, it would suggest the involvement of a retrograde trophic activity of GABA in these synapses.

7.1.2 Role of chloride switch on the elimination phase

The possible role of the timing of chloride switch on the elimination phase of the

MNTB-LSO connections can be tested in two ways. An LSO specific knockout of chloride transporter KCC2 would be ideal to keep the intracellular chloride concentration higher in the LSO cells and delay the switch of GABA/Glycine from depolarizing to hyperpolarizing. At P 2-3, GABA/Glycine /glutamate released from MNTB activates $GABA_AR$, $GABA_BR$, GlyRs as well as AMPAR and NMDARs leading to the initial high convergence. In the continued presence of high intracellular chloride in the LSO cells at P 5-6, I would predict that GABA/Glycine/glutamate mediated depolarization would lead to retention of all inputs as well as keep the inputs weak due to high $GABA_BR$ activation. At P 9-13, however, as GABA content reduces, I would expect all the maintained inputs to strengthen under SGC mediated patterned spontaneous activity. So at P 9-13 I would expect many strong inputs leading to a high maximal response of LSO cells than in the wild type animals.

A second way to test the role of chloride switch would be to constitutively express KCC2 in the LSO cells before P 2-3 (possibly by viral vector injection). KCC2 expression would prematurely lower the intracellular chloride concentration in the LSO leading to hyperpolarization by GABA/Glycine release at P 2-3. But the $GABA_BR$ activation would be intact and will be more prominent even at P 2-3 leading to early elimination. In that case I would expect few weak inputs at P 2-3 and P 5-6, and few strong inputs at P 9-13 (strengthening would occur normally after P 5-6). This result would help explain the tight correlation between intracellular chloride concentration and the elimination step in the MNTB-LSO refinement.

7.1.3 Role of patterned activity in strengthening

From studies on Pachanga and *otoferlin-/-* mice (where inner hair cells do not release glutamate and hence cannot give rise to spontaneous activity) it is evident that IHC mediated spontaneous activity may not be crucial for MNTB-LSO refinement (Noh et al., 2010). However, the results of recent studies suggest that the loss of structured spontaneous activity in alpha 9 KO mice leads to impaired strengthening as well as elimination in the developing MNTB-LSO circuit. From my hypothesized model, I also predict an important role of patterned activity on the strengthening of both medial and lateral MNTB-LSO connections. I predict that the spontaneous firing of spiral ganglion cells that begins at around P 2-3 and becomes burst like and more frequent at around P 8 guides the strengthening of the MNTB-LSO connections between P 5-6 and P 9-13. If we knockout VGlut1 (specifically expressed in auditory nerve endings) in the spiral ganglion cells, we can disrupt the SGC mediated spontaneous activity. In absence of such spontaneous activity, I expect to see weak inputs even at P 9-13 implicating the role of spontaneous bursting activity in the strengthening phase of pre-hearing refinement in the MNTB-LSO circuit.

Table 7.1: **Summary of future experiments and their expected results**

Experimental manipulation	P 2-3	P 5-6	P 9-13	Inference
$GABA_BR$ KO in LSO	many strong connections	many strong connections	many strong connections	$GABA_BR$ mediated LTD required for elimination as well as keeping input strength low
Baclofen injections in wild type after P 3	many weak connections	few weak connections	few weak connections	$GABA_BR$ mediated LTD keeps connections weak
MNTB specific GABA KO	few weak connections	few stronger connections	few strong connections	role of GABA in the lag between elimination and strengthening
LSO specific GABA KO	few weak connections	few weak connections	few strong connections	possible trophic role of retrograde GABA release from LSO
Chloride switch after P 9 (LSO specific KCC2 KO)	many weak connections	many weak connections	many strong connections	low intracellular chloride needed for proper elimination
Chloride switch before P 2-3 (constitutive KCC2 expression)	few weak connections	few weak connections	few strong connections	low intracellular chloride causes premature elimination
SGC specific VGlut1 KO	many weak connections	few weak connections	few weak connections	spontaneous activity required for strengthening of connections

Bibliography

Antonella Antonini, Michael P Stryker, et al. Rapid remodeling of axonal arbors in the visual cortex. *Science*, 260(5115):1819–1821, 1993.

Hideo Asada, Yuuki Kawamura, Kei Maruyama, Hideaki Kume, Ria-Go Ding, Nobuko Kanbara, Hiroko Kuzume, Makoto Sanbo, Takeshi Yagi, and Kunihiko Obata. Cleft palate and decreased brain γ-aminobutyric acid in mice lacking the 67-kda isoform of glutamic acid decarboxylase. *Proceedings of the National Academy of Sciences*, 94(12):6496–6499, 1997.

Veeramuthu Balakrishnan, Michael Becker, Stefan Löhrke, Hans Gerd Nothwang, Erdem Güresir, and Eckhard Friauf. Expression and function of chloride transporters during development of inhibitory neurotransmission in the auditory brainstem. *The Journal of neuroscience*, 23(10):4134–4145, 2003.

Rita J Balice-Gordon and Jeff W Lichtman. In vivo observations of pre-and post-synaptic changes during the transition from multiple to single innervation at de-

veloping neuromuscular junctions. *The Journal of neuroscience*, 13(2):834–855, 1993.

Rita J Balice-Gordon and Jeff W Lichtman. Long-term synapse loss induced by focal blockade of postsynaptic receptors. *Nature*, 372(6506):519–524, 1994.

Rita J Balice-Gordon, Christine K Chua, Carla C Nelson, and Jeff W Lichtman. Gradual loss of synaptic cartels precedes axon withdrawal at developing neuromuscular junctions. *Neuron*, 11(5):801–815, 1993.

Margaret Barnes-Davies, Matthew C Barker, Fatima Osmani, and Ian D Forsythe. Kv1 currents mediate a gradient of principal neuron excitability across the tonotopic axis in the rat lateral superior olive. *European Journal of Neuroscience*, 19 (2):325–333, 2004.

Ranjan Batra, Shigeyuki Kuwada, and Douglas C Fitzpatrick. Sensitivity to interaural temporal disparities of low-and high-frequency neurons in the superior olivary complex. ii. coincidence detection. *Journal of neurophysiology*, 78(3):1237–1247, 1997.

Yehezkel Ben-Ari. Excitatory actions of gaba during development: the nature of the nurture. *Nature Reviews Neuroscience*, 3(9):728–739, 2002.

Yehezkel Ben-Ari, Jean-Luc Gaiarsa, Roman Tyzio, and Rustem Khazipov. Gaba: a pioneer transmitter that excites immature neurons and generates primitive oscillations. *Physiological Reviews*, 87(4):1215–1284, 2007.

Yehezkel Ben-Ari, Melanie A Woodin, Evelyne Sernagor, Laura Cancedda, Laurent Vinay, Claudio Rivera, Pascal Legendre, Heiko J Luhmann, Angelique Bordey, Peter Wenner, et al. Refuting the challenges of the developmental shift of polarity of gaba actions: Gaba more exciting than ever! *Frontiers in cellular neuroscience*, 6, 2012.

Caroline Borday, A Coutinho, Isabelle Germon, J Champagnat, and G Fortin. Pre-/post-otic rhombomeric interactions control the emergence of a fetal-like respiratory rhythm in the mouse embryo. *Journal of neurobiology*, 66(12):1285–1301, 2006.

Joachim Bormann. The abcof gaba receptors. *Trends in Pharmacological Sciences*, 21(1):16–19, 2000.

Laurens WJ Bosman and Arthur Konnerth. Activity-dependent plasticity of developing climbing fiber–purkinje cell synapses. *Neuroscience*, 162(3):612–623, 2009.

Laurens WJ Bosman, Hajime Takechi, Jana Hartmann, Jens Eilers, and Arthur Konnerth. Homosynaptic long-term synaptic potentiation of the winner climbing fiber synapse in developing purkinje cells. *The Journal of Neuroscience*, 28(4):798–807, 2008.

James C Boudreau and Chiyeko Tsuchitani. Binaural interaction in the cat superior olive s segment. *Journal of Neurophysiology*, 31(3):442–454, 1968.

Igor Branchi, Daniela Santucci, Augusto Vitale, and Enrico Alleva. Ultrasonic vocal-

izations by infant laboratory mice: a preliminary spectrographic characterization under different conditions. *Developmental psychobiology*, 33(3):249–256, 1998.

Stephen G Brickley, Stuart G Cull-Candy, and Mark Farrant. Development of a tonic form of synaptic inhibition in rat cerebellar granule cells resulting from persistent activation of gabaa receptors. *The Journal of physiology*, 497(Pt 3):753–759, 1996.

Giuseppe Busetto, Mario Buffelli, Enrico Tognana, Francesco Bellico, and Alberto Cangiano. Hebbian mechanisms revealed by electrical stimulation at developing rat neuromuscular junctions. *The Journal of Neuroscience*, 20(2):685–695, 2000.

D Caird and R Klinke. Processing of binaural stimuli by cat superior olivary complex neurons. *Experimental Brain Research*, 52(3):385–399, 1983.

Nell Beatty Cant and JH Casseday. Projections from the anteroventral cochlear nucleus to the lateral and medial superior olivary nuclei. *Journal of Comparative Neurology*, 247(4):457–476, 1986.

Nell Beatty Cant and Richard L Hyson. Projections from the lateral nucleus of the trapezoid body to the medial superior olivary nucleus in the gerbil. *Hearing research*, 58(1):26–34, 1992.

Daniel T Case and Deda C Gillespie. Pre-and postsynaptic properties of glutamatergic transmission in the immature inhibitory mntb-lso pathway. *Journal of Neurophysiology*, 106(5):2570–2579, 2011.

Eric H Chang, Vibhakar C Kotak, and Dan H Sanes. Long-term depression of synaptic inhibition is expressed postsynaptically in the developing auditory system. *Journal of neurophysiology*, 90(3):1479–1488, 2003.

Jean-Pierre Changeux and Antoine Danchin. Selective stabilisation of developing synapses as a mechanism for the specification of neuronal networks. 1976.

Bidisha Chattopadhyaya, Graziella Di Cristo, Hiroyuki Higashiyama, Graham W Knott, Sandra J Kuhlman, Egbert Welker, and Z Josh Huang. Experience and activity-dependent maturation of perisomatic gabaergic innervation in primary visual cortex during a postnatal critical period. *The Journal of neuroscience*, 24(43): 9598–9611, 2004.

Bidisha Chattopadhyaya, Graziella Di Cristo, Cai Zhi Wu, Graham Knott, Sandra Kuhlman, Yu Fu, Richard D Palmiter, and Z Josh Huang. Gad67-mediated gaba synthesis and signaling regulate inhibitory synaptic innervation in the visual cortex. *Neuron*, 54(6):889–903, 2007.

Chinfei Chen and Wade G Regehr. Developmental remodeling of the retinogeniculate synapse. *Neuron*, 28(3):955–966, 2000.

Chu Chen. Hyperpolarization-activated current (¡ i¿ i¡/i¿¡ sub¿ h¡/sub¿) in primary auditory neurons. *Hearing research*, 110(1):179–190, 1997.

Enrico Cherubini, Jean L Gaiarsa, and Yehezkel Ben-Ari. Gaba: an excitatory transmitter in early postnatal life. *Trends in neurosciences*, 14(12):515–519, 1991.

David H Chi and Karl Kandler. Cannabinoid receptor expression at the mntb-lso synapse in developing rats. *Neuroscience letters*, 509(2):96–100, 2012.

Susana Cohen-Cory. The developing synapse: construction and modulation of synaptic structures and circuits. *Science*, 298(5594):770–776, 2002.

H Colman, J Nabekura, and JW Lichtman. Alterations in synaptic strength preceding axon withdrawal. *Science*, 275(5298):356–361, 1997.

Francis Crepel, Jean Mariani, and Nicole Delhaye-Bouchaud. Evidence for a multiple innervation of purkinje cells by climbing fibers in the immature rat cerebellum. *Journal of neurobiology*, 7(6):567–578, 1976.

Robert J Dooling. Auditory perception in birds. *Acoustic communication in birds*, 1: 95–130, 1982.

Shannon T Dupuy and Carolyn R Houser. Prominent expression of two forms of glutamate decarboxylase in the embryonic and early postnatal rat hippocampal formation. *The Journal of neuroscience*, 16(21):6919–6932, 1996.

JC Eccles, R Llinas, and K Sasaki. The excitatory synaptic action of climbing fibres on the purkinje cells of the cerebellum. *The Journal of Physiology*, 182(2):268–296, 1966.

Günter Ehret. Development of absolute auditory thresholds in the house mouse (mus musculus). *Ear and Hearing*, 1(5):179–184, 1976.

Ingrid Ehrlich, Stefan Löhrke, and Eckhard Friauf. Shift from depolarizing to hyperpolarizing glycine action in rat auditory neurones is due to age-dependent cl-regulation. *The Journal of physiology*, 520(1):121–137, 1999.

F Aura Ene, Abigail Kalmbach, and Karl Kandler. Metabotropic glutamate receptors in the lateral superior olive activate trp-like channels: age-and experience-dependent regulation. *Journal of neurophysiology*, 97(5):3365, 2007.

Silvia Fellippa-Marques, Laurent Vinay, and François Clarac. Spontaneous and locomotor-related gabaergic input onto primary afferents in the neonatal rat. *European Journal of Neuroscience*, 12(1):155–164, 2000.

Carolyn Ferguson, Steven L Hardy, David F Werner, Stanley M Hileman, Timothy M DeLorey, and Gregg E Homanics. New insight into the role of the β3 subunit of the gabaa-r in development, behavior, body weight regulation, and anesthesia revealed by conditional gene knockout. *BMC neuroscience*, 8(1):85, 2007.

Alexander C Flint, Xiaolin Liu, and Arnold R Kriegstein. Nonsynaptic glycine receptor activation during early neocortical development. *Neuron*, 20(1):43–53, 1998.

Moritz J Frech, Joachim W Deitmer, and Kurt H Backus. Intracellular chloride and calcium transients evoked by γ-aminobutyric acid and glycine in neurons of the rat inferior colliculus. *Journal of neurobiology*, 40(3):386–396, 1999.

E Friauf and J Ostwald. Divergent projections of physiologically characterized rat

ventral cochlear nucleus neurons as shown by intra-axonal injection of horseradish peroxidase. *Experimental brain research*, 73(2):263–284, 1988.

Eckhard Friauf. Tonotopic order in the adult and developing auditory system of the rat as shown by c-fos immunocytochemistry. *European journal of Neuroscience*, 4 (9):798–812, 1992.

JM Fritschy, J Paysan, A Enna, and H Mohler. Switch in the expression of rat gabaa-receptor subtypes during postnatal development: an immunohistochemical study. *The Journal of neuroscience*, 14(9):5302–5324, 1994.

Kiyohiro Fujino, Konomi Koyano, and Harunori Ohmori. Lateral and medial olivocochlear neurons have distinct electrophysiological properties in the rat brain slice. *Journal of neurophysiology*, 77(5):2788–2804, 1997.

Aristea S Galanopoulou. Gabaa receptors in normal development and seizures: friends or foes? *Current neuropharmacology*, 6(1):1, 2008.

Wen-Biao Gan and Jeff W Lichtman. Synaptic segregation at the developing neuromuscular junction. *Science*, 282(5393):1508–1511, 1998.

Deda C Gillespie, Gunsoo Kim, and Karl Kandler. Inhibitory synapses in the developing auditory system are glutamatergic. *Nature neuroscience*, 8(3):332–338, 2005.

KK Glendenning, KA Hutson, RJ Nudo, and RB Masterton. Acoustic chiasm ii: anatomical basis of binaurality in lateral superior olive of cat. *Journal of Comparative Neurology*, 232(2):261–285, 1985.

Corey S Goodman and Carla J Shatz. Developmental mechanisms that generate precise patterns of neuronal connectivity. *Cell*, 72:77–98, 1993.

Benjamin EF Gourbal, Mathieu Barthelemy, Gilles Petit, and Claude Gabrion. Spectrographic analysis of the ultrasonic vocalisations of adult male and female balb/c mice. *Naturwissenschaften*, 91(8):381–385, 2004.

Christelle Gras, Etienne Herzog, Gian Carlo Bellenchi, Véronique Bernard, Philippe Ravassard, Michel Pohl, Bruno Gasnier, Bruno Giros, and Salah El Mestikawy. A third vesicular glutamate transporter expressed by cholinergic and serotoninergic neurons. *The Journal of neuroscience*, 22(13):5442–5451, 2002.

Benedikt Grothe and Dan H Sanes. Synaptic inhibition influences the temporal coding properties of medial superior olivary neurons: an in vitro study. *The Journal of neuroscience*, 14(3):1701–1709, 1994.

Paolo Gubellini, Yehezkel Ben-Ari, and Jean-Luc Gaïarsa. Activity-and age-dependent gabaergic synaptic plasticity in the developing rat hippocampus. *European Journal of Neuroscience*, 14(12):1937–1946, 2001.

John J Guinan, Shelley S Guinan, and Barbara E Norris. Single auditory units in the superior olivary complex: I: Responses to sounds and classifications based

on physiological properties. *International Journal of Neuroscience*, 4(3):101–120, 1972a.

John J Guinan, Barbara E Norris, and Shelley S Guinan. Single auditory units in the superior olivary complex: Ii: locations of unit categories and tonotopic organization. *International Journal of Neuroscience*, 4(4):147–166, 1972b.

Aziz Hafidi, Joel A Katz, and Dan H Sanes. Differential expression of mag, mbp and l1 in the developing lateral superior olive. *Brain research*, 736(1):35–43, 1996.

M Gartz Hanson and Lynn T Landmesser. Characterization of the circuits that generate spontaneous episodes of activity in the early embryonic mouse spinal cord. *The Journal of neuroscience*, 23(2):587–600, 2003.

Kouichi Hashimoto and Masanobu Kano. Functional differentiation of multiple climbing fiber inputs during synapse elimination in the developing cerebellum. *Neuron*, 38(5):785–796, 2003.

Kouichi Hashimoto and Masanobu Kano. Postnatal development and synapse elimination of climbing fiber to purkinje cell projection in the cerebellum. *Neuroscience research*, 53(3):221–228, 2005.

Kouichi Hashimoto, Ryoichi Ichikawa, Kazuo Kitamura, Masahiko Watanabe, and Masanobu Kano. Translocation of a winner climbing fiber to the purkinje cell dendrite and subsequent elimination of losers from the soma in developing cerebellum. *Neuron*, 63(1):106–118, 2009.

Benjamin Hassfurth, Anna K Magnusson, Benedikt Grothe, and Ursula Koch. Sensory deprivation regulates the development of the hyperpolarization-activated current in auditory brainstem neurons. *European Journal of Neuroscience*, 30(7): 1227–1238, 2009.

Craig K Henkel and Judy K Brunso-Bechtold. Calcium-binding proteins and gaba reveal spatial segregation of cell types within the developing lateral superior olivary nucleus of the ferret. *Microscopy research and technique*, 41(3):234–245, 1998.

E Herzog, J Gilchrist, C Gras, A Muzerelle, P Ravassard, B Giros, P Gaspar, and S El Mestikawy. Localization of vglut3, the vesicular glutamate transporter type 3, in the rat brain. *Neuroscience*, 123(4):983–1002, 2004.

Brian K Hoffpauir, Janelle L Grimes, Peter H Mathers, and George A Spirou. Synaptogenesis of the calyx of held: rapid onset of function and one-to-one morphological innervation. *The Journal of neuroscience*, 26(20):5511–5523, 2006.

Brian K Hoffpauir, Douglas R Kolson, Peter H Mathers, and George A Spirou. Maturation of synaptic partners: functional phenotype and synaptic organization tuned in synchrony. *The Journal of physiology*, 588(22):4365–4385, 2010.

Paul S Holcomb, Brian K Hoffpauir, Mitchell C Hoyson, Dakota R Jackson, Thomas J Deerinck, Glenn S Marrs, Marlin Dehoff, Jonathan Wu, Mark H Ellisman, and George A Spirou. Synaptic inputs compete during rapid formation of the calyx of

held: A new model system for neural development. *The Journal of Neuroscience*, 33(32):12954–12969, 2013.

Z Josh Huang. Activity-dependent development of inhibitory synapses and innervation pattern: role of gaba signalling and beyond. *The Journal of Physiology*, 587 (9):1881–1888, 2009.

Taeko Ichise, Masanobu Kano, Kouichi Hashimoto, Dai Yanagihara, Kazuki Nakao, Ryuichi Shigemoto, Motoya Katsuki, and Atsu Aiba. mglur1 in cerebellar purkinje cells essential for long-term depression, synapse elimination, and motor coordination. *Science*, 288(5472):1832–1835, 2000.

S Ito and E Cherubini. Strychnine-sensitive glycine responses of neonatal rat hippocampal neurones. *The journal of physiology*, 440(1):67–83, 1991.

Peter Jonas, Josef Bischofberger, and Jürgen Sandkühler. Corelease of two fast neurotransmitters at a central synapse. *Science*, 281(5375):419–424, 1998.

Timothy A Jones, Sherri M Jones, and Kristina C Paggett. Primordial rhythmic bursting in embryonic cochlear ganglion cells. *The Journal of Neuroscience*, 21 (20):8129–8135, 2001.

Timothy A Jones, Patricia A Leake, Russell L Snyder, Olga Stakhovskaya, and Ben Bonham. Spontaneous discharge patterns in cochlear spiral ganglion cells before the onset of hearing in cats. *Journal of neurophysiology*, 98(4):1898–1908, 2007.

Philip X Joris and TC Yin. Envelope coding in the lateral superior olive. i. sensitivity to interaural time differences. *Journal of Neurophysiology*, 73(3):1043–1062, 1995.

Philip X Joris, Philip H Smith, and TC Yin. Enhancement of neural synchronization in the anteroventral cochlear nucleus. ii. responses in the tuning curve tail. *Journal of neurophysiology*, 71(3):1037–1051, 1994.

Philip X Joris, Philip H Smith, and Tom CT Yin. Coincidence detection in the auditory system: 50 years after jeffress. *Neuron*, 21(6):1235–1238, 1998.

Jose M Juiz, Robert H Helfert, Joann M Bonneau, Robert J Wenthold, and Richard A Altschuler. Three classes of inhibitory amino acid terminals in the cochlear nucleus of the guinea pig. *Journal of Comparative Neurology*, 373(1):11–26, 1996.

Karl Kandler and Eckhard Friauf. Pre-and postnatal development of efferent connections of the cochlear nucleus in the rat. *Journal of Comparative Neurology*, 328(2): 161–184, 1993.

Karl Kandler and Eckhard Friauf. Development of glycinergic and glutamatergic synaptic transmission in the auditory brainstem of perinatal rats. *The Journal of neuroscience*, 15(10):6890–6904, 1995a.

Karl Kandler and Eckhard Friauf. Development of electrical membrane properties and discharge characteristics of superior olivary complex neurons in fetal and postnatal rats. *European Journal of Neuroscience*, 7(8):1773–1790, 1995b.

Karl Kandler, Amanda Clause, and Jihyun Noh. Tonotopic reorganization of developing auditory brainstem circuits. *Nature neuroscience*, 12(6):711–717, 2009.

Christoph Kapfer, Armin H Seidl, Hermann Schweizer, and Benedikt Grothe. Experience-dependent refinement of inhibitory inputs to auditory coincidence-detector neurons. *Nature neuroscience*, 5(3):247–253, 2002.

Larry C Katz and Carla J Shatz. Synaptic activity and the construction of cortical circuits. *Science*, 274(5290):1133–1138, 1996.

Daniel L Kaufman, Carolyn R Houser, and Allan J Tobin. Two forms of the γ-aminobutyric acid synthetic enzyme glutamate decarboxylase have distinct intraneuronal distributions and cofactor interactions. *Journal of neurochemistry*, 56(2): 720–723, 1991.

Yoshinobu Kawamura, Hisako Nakayama, Kouichi Hashimoto, Kenji Sakimura, Kazuo Kitamura, and Masanobu Kano. Spike timing-dependent selective strengthening of single climbing fibre inputs to purkinje cells during cerebellar development. *Nature communications*, 4, 2013.

Jonathan Kil, Glenn Hkageyama, Malcolm N Semple, and Leonard M Kitzes. Development of ventral cochlear nucleus projections to the superior olivary complex in gerbil. *Journal of Comparative Neurology*, 353(3):317–340, 1995.

Gunsoo Kim and Karl Kandler. Elimination and strengthening of glyciner-

gic/gabaergic connections during tonotopic map formation. *Nature neuroscience*, 6(3):282–290, 2003.

Gunsoo Kim and Karl Kandler. Synaptic changes underlying the strengthening of gaba/glycinergic connections in the developing lateral superior olive. *Neuroscience*, 171(3):924–933, 2010.

Matthias Kneussel and Heinrich Betz. Clustering of inhibitory neurotransmitter receptors at developing postsynaptic sites: the membrane activation model. *Trends in neurosciences*, 23(9):429–435, 2000.

Sailaja Korada and Ilsa R Schwartz. Development of gaba, glycine, and their receptors in the auditory brainstem of gerbil: a light and electron microscopic study. *Journal of Comparative Neurology*, 409(4):664–681, 1999.

Vibhakar C Kotak and Dan H Sanes. Long-lasting inhibitory synaptic depression is age-and calcium-dependent. *The Journal of Neuroscience*, 20(15):5820–5826, 2000.

Vibhakar C Kotak and DH Sanes. Synaptically evoked prolonged depolarizations in the developing auditory system. *Journal of neurophysiology*, 74(4):1611–1620, 1995.

Vibhakar C Kotak, Sailaja Korada, Ilsa R Schwartz, and Dan H Sanes. A developmental shift from gabaergic to glycinergic transmission in the central auditory system. *The Journal of neuroscience*, 18(12):4646–4655, 1998.

Vibhakar C Kotak, Christopher DiMattina, and Dan H Sanes. Gaba˜ b and trk receptor signaling mediates long-lasting inhibitory synaptic depression. *Journal of neurophysiology*, 86(1):536–540, 2001.

Udo Kraushaar and Kurt H Backus. Characterization of gabaa and glycine receptors in neurons of the developing rat inferior colliculus. *Pflügers Archiv*, 445(2):279–288, 2002.

Paul HM Kullmann and Karl Kandler. Glycinergic/gabaergic synapses in the lateral superior olive are excitatory in neonatal c57bl/6j mice. *Developmental Brain Research*, 131(1):143–147, 2001.

Paul HM Kullmann and Karl Kandler. Dendritic ca¡ sup¿ 2+¡/sup¿ responses in neonatal lateral superior olive neurons elicited by glycinergic/gabaergic synapses and action potentials. *Neuroscience*, 154(1):338–345, 2008.

Paul HM Kullmann, F Aura Ene, and Karl Kandler. Glycinergic and gabaergic calcium responses in the developing lateral superior olive. *European Journal of Neuroscience*, 15(7):1093–1104, 2002.

Hui Kuo, Donald K Ingram, Ronald G Crystal, and Andrea Mastrangeli. Retrograde transfer of replication deficient recombinant adenovirus vector in the central nervous system for tracing studies. *Brain research*, 705(1):31–38, 1995.

Andreas Kyrozis, Ondrej Chudomel, Solomon L Moshé, and Aristea S Galanopoulou.

Sex-dependent maturation of gaba¡ sub¿ a¡/sub¿ receptor-mediated synaptic events in rat substantia nigra reticulata. *Neuroscience letters*, 398(1):1–5, 2006.

Katarina E Leao, Richardson N Leao, Hong Sun, Robert EW Fyffe, and Bruce Walmsley. Hyperpolarization-activated currents are differentially expressed in mice brainstem auditory nuclei. *The Journal of physiology*, 576(3):849–864, 2006.

Katarina E Leao, Richardson N Leao, and Bruce Walmsley. Modulation of dendritic synaptic processing in the lateral superior olive by hyperpolarization-activated currents. *European Journal of Neuroscience*, 33(8):1462–1470, 2011.

Xavier Leinekugel, Vadim Tseeb, Yezekiel Ben-Ari, and Piotr Bregestovski. Synaptic gabaa activation induces ca2+ rise in pyramidal cells and interneurons from rat neonatal hippocampal slices. *The Journal of physiology*, 487(Pt 2):319–329, 1995.

Jeff W Lichtman and Howard Colman. Synapse elimination and indelible memory. *neuron*, 25(2):269–278, 2000.

DJ Lim and J Rueda. Structural development of the cochlea. *Development of auditory and vestibular systems*, 2:33–58, 1992.

Man-Hway Lin, Masanori P Takahashi, Yoshifumi Takahashi, and Tadaharu Tsumoto. Intracellular calcium increase induced by gaba in visual cortex of fetal and neonatal rats and its disappearance with development. *Neuroscience research*, 20(1):85–94, 1994.

Ann M Lohof, Nicole Delhaye-Bouchard, and Jean Mariani. Synapse elimination in the central nervous system: functional significance and cellular mechanisms. *Reviews in the Neurosciences*, 7(2):85–102, 1996.

Stefan Löhrke, Geetha Srinivasan, Martin Oberhofer, Ekaterina Doncheva, and Eckhard Friauf. Shift from depolarizing to hyperpolarizing glycine action occurs at different perinatal ages in superior olivary complex nuclei. *European Journal of Neuroscience*, 22(11):2708–2722, 2005.

HJ Luhmann and DA Prince. Postnatal maturation of the gabaergic system in rat neocortex. *Journal of Neurophysiology*, 65(2):247–263, 1991.

Wu Ma, Toby Behar, and Jeffery L Barker. Transient expression of gaba immunoreactivity in the developing rat spinal cord. *Journal of Comparative Neurology*, 325 (2):271–290, 1992.

Takashi Maejima, Kouichi Hashimoto, Takayuki Yoshida, Atsu Aiba, and Masanobu Kano. Presynaptic inhibition caused by retrograde signal from metabotropic glutamate to cannabinoid receptors. *Neuron*, 31(3):463–475, 2001.

John C Maggio, Jeanne H Maggio, and Glayde Whitney. Experience-based vocalization of male mice to female chemosignals. *Physiology & behavior*, 31(3):269–272, 1983.

Anna K Magnusson, Thomas J Park, Michael Pecka, Benedikt Grothe, and Ursula

Koch. Retrograde gaba signaling adjusts sound localization by balancing excitation and inhibition in the brainstem. *Neuron*, 59(1):125–137, 2008.

Robert C Malenka and Mark F Bear. Ltp and ltd: an embarrassment of riches. *Neuron*, 44(1):5–21, 2004.

Nima Marandi, Arthur Konnerth, and Olga Garaschuk. Two-photon chloride imaging in neurons of brain slices. *Pflügers Archiv*, 445(3):357–365, 2002.

Glen S Marrs, Warren J Morgan, David M Howell, George A Spirou, and Peter H Mathers. Embryonic origins of the mouse superior olivary complex. *Developmental neurobiology*, 2013.

Carol A Mason, Sylvia Christakos, and Susan M Catalano. Early climbing fiber interactions with purkinje cells in the postnatal mouse cerebellum. *Journal of Comparative Neurology*, 297(1):77–90, 1990.

Bruce Masterton, Henry Heffner, and Richard Ravizza. The evolution of human hearing. *The Journal of the Acoustical Society of America*, 45(4):966–985, 2005.

Ruth M McKernan and Paul J Whiting. Which gaba¡ sub¿ a¡/sub¿-receptor subtypes really occur in the brain? *Trends in neurosciences*, 19(4):139–143, 1996.

Guido Michels and Stephen J Moss. Gabaa receptors: properties and trafficking. *Critical reviews in biochemistry and molecular biology*, 42(1):3–14, 2007.

Mariko Miyata, Elizabeth A Finch, Leonard Khiroug, Kouichi Hashimoto, Shizu Hayasaka, Sen-Ichi Oda, Minoru Inouye, Yoshiko Takagishi, George J Augustine, and Masanobu Kano. Local calcium release in dendritic spines required for long-term synaptic depression. *Neuron*, 28(1):233–244, 2000.

H Mohler, B Luscher, J-M Fritschy, D Benke, J Benson, and U Rudolph. Gaba¡ sub¿ a¡/sub¿-receptor assembly in vivo: Lessons from subunit mutant mice. *Life sciences*, 62(17):1611–1615, 1998.

Richard Mooney, Anna A Penn, Roberto Gallego, and Carla J Shatz. Thalamic relay of spontaneous retinal activity prior to vision. *Neuron*, 17(5):863–874, 1996.

Junichi Nabekura, Shutaro Katsurabayashi, Yasuhiro Kakazu, Shumei Shibata, Atsushi Matsubara, Shozo Jinno, Yoshito Mizoguchi, Akira Sasaki, and Hitoshi Ishibashi. Developmental switch from gaba to glycine release in single central synaptic terminals. *Nature neuroscience*, 7(1):17–23, 2003.

Hisako Nakayama, Taisuke Miyazaki, Kazuo Kitamura, Kouichi Hashimoto, Yuchio Yanagawa, Kunihiko Obata, Kenji Sakimura, Masahiko Watanabe, and Masanobu Kano. Gabaergic inhibition regulates developmental synapse elimination in the cerebellum. *Neuron*, 74(2):384–396, 2012.

Mark Namchuk, LeAnn Lindsay, Christoph W Turck, Jamil Kanaani, and Steinunn Baekkeskov. Phosphorylation of serine residues 3, 6, 10, and 13 distinguishes membrane anchored from soluble glutamic acid decarboxylase 65 and is restricted to

glutamic acid decarboxylase 65α. *Journal of Biological Chemistry*, 272(3):1548–1557, 1997.

Quyen T Nguyen and Jeff W Lichtman. Mechanism of synapse disassembly at the developing neuromuscular junction. *Current opinion in neurobiology*, 6(1):104–112, 1996.

Jihyun Noh, Rebecca P Seal, Jessica A Garver, Robert H Edwards, and Karl Kandler. Glutamate co-release at gaba/glycinergic synapses is crucial for the refinement of an inhibitory map. *Nature neuroscience*, 13(2):232–238, 2010.

Z Nusser, E Mulvihill, P Streit, and P Somogyi. Subsynaptic segregation of metabotropic and ionotropic glutamate receptors as revealed by immunogold localization. *Neuroscience*, 61(3):421–427, 1994.

Richard W Olsen and Werner Sieghart. Gaba¡ sub¿ a¡/sub¿ receptors: Subtypes provide diversity of function and pharmacology. *Neuropharmacology*, 56(1):141–148, 2009.

Hans-Christian Pape. Queer current and pacemaker: the hyperpolarization-activated cation current in neurons. *Annual review of physiology*, 58(1):299–327, 1996.

Alexandros Poulopoulos, Gayane Aramuni, Guido Meyer, Tolga Soykan, Mrinalini Hoon, Theofilos Papadopoulos, Mingyue Zhang, Ingo Paarmann, Céline Fuchs, Kirsten Harvey, et al. Neuroligin 2 drives postsynaptic assembly at perisomatic inhibitory synapses through gephyrin and collybistin. *Neuron*, 63(5):628–642, 2009.

Dale Purves and Jeff W Lichtman. Specific connections between nerve cells. *Annual review of physiology*, 45(1):553–565, 1983.

Dale Purves and Jeff W Lichtman. *Principles of neural development*. Sinauer Associates Sunderland, MA, 1985.

Heike-Jana Rietzel and Eckhard Friauf. Neuron types in the rat lateral superior olive and developmental changes in the complexity of their dendritic arbors. *The Journal of comparative neurology*, 390(1):20–40, 1998.

Claudio Rivera, Juha Voipio, John A Payne, Eva Ruusuvuori, Hannele Lahtinen, Karri Lamsa, Ulla Pirvola, Mart Saarma, and Kai Kaila. The k+/cl- co-transporter kcc2 renders gaba hyperpolarizing during neuronal maturation. *Nature*, 397(6716): 251–255, 1999.

Claudio Rivera, Juha Voipio, and Kai Kaila. Two developmental switches in gabaergic signalling: the k+–cl- cotransporter kcc2 and carbonic anhydrase cavii. *The Journal of physiology*, 562(1):27–36, 2005.

F Anne Russell and David R Moore. Afferent reorganisation within the superior olivary complex of the gerbil: development and induction by neonatal, unilateral cochlear removal. *Journal of Comparative Neurology*, 352(4):607–625, 1995.

Robert Sandler and A David Smith. Coexistence of gaba and glutamate in mossy fiber terminals of the primate hippocampus: an ultrastructural study. *Journal of comparative neurology*, 303(2):177–192, 1991.

Dan H Sanes and Parag Chokshi. Glycinergic transmission influences the development of dendrite shape. *Neuroreport*, 3(4):323–326, 1992.

Dan H Sanes and EW Rubel. The ontogeny of inhibition and excitation in the gerbil lateral superior olive. *The Journal of neuroscience*, 8(2):682–700, 1988.

Dan H Sanes and Veronica Siverls. Development and specificity of inhibitory terminal arborizations in the central nervous system. *Journal of neurobiology*, 22(8):837–854, 1991.

Dan H Sanes and Catherine Takács. Activity-dependent refinement of inhibitory connections. *European Journal of Neuroscience*, 5(6):570–574, 1993.

Dan H Sanes and G Frederick Wooten. Development of glycine receptor distribution in the lateral superior olive of the gerbil. *The Journal of neuroscience*, 7(11): 3803–3811, 1987.

Dan H Sanes, Michael Merickel, and Edwin W Rubel. Evidence for an alteration of the tonotopic map in the gerbil cochlea during development. *Journal of Comparative Neurology*, 279(3):436–444, 1989.

Dan H Sanes, Nira A Goldstein, Masoud Ostad, and Dean E Hillman. Dendritic morphology of central auditory neurons correlates with their tonotopic position. *Journal of Comparative Neurology*, 294(3):443–454, 1990.

Dan H Sanes, Scott Markowitz, Joseph Bernstein, and Jesse Wardlow. The influence of inhibitory afferents on the development of postsynaptic dendritic arbors. *Journal of Comparative Neurology*, 321(4):637–644, 1992a.

Dan H Sanes, John Song, and James Tyson. Refinement of dendritic arbors along the tonotopic axis of the gerbil lateral superior olive. *Developmental brain research*, 67 (1):47–55, 1992b.

Joshua R Sanes and Jeff W Lichtman. Development of the vertebrate neuromuscular junction. *Annual review of neuroscience*, 22(1):389–442, 1999.

Isabella Sarto-Jackson and Werner Sieghart. Assembly of gabaa receptors (review). *Molecular Membrane Biology*, 25(4):302–310, 2008.

Minako Sato, Patricia A Leake, and Gary T Hradek. Postnatal development of the organ of corti in cats: a light microscopic morphometric study. *Hearing research*, 127(1):1–13, 1999.

Martin K-H Schäfer, Hélène Varoqui, Norah Defamie, Eberhard Weihe, and Jeffrey D Erickson. Molecular cloning and functional identification of mouse vesicular glutamate transporter 3 and its expression in subsets of novel excitatory neurons. *Journal of Biological Chemistry*, 277(52):50734–50748, 2002.

Rebecca P Seal, Omar Akil, Eunyoung Yi, Christopher M Weber, Lisa Grant, Jong Yoo, Amanda Clause, Karl Kandler, Jeffrey L Noebels, Elisabeth Glowatzki, et al.

Sensorineural deafness and seizures in mice lacking vesicular glutamate transporter 3. *Neuron*, 57(2):263–275, 2008.

RP Seal and RH Edwards. The diverse roles of vesicular glutamate transporter 3. In *Neurotransmitter Transporters*, pages 137–150. Springer, 2006.

Aasef G Shaikh and Paul G Finlayson. Hyperpolarization-activated (i¡ sub¿ h¡/sub¿) conductances affect brainstem auditory neuron excitability. *Hearing research*, 183 (1):126–136, 2003.

Carla J Shatz. Impulse activity and the patterning of connections during cns development. *Neuron*, 5(6):745–756, 1990.

W Sieghart, K Fuchs, V Tretter, V Ebert, M Jechlinger, H Höger, and D Adamiker. Structure and subunit composition of gaba¡ sub¿ a¡/sub¿ receptors. *Neurochemistry international*, 34(5):379–385, 1999.

Joshua H Singer, Edmund M Talley, Douglas A Bayliss, Albert J Berger, et al. Development of glycinergic synaptic transmission to rat brain stem motoneurons. *Journal of Neurophysiology*, 80:2608–2620, 1998.

Philip H Smith, Philip X Joris, and Tom CT Yin. Projections of physiologically characterized spherical bushy cell axons from the cochlear nucleus of the cat: evidence for delay lines to the medial superior olive. *Journal of Comparative Neurology*, 331 (2):245–260, 1993.

Philip H Smith, Philip X Joris, and Tom CT Yin. Anatomy and physiology of principal cells of the medial nucleus of the trapezoid body (mntb) of the cat. *Journal of Neurophysiology*, 79(6):3127–3142, 1998.

Jean-Jacques Soghomonian and David L Martin. Two isoforms of glutamate decarboxylase: why? *Trends in pharmacological sciences*, 19(12):500–505, 1998.

Jozsef Somogyi, Agnès Baude, Yuko Omori, Hidemi Shimizu, Salah El Mestikawy, Masahiro Fukaya, Ryuichi Shigemoto, Masahiko Watanabe, and Peter Somogyi. Gabaergic basket cells expressing cholecystokinin contain vesicular glutamate transporter type 3 (vglut3) in their synaptic terminals in hippocampus and isocortex of the rat. *European Journal of Neuroscience*, 19(3):552–569, 2004.

Kevin M Spangler, W Bruce Warr, and Craig K Henkel. The projections of principal cells of the medial nucleus of the trapezoid body in the cat. *Journal of Comparative Neurology*, 238(3):249–262, 1985.

Christian G Specht and Ralf Schoepfer. Deletion of the alpha-synuclein locus in a subpopulation of c57bl/6j inbred mice. *BMC neuroscience*, 2(1):11, 2001.

MW Spitzer and MN Semple. Neurons sensitive to interaural phase disparity in gerbil superior olive: diverse monaural and temporal response properties. *Journal of neurophysiology*, 73(4):1668–1690, 1995.

Jessica C Sterenborg, Nadia Pilati, Craig J Sheridan, Osvaldo D Uchitel, Ian D Forsythe, and Margaret Barnes-Davies. Lateral olivocochlear (loc) neurons of the

mouse lso receive excitatory and inhibitory synaptic inputs with slower kinetics than lso principal neurons. *Hearing research*, 270(1):119–126, 2010.

Ann M Thompson. Serotonin immunoreactivity in auditory brainstem neurons of the postnatal monoamine oxidase-a knockout mouse. *Brain research*, 1228:58–67, 2008.

Ann M Thompson and Glenn C Thompson. Experimental evidence that the serotonin transporter mediates serotonin accumulation in lso neurons of the postnatal mouse. *Brain research*, 1253:60–68, 2009a.

Ann M Thompson and Glenn C Thompson. Serotonin-immunoreactive neurons in the postnatal mao-a ko mouse lateral superior olive project to the inferior colliculus. *Neuroscience letters*, 460(1):47–51, 2009b.

AJ Todd, C Watt, RC Spike, and W Sieghart. Colocalization of gaba, glycine, and their receptors at synapses in the rat spinal cord. *The Journal of neuroscience*, 16 (3):974–982, 1996.

Daniel J Tollin and Tom CT Yin. Interaural phase and level difference sensitivity in low-frequency neurons in the lateral superior olive. *The Journal of neuroscience*, 25(46):10648–10657, 2005.

Daniel J Tollin, Kanthaiah Koka, and Jeffrey J Tsai. Interaural level difference discrimination thresholds for single neurons in the lateral superior olive. *The Journal of Neuroscience*, 28(19):4848–4860, 2008.

Nicolas X Tritsch and Dwight E Bergles. Developmental regulation of spontaneous activity in the mammalian cochlea. *The Journal of Neuroscience*, 30(4):1539–1550, 2010.

Nicolas X Tritsch, Eunyoung Yi, Jonathan E Gale, Elisabeth Glowatzki, and Dwight E Bergles. The origin of spontaneous activity in the developing auditory system. *Nature*, 450(7166):50–55, 2007.

Nicolas X Tritsch, Adrián Rodríguez-Contreras, Tom TH Crins, Han Chin Wang, J Gerard G Borst, and Dwight E Bergles. Calcium action potentials in hair cells pattern auditory neuron activity before hearing onset. *Nature neuroscience*, 13(9): 1050–1052, 2010.

C Tsuchitani. Functional organization of lateral cell groups of cat superior olivary complex. *Journal of Neurophysiology*, 40(2):296–318, 1977.

Alain Uziel, Raymond Romand, and Michel Marot. Development of cochlear potentials in rats. *International Journal of Audiology*, 20(2):89–100, 1981.

Jacques I Wadiche and Craig E Jahr. Multivesicular release at climbing fiber-purkinje cell synapses. *Neuron*, 32(2):301–313, 2001.

Mark K Walsh and Jeff W Lichtman. In vivo time-lapse imaging of synaptic takeover associated with naturally occurring synapse elimination. *Neuron*, 37(1):67–73, 2003.

Hao Wang, Hong Liu, and Zhong-wei Zhang. Elimination of redundant synaptic inputs in the absence of synaptic strengthening. *The Journal of Neuroscience*, 31 (46):16675–16684, 2011.

Florian Werthat, Olga Alexandrova, Benedikt Grothe, and Ursula Koch. Experience-dependent refinement of the inhibitory axons projecting to the medial superior olive. *Developmental neurobiology*, 68(13):1454–1462, 2008.

Rachel OL Wong, Markus Meister, and Carla J Shatz. Transient period of correlated bursting activity during development of the mammalian retina. *Neuron*, 11(5): 923–938, 1993.

ROL Wong and DM Oakley. Changing patterns of spontaneous bursting activity of on and off retinal ganglion cells during development. *Neuron*, 16(6):1087–1095, 1996.

WL Wu, L Ziskind-Conhaim, and MA Sweet. Early development of glycine-and gaba-mediated synapses in rat spinal cord. *The Journal of neuroscience*, 12(10): 3935–3945, 1992.

Junko Yamada, Akihito Okabe, Hiroki Toyoda, Werner Kilb, Heiko J Luhmann, and Atsuo Fukuda. Cl- uptake promoting depolarizing gaba actions in immature rat neocortical neurones is mediated by nkcc1. *The Journal of physiology*, 557(3): 829–841, 2004.

Ji-jian Zheng, Seunghoon Lee, and Z Jimmy Zhou. A developmental switch in the excitability and function of the starburst network in the mammalian retina. *Neuron*, 44(5):851–864, 2004.

Xiaoxi Zhuang, Justine Masson, Jay A Gingrich, Stephen Rayport, and René Hen. Targeted gene expression in dopamine and serotonin neurons of the mouse brain. *Journal of neuroscience methods*, 143(1):27–32, 2005.